

## General Disclaimer

### One or more of the Following Statements may affect this Document

- This document has been reproduced from the best copy furnished by the organizational source. It is being released in the interest of making available as much information as possible.
- This document may contain data, which exceeds the sheet parameters. It was furnished in this condition by the organizational source and is the best copy available.
- This document may contain tone-on-tone or color graphs, charts and/or pictures, which have been reproduced in black and white.
- This document is paginated as submitted by the original source.
- Portions of this document are not fully legible due to the historical nature of some of the material. However, it is the best reproduction available from the original submission.

~~CONFIDENTIAL~~  
**CASE FILE  
COPY**

NATIONAL ADVISORY COMMITTEE FOR AERONAUTICS

~~CONFIDENTIAL~~

~~CLASSIFICATION CANCELLED~~

THIS DOCUMENT OR LOAN FROM THE FILES OF

NATIONAL ADVISORY COMMITTEE FOR AERONAUTICS  
LANGLEY AERONAUTICAL LABORATORY  
LANGLEY FIELD, HAMPTON, VIRGINIA

THIS DOCUMENT OR LOAN FROM THE FILES OF

NATIONAL ADVISORY COMMITTEE FOR AERONAUTICS  
LANGLEY AERONAUTICAL LABORATORY  
LANGLEY FIELD, HAMPTON, VIRGINIA

RETURN TO THE ABOVE ADDRESS.

REQUESTS FOR PUBLICATIONS SHOULD BE ADDRESSED  
AS FOLLOWS:

RETURN TO THE ABOVE ADDRESS.

REQUESTS FOR PUBLICATIONS SHOULD BE ADDRESSED  
AS FOLLOWS:

NATIONAL ADVISORY COMMITTEE FOR AERONAUTICS  
1721 K STREET, N.W.  
WASHINGTON 25, D.C.

MEMORANDUM REPORT

for the

NATIONAL ADVISORY COMMITTEE FOR AERONAUTICS  
1721 K STREET, N.W.  
WASHINGTON 25, D.C.

Declassified by authority  
of LaRC Security Classification  
(SC) Letter dated  
June 16, 1983, and  
STI Program Office

Air Materiel Command, Army Air Forces

TESTS OF A 1/5-SCALE MODEL OF THE REPUBLIC  
XP-84 AIRPLANE (ARMY PROJECT MX-578) IN THE  
LANGLEY 300 MPH 7- BY 10-FOOT TUNNEL

By Warren A. Tucker and Kenneth W. Goodson

Langley Memorial Aeronautical Laboratory  
Langley Field, Va.



CLASSIFIED DOCUMENT

This document contains classified information affecting the National Defense of the United States within the meaning of the Espionage Act (50:31) and 32. Its transmission or the revelation of its contents in any manner to an unauthorized person is prohibited by law. Information so classified may be imparted only to persons in the military and naval services of the United States, appropriate civilian officers and employees of the Federal Government who have a legitimate interest therein and to United States citizens of known loyalty and discretion who necessarily must be informed thereof.

~~CLASSIFICATION CANCELLED~~

~~CLASSIFICATION CHANGED TO  
CONFIDENTIAL~~

July 17, 1946

~~CONFIDENTIAL~~

Ind H 3

NACA Langley Memorial Aeronautical Laboratory

MEMORANDUM REPORT

for the **CLASSIFICATION CANCELLED**

Air Materiel Command, Army Air Forces

RESTRICTED

MR No. L6F25

TESTS OF A 1/5-SCALE MODEL OF THE REPUBLIC

XP-84 AIRPLANE (ARMY PROJECT MX-578) IN THE

LANGLEY 300 MPH 7- BY 10-FOOT TUNNEL

By Warren A. Tucker and Kenneth W. Goodson

SUMMARY

A 1/5-scale model of the Republic XP-84 airplane (Army Project MX-578) was tested in the Langley 300 MPH 7- by 10-foot tunnel. The primary object of the tests was twofold: to determine a practicable method of increasing the longitudinal stability in the landing configuration, and to investigate the effects on longitudinal and lateral stability of various external stores (fuel tanks, bombs, and rockets). The effects of the fuselage dive brakes were also determined, and the critical Mach numbers of certain of the airplane components were estimated.

The use of the revised horizontal tail (of larger aspect ratio and area than the original) seemed to be the most feasible expedient for materially increasing the longitudinal stability in the landing configuration.

The neutral-point shifts produced by the various external stores were unstable, the largest shift being about 2.5 percent mean aerodynamic chord. No appreciable aerodynamic trim changes were caused by the external stores.

From the standpoint of range, maximum speed, and rate of climb, the advantages of mounting the fuel tanks at the wing tips rather than inboard beneath the wings were clearly demonstrated by the tests.

RESTRICTED

The effective dihedral parameter  $C_{l\psi}$  was the only static lateral-stability derivative appreciably affected by the external stores. At high lift coefficients, the tip-mounted tanks caused a large increase in the effective-dihedral parameter (about  $4^\circ$  increase at a lift coefficient of 1.0). This increase was held undesirable, because the tendency toward oscillatory instability that it would cause would be heightened by the increased moments of inertia resulting from the weight of the tanks when carrying fuel.

The fuselage dive brakes, when deflected, caused a change in trim tending to nose the airplane up; the neutral point also moved rearward upon deflecting the dive brakes. The amount of elevator required to overcome the change in trim was well within the available range of deflection. It was estimated that a dive-brake deflection of  $90^\circ$  would decrease the terminal Mach number in a vertical dive by about 0.1.

The estimated critical Mach number of the V-front canopy was about 0.04 greater than that of the original canopy. Pressure-distribution tests disclosed severe pressure peaks inside the nose of the jet entrance duct. These peaks, which would lead to separation and consequently poor pressure recovery at the engine, could be reduced by using a smaller nose radius and a modified internal lip shape.

#### INTRODUCTION

At the request of the Air Materiel Command, Army Air Forces, a 1/5-scale model of the Republic XP-84 airplane (Army Project MX-578) was tested in the Langley 300 MPH 7- by 10-foot tunnel.

Previous tests of the same model in the Langley 7- by 10-foot atmospheric tunnel (reference 1) had indicated that the longitudinal stability was undesirably low, particularly in the landing configuration. One of the objects of the present investigation was therefore to determine some means of increasing the longitudinal stability in the landing configuration. To this end, tests were made of various flap modifications and also of a revised horizontal tail.

Tests were made to determine the effect of the various external stores (fuel tanks, bombs, and rockets) on the longitudinal and lateral stability characteristics. Tests were also made to determine the characteristics of the fuselage dive brakes.

Because of the high speeds expected to be attained in flight, pressure-distribution tests were made to determine the critical Mach numbers of the original canopy and of a V-front canopy. Pressures were also measured inside and outside the nose of the jet entrance duct.

#### COEFFICIENTS AND SYMBOLS

The results of the tests are presented as standard NACA coefficients of forces and moments. Rolling-, yawing-, and pitching-moment coefficients are given about the center-of-gravity location shown in figure 1 (26.45 percent of the mean aerodynamic chord). The data are referred to the stability axes, which are a system of axes having their origin at the center of gravity and in which the Z-axis is in the plane of symmetry and perpendicular to the relative wind, the X-axis is in the plane of symmetry and perpendicular to the Z-axis, and the Y-axis is perpendicular to the plane of symmetry. The positive directions of the stability axes, of angular displacements of the airplane and control surfaces, and of forces and moments are shown in figure 2.

The coefficients and symbols are defined as follows:

$C_L$	lift coefficient (Lift/qS)
$C_D$	drag coefficient (Drag/qS)
$C_X$	longitudinal-force coefficient ( $X/qS$ )
$C_Y$	lateral-force coefficient ( $Y/qS$ )
$C_l$	rolling-moment coefficient ( $L/qS_b$ )
$C_m$	pitching-moment coefficient ( $M/qS_c'$ )
$C_n$	yawing-moment coefficient ( $N/qS_b$ )

MR No. L6F25

$T_c'$  effective thrust coefficient based on wing area ( $T_e/qS$ )

$P$  pressure coefficient  $\left( \frac{p - p_0}{q} \right)$

Lift =  $-Z$

Drag =  $-X$  (only at  $\psi = 0^\circ$ )

$X\}$  forces along axes, pounds  
 $Y\}$   
 $Z\}$

$L\}$  moments about axes, pound feet  
 $M\}$   
 $N\}$

$T_e$  effective thrust, pounds

$p$  local static pressure, pounds per square foot

$p_0$  free-stream static pressure, pounds per square foot

$q$  free-stream dynamic pressure, pounds per square foot ( $\rho V^2/2$ )

$S$  wing area (10.40 sq ft on model)

$c'$  wing mean aerodynamic chord (M.A.C.) (1.48 ft on model)

$b$  wing span (7.28 ft on model)

$h$  distance from thrust line to center of gravity, positive when thrust line is above center of gravity (-0.0165 ft on model)

$A$  area of duct inlet (0.0872 sq ft on model)

$l$  distance from duct inlet to center of gravity (2.97 ft on model)

$V$  free-stream air velocity, feet per second

$V_i$  average air velocity at minimum cross section of duct inlet, feet per second

$\rho$	mass density of air, slug per cubic foot
$\alpha$	angle of attack of fuselage reference line, degrees
$\psi$	angle of yaw, degrees
$i_t$	angle of stabilizer with respect to fuselage reference line, degrees; positive when trailing edge is down
$\delta_e$	elevator deflection with respect to stabilizer chord line, degrees; positive when trailing edge is down
$C_{L\alpha}$	slope of lift curve, per degree
$n_p$	neutral-point location, percent wing mean aerodynamic chord (center-of-gravity location for neutral longitudinal stability in trimmed flight)
$k_x$	radius of gyration about X-axis, feet
$k_z$	radius of gyration about Z-axis, feet
$\mu$	relative density factor ( $m/\rho S_b$ )
$m$	mass of airplane, slugs
Subscript:	
$\psi$	denotes partial derivative of a coefficient with respect to angle of yaw (example: $C_{L\psi} = \partial C_L / \partial \psi$ )

## AIRPLANE, MODEL, AND APPARATUS

The Republic XP-84 airplane is a single-place, single-jet, low-midwing fighter, with tricycle landing gear. The jet power plant of the airplane is completely enclosed within the fuselage, with the intake duct in the fuselage nose and the jet exit at the tail. The airplane has been designed to carry auxiliary fuel tanks, bombs, rockets, or a combination of these external stores,

depending upon the tactical use of the airplane (long-range fighter, fighter-bomber, etc.). The airplane physical characteristics as supplied by the manufacturer are presented in table I.

The model, which has been tested previously in the Langley 7- by 10-foot atmospheric tunnel, was supplied by the Republic Aviation Corporation. A three-view drawing of the 1/5-scale model with the original horizontal tail and a photograph of the model in the landing configuration (split flaps deflected 60°) mounted in the Langley 300 MPH 7- by 10-foot tunnel are shown in figures 1 and 3, respectively. The model was equipped with a 40-percent-span slotted flap, the chord of which varied from 24.9 percent of the wing chord at the inboard end to 26.6 percent of the wing chord at the outboard end. The flap position when deflected 30° is shown in figure 4. Provisions were also made for testing with a 40-percent-span split flap having a constant-percentage chord of 25 percent of the wing chord.

The revised horizontal tail, which was formed by adding area at the root section of the original tail (thereby increasing the span), is compared in figure 5 with the original tail. It will be noted that the revision did not affect the dimensions of the elevator.

Drawings of the fuel tanks in the two positions tested are shown in figures 6 and 7. A photograph of the fuel tanks mounted in the tip position is shown in figure 8. The bombs were also located in two positions. (See fig. 9.) The rockets were located under the fuselage as shown in figure 10. The fuselage dive brakes are shown in figure 11.

The locations of the pressure orifices are shown in figure 12. When the pressure orifices were being installed in the nose, it was noticed that a template made from the dimensions given in Republic drawings SK-30-1 and SK-30-7 was not a good fit with the actual nose. A comparison of the actual nose with the design nose is given in figure 13.

Photographs of the original and the V-front canopies are given in figures 14 and 15.

The model was tested in the cruising configuration (landing gear and flaps retracted) and the landing configuration (landing gear and flaps extended).

The model was equipped with a single-stage axial-flow blower driven by an electric motor. This unit, located within the fuselage, produced a cold jet which was used to simulate the airplane jet for the pressure-distribution tests. Because the inlet velocity could not conveniently be measured directly, the average velocity was measured at the jet exit and converted to average inlet velocity by using continuity considerations. The exit velocity was measured by a single pitot-static tube so located as to measure the average velocity at the jet exit; the location of the tube was obtained from a series of preliminary tests in the Langley 7- by 10-foot tunnel.

## TESTS AND RESULTS

### Test Conditions

The flap modification tests were made at a dynamic pressure chosen to give a Reynolds number equal to the effective Reynolds number of the tests made in the Langley 7- by 10-foot atmospheric tunnel. The remainder of the tests were made at dynamic pressures conditioned mainly by the strength of the model components. The values of dynamic pressure, Reynolds number, and Mach number for each group of tests are listed below.

Tests	$q$ (lb/sq ft)	R	M
Flap modifications	41.8	$1.78 \times 10^6$	0.17
Dive brakes, rocket drag	110.0	2.87	.28
Pressure distributions	27.9	1.46	.14
All others	55.6	2.04	.20

### Corrections

Because of the limited time available for the tests, the tares caused by the model support-strut system were not determined. Because a large number of the tests were made for comparisons with each other, the omission of tares is not too important.

Jet-boundary corrections have been applied to the angles of attack, the longitudinal force coefficients,

and the tail-on pitching-moment coefficients. The following corrections, obtained from reference 2, were added to the test data:

$$\Delta\alpha = 1.00C_L$$

$$\Delta C_X = -0.0175C_L^2$$

$$\Delta C_m = -8.65C_L \left( \frac{0.216}{\sqrt{q_t/q}} - 0.166 \right) \left( \frac{\Delta C_m}{\Delta t} \right)$$

where  $\Delta\alpha$  is in degrees.

Because all the model tests, with the exception of the pressure-distribution tests, were made power-off (model blower unit inoperative), the variations with  $C_L$  of airplane  $T_c'$  and  $V_i/V$  were not duplicated. Therefore, whenever pitching-moment data were desired for the idling-power condition, it was necessary to correct for the effect of  $T_c'$  and  $V_i/V$ . The correction for the direct thrust moment is given by

$$\Delta C_m = -\frac{h}{c'} (T_c') = -0.0112T_c'$$

where  $T_c'$  is for the idling-power condition. The variation of  $T_c'$  with  $C_L$  for the idling-power condition of the airplane is given in figure 16. These data were supplied by the Republic Corporation. The correction for the turning of the air at the nose is given by

$$\Delta C_m = \left( \Delta \frac{V_i}{V} \right) \frac{2Al}{Sc'} \sin \alpha \approx 0.000568 \left( \Delta \frac{V_i}{V} \right) \alpha^\circ$$

where  $\Delta \frac{V_i}{V}$  is the difference in inlet-velocity ratio between the model and the idling-power condition of the airplane. (See fig. 17.) The data of figure 17 were supplied by the Republic Corporation. Both these corrections, which have been derived in reference 1, were added to the power-off data. The combined correction was

destabilizing but small, causing a forward shift of the neutral point always less than 1 percent mean aerodynamic chord.

#### Test Procedure

Except for the pressure-distribution tests, all tests were made power-off (model blower unit inoperative). For those cases in which it was desirable to have pitching-moment data for the idling-power condition, thus allowing a more direct comparison with power-on data from the Langley 7- by 10-foot tunnel, the power-off pitching-moment data were corrected to the idling-power condition by the methods previously explained.

In making the pressure-distribution tests, a different procedure was necessary, since the distribution of pressure, particularly over the nose of the entrance duct, depends on the inlet-velocity ratio. Therefore, the variation of airplane inlet-velocity ratio with lift coefficient (see fig. 17) was duplicated for the pressure-distribution tests. The trim-lift curve used in making the tests is shown in figure 18. This curve was obtained from the test data. For a selected angle of attack of the model, the trim lift coefficient read from figure 18 was used to determine the corresponding inlet-velocity ratio from the appropriate curve of figure 17. This inlet-velocity ratio was then obtained by suitable operation of the blower unit.

An explanation of figure 17 will prove helpful in evaluating the data. The two curves of figure 17 were supplied by the Republic Corporation. The curve marked "power condition A" was given as the variation of  $V_i/V$  with  $C_L$  for idling power (80 percent rpm) at sea level and the curve marked "power condition B" was given as the variation for full power (100 percent rpm) at sea level. Later calculations at the Laboratory disclosed that the curve labeled power condition A also closely represented the variation of  $V_i/V$  with  $C_L$  for full power at 30,000 feet (at any  $C_L$ , the calculated value of  $V_i/V$  for full power at 30,000 feet is about 0.1 less than the value for idling power at sea level). Three power conditions were thus simulated in the tests: full power at sea level, approximately full power at 30,000 feet, and idling power at sea level.

There is one further point of interest regarding the curves of figure 17. The data from the company apparently were worked out neglecting compressibility effects. Had the effect of compressibility been taken into account, the inlet-velocity ratio for power condition B at  $C_L = 0.5$  would have been about 0.15 less (at higher values of  $C_L$ , the difference becomes smaller). The use of the incompressible curves in estimating the critical Mach number of the outer part of the nose of the entrance duct is therefore slightly unconservative.

The lateral stability derivatives at small angles of yaw were obtained from tests through the angle-of-attack range at angles of yaw of  $\pm 5^\circ$  by assuming a straight-line variation between these points.

Because much of the program involved the determination of groups of relatively small incremental effects, the tests of the clean model were repeated for each group, thereby assuring that any small changes in the clean model condition would not introduce errors into the determination of the increments.

#### Presentation of Results

An outline of the figures presenting the results is given below:

#### Figure

##### A. Flap modifications and revised tail:

Stabilizer tests, original tail . . . . .	19
Stabilizer tests, revised tail . . . . .	20
Elevator tests, revised tail . . . . .	21
Neutral points for flap modifications . . . . .	22
Neutral points for original and revised tails .	23

##### B. Longitudinal stability with external stores on wing:

Stabilizer tests . . . . .	24
Neutral points . . . . .	25

Figure

C. Lateral stability with external stores on wing:	
Lateral stability derivatives at small angles	
of yaw . . . . .	26
Stability boundaries . . . . .	27
Tests through yaw range:	
Inboard tanks . . . . .	28
Tip tanks . . . . .	29
Tanks and bombs . . . . .	30
D. Rockets:	
Stabilizer tests . . . . .	31
Effect of rockets . . . . .	32
Neutral points . . . . .	33
E. Fuselage dive brakes:	
Stabilizer tests . . . . .	34
Terminal Mach numbers . . . . .	35
F. Pressure distributions:	
Original canopy . . . . .	36
V-front canopy . . . . .	37
Nose of entrance duct . . . . .	38
Critical Mach number of canopies . . . . .	39
Critical Mach number of nose . . . . .	40

## DISCUSSION

Effect of flap modifications.— The flap modifications ( $30^\circ$  slotted flaps with ailerons drooped  $15^\circ$ , and  $60^\circ$  split flaps) were tested with an eye to improving the stability over that with the  $30^\circ$  slotted flaps, without imposing too severe a penalty on the maximum lift coefficient obtainable. As shown by the stick-fixed neutral points of figure 22, the incorporation of  $15^\circ$  aileron droop actually decreased the stability over the range of lift coefficient in which the flaps would be deflected. Below a lift coefficient of 1.25, the stability with  $60^\circ$  split flaps is slightly greater (1 or 2 percent mean aerodynamic chord neutral point) than that with  $30^\circ$  slotted flaps, but above  $C_L = 1.25$  the stability with the split flaps is less. The results of reference 1 indicate that the stability with  $60^\circ$  split flaps will be greater over the entire lift range.

The values of trim  $C_{L_{max}}$  for the various flap configurations were obtained from figure 19, and are tabulated below. Because of the low Reynolds number of the tests, the absolute values of  $C_{L_{max}}$  are doubtless not those that will be obtained on the full-scale airplane.

Flap configuration	Trim $C_{L_{max}}$
30° slotted flaps	1.53
30° slotted flaps, 15° aileron droop	1.69
60° split flaps	1.46

Hence, if it is decided to use split flaps on the basis of the test results from the Langley 7- by 10-foot tunnel, the decrease in  $C_{L_{max}}$  will be only about 0.07. Split flaps would also present a simpler construction problem.

Effect of revised horizontal tail.—The increase in stability afforded by the revised horizontal tail is illustrated in figure 23, in which the stick-fixed neutral points of the model with the revised tail are compared with those for the model with the original tail. Calculations had indicated that the revised tail should give a 5 percent favorable neutral-point shift at low lift coefficients, with the model in the cruising configuration; the neutral points of figure 23 show a shift of about 6 percent, which is considered good agreement.

Since the revised tail was derived from the original tail by adding fixed area without increasing the amount of movable area (see fig. 5), it was considered advisable to determine the elevator effectiveness of the revised tail. From the data of figure 21, the average elevator effectiveness  $\partial\delta_e/\partial C_L$  was determined; the values obtained are compared below with the corresponding values for the original tail. The values of  $\partial\delta_e/\partial C_L$  for the original tail were obtained from reference 1, since no elevator tests with the original tail were made in the Langley 300 MPH 7- by 10-foot tunnel.

Horizontal tail	Average $\delta\delta_e/\delta C_L$	
	Cruising configuration	Landing configuration ( $60^\circ$ split flaps)
Original (reference 1)	-4.51	<sup>a</sup> -5.99
Revised	-7.75	-7.89

<sup>a</sup>Estimated from isolated tail tests and stabilizer tests on complete model.

These values indicate that to execute a given maneuver, a greater change in elevator deflection will be required with the revised tail.

Effect of fuel tanks and bombs on longitudinal stability and drag (original horizontal tail). - An inspection of the stabilizer curves of figure 24 reveals that for a given center-of-gravity location, the trim changes caused by the various fuel tank and bomb configurations are negligible. This is of interest since it indicates that upon dropping the bombs, for example, the only trim changes which must be overcome by the pilot will be those caused by any center-of-gravity shift occurring when the bombs are released.

The neutral-point shift caused by the various fuel tank and bomb configurations is in general slightly unstable, the maximum unstable shift being about 2.5 percent mean aerodynamic chord. (See fig. 25.) Any actual change in static margin will depend on any possible changes in center-of-gravity location caused by the presence of the external stores.

To aid in evaluating the relative merits of the different configurations, particularly from the stand-point of their effect on the range of the aircraft, certain quantities obtained from enlarged-scale plots of the data of figure 24, for a stabilizer setting of  $-1.0^\circ$ , are presented in the following table. In obtaining the test data, no attempt was made to fix boundary-layer transition on either the stores or the wing; some preliminary tests indicated that on the fuel tanks transition occurred very near the nose.

External stores	$(C_L/C_D)_{max}$	$C_L$ for $(C_L/C_D)_{max}$	$C_D$ at $(C_L/C_D)_{max}$	$C_D$ at $C_L = 0.1$	$C_{L_d}$
None	12.3	0.57	0.0463	0.0240	0.079
Right inboard tank	11.7	.62	.0530	.0282	.076
Both inboard tanks	11.2	.61	.0544	.0302	.075
Right tip tank	12.3	.58	.0472	.0251	.080
Both tip tanks	12.9	.58	.0450	.0252	.088
Both tip tanks + left inboard bomb	11.8	.62	.0526	.0288	.086
Two tip bombs + left inboard bomb	10.8	.65	.0601	.0325	.079

11

An inspection of the values of  $(C_L/C_D)_{max}$  indicates that for a negligible weight increase (tanks empty) the tip-mounted tanks would give a 5-percent increase in range over the airplane with no fuel tanks, whereas the inboard-mounted tanks would decrease the range about 9 percent.

The values of drag coefficient at  $C_L = 0.1$ , qualitatively illustrate the less drastic reduction imposed on the maximum level-flight speed by the tip-mounted tanks, as compared to the inboard-tank installation. Calculations indicated that the tip-mounted tanks would decrease the top speed about 10 miles per hour, whereas the inboard-mounted tanks would give a reduction of about 50 miles per hour. It is reasonable to suppose that the tip tanks, because of their cleaner installation, would be less susceptible to early compressibility shock than would the inboard tanks.

The same calculations also indicated that the maximum rate of climb was not affected by the tip tanks, whereas the inboard tank installation appeared to decrease the maximum rate of climb by about 200 feet per minute. These figures should not be interpreted as quantitative performance estimations, but as indications of the relative merits of the two tank installations.

Effect of fuel tanks and bombs on lateral stability. - Only small effects on the parameters  $C_{l\psi}$  and  $C_{Y\psi}$  are shown by the plots against  $C_L$  of the lateral-stability derivatives  $C_{l\psi}$ ,  $C_{n\psi}$ , and  $C_{Y\psi}$  at small angles of yaw (fig. 26), which provide an over-all picture of the effects of the various fuel tank and bomb configurations.

The only derivative affected to any marked degree is  $C_{l\psi}$ , the effective-dihedral parameter. The effect of the inboard tanks on this parameter is small, but the effect of the tip-mounted tanks, either alone or in conjunction with a single inboard bomb, is to increase the positive value of  $C_{l\psi}$  by an amount proportional to the lift coefficient.

However, with two tip bombs and a single inboard bomb, the parameter  $C_{l\psi}$  is reduced by a practically constant amount over the lift range.

It was considered desirable to investigate the dynamic lateral stability characteristics of the airplane when the tip tanks are carrying fuel, because in this condition the high moments of inertia, combined with the increased  $C_{l\psi}$ , would be expected to give a tendency toward undamped oscillations. Accordingly, the equations of appendix I of reference 3 were used to compute the boundaries for spiral and oscillatory stability for level flight at 20,000 feet for lift coefficients of 0.24 and 0.80. (See fig. 27.) In computing the boundaries, no attempt was made to estimate the effect of the wing tanks on the damping derivatives; it is thought that this effect would be relatively small. The large symbols are the values given by the test data; the position of these symbols in relation to the boundaries indicates the type of stability or instability.

It will be noted that at  $C_L = 0.80$  the test symbol lies in the region of spiral instability. Flight

experience has indicated that a moderate amount of spiral instability can be tolerated, and has little bearing on the ability of the pilot to fly the airplane efficiently. It is greatly desired, however, to have a high degree of damping of the lateral oscillations.

The nearest approach to oscillatory instability occurs with the full tanks at  $C_L = 0.80$ , where the test point falls very near the oscillatory boundary. The condition of level flight at  $C_L = 0.80$  at 20,000 feet is rather extreme, so that it is unlikely that the oscillations will become undamped for any flight condition. However, because the degree of damping of the oscillations becomes smaller as the boundary is approached, it may be that in some cases the oscillations will be so lightly damped as to become objectionable to the pilot. It appears that the airplane could have been designed with 3° or 4° less geometric dihedral (note that even in the three-bomb configuration (fig. 26(c)),  $C_{L\Psi}$  would still be positive).

The slopes of the curves of  $C_l$ ,  $C_n$ , and  $C_y$  plotted against  $\Psi$  for two selected angles of attack (figs. 28 to 30) agree both qualitatively and quantitatively with the curves of figure 26. In addition, the curves of figures 28 and 29 indicate that at an angle of attack of 8.7° ( $C_L \approx 0.7$ ) a single fuel tank mounted on the right wing either inboard or at the tip shifts the rolling-moment curve, the shift being positive for the inboard tank and negative for the tip tank. Not shown in figures 28 and 29 is the fact that a single tank, particularly when full, will cause an appreciable lateral shift of the center of gravity. The importance of a lateral center-of-gravity shift has been shown in reference 4. In order to check the ability of the controls to overcome the combined effects of the asymmetric aerodynamic forces and the lateral shift of the center of gravity, the rudder deflections, aileron deflections, and sideslip angles required for trim in a full-power wing-level climb at  $C_L = 0.7$  have been calculated, using the control-effectiveness data of reference 5. In making the estimates, the asymmetry of the model was taken into account by assuming that at  $\Psi = 0$  with the tanks off, the rolling and yawing moments should be zero. A gross weight of 13,000 pounds (tanks off) was assumed; the weight of a single full tank was assumed

to be 1300 pounds. (The tank capacity was estimated as about 200 gallons.) The results are tabulated below:

	Rudder (deg)	Total aileron (deg)	Sideslip angle (deg)
Right tip tank			
Tank full	10.4 left	8.5 left	2.8 right
Tank empty	2.5 left	7.5 right	.7 right
Right inboard tank			
Tank full	5.0 left	12.4 left	1.4 right
Tank empty	0	2.7 left	0

The calculated values show that the control deflections required are well within the range of the available deflections ( $\pm 25^\circ$  rudder,  $\pm 34^\circ$  total aileron). At lower speeds the deflections required will probably be somewhat greater.

Effect of rockets.- At low lift coefficients, the drag increment contributed by the two rockets beneath the fuselage was only about 0.001, as shown by the longitudinal-force-coefficient curves of figure 32. At lift coefficients greater than 0.4, no drag increment due to the rockets could be detected. The effects of the rockets on trim and neutral point were negligible. (See figs. 32 and 33.)

Effect of fuselage dive brakes.- Examination of the pitching-moment data of figure 34 indicates that deflection of the fuselage dive brakes causes a pitching-moment change which tends to nose the airplane up. Because of the low location of the dive brakes, it might be supposed that the drag forces acting on them would give a diving moment. Apparently, however, when the brakes are deflected, the flow over the wing and tail is changed in such a manner as to give a net nose-up moment. This change in trim may not be objectionable if the fuselage brakes are to be used only as a means of limiting the speed in a dive (at a lift coefficient of 0.1, the change in trim corresponding to a dive-brake deflection of  $90^\circ$  amounts to a change in elevator

deflection of about  $5^\circ$ ). If the nose-up change in trim is maintained at high Mach numbers, the dive brakes could be utilized as a dive recovery device. However, if the brakes were to be used as fighter brakes to check the speed of the aircraft when approaching a target, so as to allow a longer firing time before contact must be broken, the change in trim resulting from application of the brakes would be most disturbing to the pilot, since it would throw the line of fire off the target.

The tail-off curves show that, at the low lift coefficients that will be reached in dives, the tail load for trim with the dive brakes deflected will be somewhat less than that required when the dive-brakes are not used.

The stabilizer curves show that dive-brake deflection is accompanied by an increase in longitudinal stability. The increase amounts to a rearward neutral-point shift of about 6 percent mean aerodynamic chord for the  $60^\circ$  deflection, and about 8 percent mean aerodynamic chord for the  $90^\circ$  deflection. About one-half the increase in each case seems to be the result of a shift of the aerodynamic center of the wing-fuselage combination, the other half being caused by a lower rate of change of downwash at the tail.

Because the primary function of the fuselage dive brakes is to limit the diving speed, it is desirable to see what speed reduction can be effected by use of the brakes. As an indication of the effectiveness of the brakes, the terminal Mach numbers in vertical dives have been estimated. The estimations were made using the data of figure 34 in conjunction with the method of reference 6. The results, shown in figure 35, indicate that a  $90^\circ$  dive brake deflection will reduce the terminal Mach number by roughly 0.1. The additional decrement in terminal Mach number resulting from filling the spaces in the  $90^\circ$  brakes is only about 0.01. The relatively low scale at which the test data were obtained necessitates that the absolute values of the terminal Mach number be regarded with some caution.

Subsequent to the tests, information was received from the Republic Corporation that changes in the size, shape, and location of the fuselage dive brakes were being considered. The data for the original dive brakes are included in this report for possible aid in future design.

Pressures inside nose of inlet duct.—The data of figure 38 show that severe pressure peaks occur inside the nose of the entrance duct. These peaks will be flattened somewhat at full-scale Mach numbers (the model tests were made at a Mach number of 0.14), but they will doubtless still be severe enough to cause internal separation, with a consequent decrease in pressure recovery at the engine. It is thought that a smaller radius (perhaps half the present value) and a change in the lower inner lip shape, bringing the lip straight back for a short distance instead of immediately starting the rather rapid drop-off now present, would do much to eliminate the sharp pressure peaks.

It is interesting to note that the duct surveys of reference 1 show a nonuniform velocity distribution across the duct, the velocity at the wall of the duct (where the pressures of the present tests were measured) being considerably higher than the average inlet velocity.

Critical Mach numbers.—The pressure-distribution data presented in figures 36 and 37 have been used to estimate the critical Mach numbers of the various airplane components. The von Kármán-Tsien method (reference 7) was used in making the estimations; the critical Mach number as defined in reference 7 is the Mach number of the undisturbed flow for which the local velocity at some point on the surface reaches the local velocity of sound.

The estimated critical Mach numbers for the original and the V-front canopies are compared in figure 39. As an aid in evaluating the results, the flight Mach numbers at two altitudes, for a gross weight of 12,500 pounds, are also plotted. It should be noted that in computing the critical Mach number for the V-front canopy, the pressure readings at the orifice 25.95 inches from the nose (see fig. 37) have been disregarded. These readings are considered unreliable, and are thought to be the result of a slight unfairness in the model canopy immediately ahead of the orifice. It should also be borne in mind that since pressure orifices were installed only in the plane of symmetry, the maximum suction pressure on the canopy may not have been measured, so that the estimated critical Mach numbers may be too high. A comprehensive investigation of the pressure distribution over canopies (reference 8) has indicated that the critical Mach number determined from pressure readings in

the plane of symmetry will, in general, be not more than 0.05 too high.

In computing the critical Mach numbers of the canopies, it was noticed that the effect of power was too small to be detected. Therefore, only one curve for each canopy is shown on figure 39. The results indicate that the critical Mach number of the V-front canopy is only slightly (about 0.04) greater than that of the original canopy. If the airplane is assumed to reach a Mach number of 0.8 at either altitude, the critical Mach number of either canopy will be exceeded at this flight Mach number. Because of the relatively small variation of critical Mach number with lift coefficient, the flight Mach number at which the critical Mach number of either canopy is reached does not vary greatly with altitude.

The estimated critical Mach numbers of the outside of the upper nose of the entrance duct are presented in figure 40, together with the flight Mach number. It should be noted that the plots of figure 38 do not in every case extend to the distance from the nose at which the peak pressure on the outside nose is reached; the critical Mach numbers of the outside nose were estimated from separate plots of the data presented in figure 36. The effect of power is quite evident. At sea level, for example, as the power is increased, at any lift coefficient the inlet-velocity ratio is increased so that correspondingly less air is diverted to the outside of the nose and the critical Mach number is increased. If as before a maximum flight Mach number of 0.8 is assumed, the curves of figure 40 indicate that at sea level or at altitude the critical Mach number of the outer upper nose is never reached, for either power condition represented.

Because of the position of the nose wheel well, the pressure measurements on the lower part of the outer nose did not extend far enough back to permit a complete determination of the critical Mach number. However, the outer lower nose is less critical than the outer upper nose for any positive angle of attack, so the omission is not important.

MR No. L6F25

## CONCLUSIONS

The following conclusions are based on the results of tests of a 1/5-scale model of the Republic XP-84 airplane (Army Project MX-578) in the Langley 300 MPH 7- by 10-foot tunnel:

1. The substitution of split flaps for the original slotted flaps afforded a stable neutral-point shift of only 1 or 2 percent mean aerodynamic chord below  $C_L = 1.25$ . Above  $C_L = 1.25$ , the stability with split flaps was less than with the original slotted flaps. The adoption of the revised horizontal tail (of greater aspect ratio and area than the original) appeared the most feasible means of materially increasing the longitudinal stability in the landing configuration.
2. The presence of the various external stores caused unstable neutral-point shifts, the largest shift being about 2.5 percent mean aerodynamic chord. Aerodynamic trim changes caused by the external stores were negligible.
3. From the standpoint of range, maximum speed, and rate of climb, the fuel tanks mounted at the wing tips showed themselves superior to the tanks mounted inboard beneath the wings. With the tanks carrying no fuel, the range of the airplane with the tip-mounted tanks was estimated to be 5 percent greater than the range with no tanks, while the range with the inboard-mounted tanks was about 9 percent less than that with no tanks. The decreases in maximum speed and rate of climb were indicated to be considerably less for the tip-mounted tanks than for the inboard-mounted tanks.
4. The only static lateral-stability parameter affected materially by the presence of the external stores was  $C_{l\psi}$ , the effective-dihedral parameter. The effect of the inboard tanks on  $C_{l\psi}$  was small, the effect of the tip-mounted tanks was to increase the positive value of  $C_{l\psi}$  by an amount proportional to the lift coefficient and the effect of the three bombs was to decrease  $C_{l\psi}$  by a constant amount over the lift range.

## DISCUSSION

The large increase in  $C_{l\psi}$  at high lift coefficients caused by the tip-mounted tanks was regarded as undesirable because of the tendency it gave toward aerodynamic oscillatory instability; this tendency was aggravated by the increased moments of inertia resulting from the weight of the full tanks.

5. For a full-power wing-level climb at  $C_L = 0.7$ , the estimated rudder and aileron deflections required to trim out the asymmetric moments resulting from the presence of a single full fuel tank mounted either inboard or at the tip were well within the available range of deflections.

6. The aerodynamic effects of the rockets were negligible.

7. Deflection of the fuselage dive-brakes caused a nose-up change in trim and a rearward (stable) shift of the neutral point. The amount of elevator required to overcome the change in trim was well within the available range of deflection. It was estimated that a dive-brake deflection of  $90^\circ$  would decrease the terminal Mach number in a vertical dive by about 0.1.

8. The critical Mach number of the V-front canopy, as estimated from pressure-distribution data obtained at a low Mach number, was about 0.04 greater than the critical Mach number of the original canopy. The effect of power on the critical Mach number of either canopy was negligible.

9. The estimated critical Mach number of the outside nose of the jet entrance duct was greater than the flight Mach number for both power conditions tested. Pressure-distribution tests showed sharp internal pressure peaks which would lead to separation and, consequently, a decrease in pressure recovery at the engine. It was

MR No. L6F25

suggested that a smaller nose radius and a change in the internal lip shape would help to alleviate the pressure peaks.

Langley Memorial Aeronautical Laboratory  
National Advisory Committee for Aeronautics  
Langley Field, Va.

*Warren G. Tucker*

Warren A. Tucker  
Aeronautical Engineer

*Kenneth W. Goodson*  
Kenneth W. Goodson  
Aeronautical Engineer

Approved: *Thomas G. Harris*  
for *Hartley A. Soule*  
Chief of Stability Research Division

## REFERENCES

1. Gillis, Clarence L., and Andrews, Thomas B., Jr.: Wind-Tunnel Tests of a 1/5-Scale Model of the Republic XP-84 Airplane (Army Project MX-578). I - Longitudinal Static Stability and Control. NACA MR No. L6D05, Army Air Forces, 1946.
2. Gillis, Clarence L., Polhamus, Edward C., and Gray, Joseph L., Jr.: Charts for Determining Jet-Boundary Corrections for Complete Models in 7- by 10-Foot Closed Rectangular Wind Tunnels. NACA ARR No. L5G31, 1945.
3. Zimmerman, Charles H.: An Analysis of Lateral Stability in Power-Off Flight with Charts for Use in Design. NACA Rep. No. 589, 1937.
4. Phillips, W. H., Crane, H. L., and Hunter, P. A.: Effect of Lateral Shift of Center of Gravity on Rudder Deflection Required for Trim. NACA RB No. L4I06, 1944.
5. Gillis, Clarence L., and Delftchmann, Seymour J.: Wind-Tunnel Tests of a 1/5-Scale Model of the Republic XP-84 Airplane (Army Project MX-578). II - Lateral Stability and Control. NACA MR No. L6D15, Army Air Forces, 1946.
6. Bielat, Ralph P.: A Simple Method for Estimating Terminal Velocity Including Effect of Compressibility on Drag. NACA ACR No. L5G31, 1945.
7. von Kármán, Th.: Compressibility Effects in Aerodynamics. Jour. Aero. Sci., vol. 8, no. 9, July 1941, pp. 337-356.
8. Delano, James B., and Wright, Ray H.: Investigation of Drag and Pressure Distribution of Windshields at High Speeds. NACA ARR, Jan. 1942.

TABLE I

## PHYSICAL CHARACTERISTICS OF THE REPUBLIC XP-84 AIRPLANE

Type . . . . . Jet-propelled fighter

## Wing:

Area, sq ft . . . . .	260
Span, ft . . . . .	36.42
Aspect ratio . . . . .	5.1
Taper ratio . . . . .	0.57
Dihedral, deg . . . . .	5
Incidence at station 27 in. from center line . . . . .	0
Sweepback, 25-percent chord line, deg . . . . .	3.08
Geometric twist, deg (washout) . . . . .	2
Mean aerodynamic chord (M.A.C.), ft . . . . .	7.39
Station zero to 50-percent chord of M.A.C., ft . . . . .	16.5
Airfoil section . . . . .	Republic R-4, 45-1512-.9

## Original horizontal tail:

Area, sq ft . . . . .	48.5
Span, ft . . . . .	15.0
Aspect ratio . . . . .	4.6
Elevator area behind hingeline, sq ft . . . . .	13
Root-mean-square chord of elevator, ft . . . . .	0.990
Airfoil section . . . . .	Republic R-4, 40-010

## Revised horizontal tail:

Area, sq ft . . . . .	57.1
Span, ft . . . . .	17.0
Aspect ratio . . . . .	5.07
Elevator area behind hinge line, sq ft . . . . .	13
Root-mean-square chord of elevator, ft . . . . .	0.990
Airfoil section . . . . .	Republic R-4, 40-010

## Vertical tail:

Total area, sq ft . . . . .	35.80
Rudder area behind hinge line, sq ft . . . . .	7.39
Height from center line of fuselage, ft . . . . .	8.10
Root-mean-square chord of rudder, ft . . . . .	1.21
Airfoil section . . . . .	Republic R-4, 40-010

## High-lift device (slotted flap):

Chord . . . . .	0.249c inboard, 0.266c outboard
Span . . .	Extends from wing-fuselage juncture to 0.51 <sup>b</sup> <sub>2</sub>

## High-lift device (split flap):

Chord . . . . .	0.25c
Span . . .	Extends from wing-fuselage juncture to 0.51 <sup>b</sup> <sub>2</sub>

MR No. L6F25

TABLE I  
PHYSICAL CHARACTERISTICS - Concluded

Weight and balance:	
Normal gross weight, lb	12,500
Wing loading, lb/sq. ft	48.1
Normal center-of-gravity position, percent	
M.A.C.	26.45
Center-of-gravity range, percent	
M.A.C.	26.45 to 30.00

NATIONAL ADVISORY  
COMMITTEE FOR AERONAUTICS

MR No. L6F25

FIGURE LEGENDS

Figure 1.- Three-view drawing of the 1/5-scale model of the Republic XP-84 airplane (Army Project MX-578) with original horizontal tail.

Figure 2.- System of axes. Positive values of forces, moments, and angles are indicated by arrows.

Figure 3.- The 1/5-scale model of the Republic XP-84 airplane (Army Project MX-578) mounted in the 300 mph 7- by 10-foot tunnel.

Figure 4.- Flap position for tests of 1/5-scale model of Republic XP-84 airplane (Army Project MX-578) with slotted flap deflected 30°.

Figure 5.- Original and revised horizontal tails tested on the 1/5-scale model of the Republic XP-84 airplane (Army Project MX-578).

Figure 6.- Inboard position of fuel tank tested on the 1/5-scale model of the Republic XP-84 airplane (Army Project MX-578).

Figure 7.- Wing-tip position of fuel tank tested on the 1/5-scale model of the Republic XP-84 airplane (Army Project MX-578).

Figure 8.- Fuel tanks mounted at the wing tips of the 1/5-scale model of the Republic XP-84 airplane (Army Project MX-578).

Figure 9.- Positions of bombs tested on the 1/5-scale model of the Republic XP-84 airplane (Army Project MX-578).

Figure 10.- Details of rockets tested on the 1/5-scale model of the Republic XP-84 airplane (Army Project MX-578).

Figure 11.- Fuselage dive brakes tested on the 1/5-scale model of the Republic XP-84 airplane (Army Project MX-578).

MR No. L6F25

FIGURE LEGENDS - Continued

Figure 12.- Location of pressure orifices on the 1/5-scale model of the Republic XP-84 airplane (Army Project MX-578).

(a) Original canopy.

(b) Nose.

Figure 12.- Concluded.

(c) V-front canopy.

Figure 13.- A comparison of ordinates for the design nose and the actual nose as tested on the 1/5-scale model of the Republic XP-84 airplane (Army Project MX-578).

Figure 14.- The original canopy tested on the 1/5-scale model of the Republic XP-84 airplane (Army Project MX-578).

Figure 15.- The V-front canopy tested on the 1/5-scale model of the Republic XP-84 airplane (Army Project MX-578).

Figure 16.- Variation of effective thrust coefficient with lift coefficient for the Republic XP-84 airplane (Army Project MX-578). Idling power (80 percent rpm) at sea level (power condition A); gross weight = 12,500 lb.

Figure 17.- Variation of inlet-velocity ratio with lift coefficient for the Republic XP-84 airplane (Army Project MX-578). Gross weight = 12,500 lb.

Figure 18.- Variation of trim lift coefficient with angle of attack used making pressure-distribution tests on the 1/5-scale model of the Republic XP-84 airplane (Army Project MX-578). Cruising configuration.

Figure 19.- Effect of stabilizer on the aerodynamic characteristics in pitch of the 1/5-scale model of the Republic XP-84 airplane with original horizontal tail. Idling power.

(a) Cruising configuration.

FIGURE LEGENDS - Continued

Figure 19.- Continued.

(b) Landing configuration (slotted flaps deflected 30°).

Figure 19.- Continued.

(c) Landing configuration (slotted flaps deflected 30°; ailerons drooped 15°).

Figure 19.- Concluded.

(d) Landing configuration (split flaps deflected 60°).

Figure 20.- Effect of stabilizer on the aerodynamic characteristics in pitch of the 1/5-scale model of the Republic XP-84 airplane with revised horizontal tail. Idling power.

(a) Cruising configuration.

Figure 20.- Concluded.

(b) Landing configuration (split flaps deflected 60°).

Figure 21.- Effect of elevator deflection on the aerodynamic characteristics in pitch of the 1/5-scale model of the Republic XP-84 airplane with revised horizontal tail. Idling power;  $it = 0^\circ$ .

(a) Cruising configuration.

Figure 21.- Concluded.

(b) Landing configuration (split flaps deflected 60°).

Figure 22.- Stick-fixed neutral points of the Republic XP-84 airplane with original horizontal tail, as determined from tests of the 1/5-scale model. Idling power, landing configuration.

MR No. L6F25

FIGURE LEGENDS - Continued

Figure 23.- Effect of revised horizontal tail on the stick-fixed neutral points of the Republic XP-84 airplane, as determined from tests of the 1/5-scale model. Idling power.

Figure 24.- Effect of external fuel tanks and bombs on the aerodynamic characteristics in pitch of the 1/5-scale model of the Republic XP-84 airplane with original horizontal tail. Power off, cruising configurations.

(a) Tanks off; bombs off.

Figure 24.- Continued.

(b) Right tank in inboard position; left tank off; bombs off.

Figure 24.- Continued.

(c) Both tanks in inboard position; bombs off.

Figure 24.- Continued.

(d) Right tank in tip position; left tank off; bombs off.

Figure 24.- Continued.

(e) Both tanks in tip position; bombs off.

Figure 24.- Continued.

(f) Both tanks in tip position; left inboard bomb on, tip bombs off.

Figure 24.- Concluded.

(g) Tanks off; left inboard bomb on, tip bombs on.

Figure 25.- Effect of external fuel tanks and bombs on the stick-fixed neutral points of the Republic XP-84 airplane, as determined from tests of the 1/5-scale model. Power off; cruising configuration.

FIGURE LEGENDS - Continued

Figure 26.- Effect of external fuel tanks and bombs on the lateral-stability derivatives at small angles of yaw of the 1/5-scale model of the Republic XP-84 airplane. Power off; cruising configuration;  $i_t = 0^\circ$ .

(a) Inboard tanks.

Figure 26.- Continued.

(b) Tip tanks.

Figure 26.- Concluded.

(c) Tanks and bombs.

Figure 27.- Effect of carrying fuel in the wing tip tanks on the dynamic lateral-stability boundaries of the XP-84 airplane. Cruising configuration.

Figure 28.- Effect of inboard fuel tanks on the aerodynamic characteristics in yaw of the 1/5-scale model of the Republic XP-84 airplane. Power off; cruising configuration;  $i_t = 0^\circ$ .

(a)  $\alpha = 0.1^\circ$ .

Figure 28.- Continued.

(a) Concluded.

Figure 28.- Continued.

(b)  $\alpha = 8.7^\circ$ .

Figure 28.- Concluded.

(b) Concluded.

Figure 29.- Effect of tip-mounted fuel tanks on the aerodynamic characteristics in yaw of the 1/5-scale model of the Republic XP-84 airplane. Power off; cruising configuration;  $i_t = 0^\circ$ .

(a)  $\alpha = 0.1^\circ$ .

FIGURE LEGENDS - Continued

Figure 29.- Continued.

(a) Concluded.

Figure 29.- Continued.

(b)  $\alpha = 8.7^\circ$ .

Figure 29.- Concluded.

(b) Concluded.

Figure 30.- Effect of fuel tanks and bombs on the aerodynamic characteristics in yaw of the 1/5-scale model of the Republic XP-84 airplane. Power off; cruising configuration;  $i_t = 0^\circ$ .

(a)  $\alpha = 0.1^\circ$ .

Figure 30.- Continued.

(a) Concluded.

Figure 30.- Continued.

(b)  $\alpha = 8.7^\circ$ .

Figure 30.- Concluded.

(b) Concluded.

Figure 31.- Effect of stabilizer on the aerodynamic characteristics in pitch of the 1/5-scale model of the Republic XP-84 airplane with revised horizontal tail. Idling power; cruising configuration. Two rockets beneath fuselage.

Figure 32.- Effect of rockets on the aerodynamic characteristics in pitch of the 1/5-scale model of the Republic XP-84 airplane with revised horizontal tail. Idling power; cruising configuration;  $i_t = 0^\circ$ .

Figure 33.- Effect of rockets on the stick-fixed neutral points of the Republic XP-84 airplane with revised horizontal tail, as determined from tests of the 1/5-scale model. Idling power; cruising configuration.

FIGURE LEGENDS - Continued

Figure 34.- Effect of fuselage dive-brake deflection on the aerodynamic characteristics in pitch of the 1/5-scale model of the Republic XP-84 airplane with original horizontal tail. Idling power, cruising configuration.

(a) Dive brakes retracted.

Figure 34.- Continued.

(b) Dive brakes deflected 60°.

Figure 34.- Concluded.

(c) Dive brakes deflected 90°.

Figure 35.- Effect of fuselage dive brakes on the estimated terminal Mach numbers of the Republic XP-84 airplane in vertical dives. Estimates based on wing critical Mach number of 0.755. Gross weight = 13,324 lb.

Figure 36.- Pressure distribution over the top of the fuselage of the 1/5-scale model of the Republic XP-84 airplane with the original canopy.

(a) Power condition A (idling power (80 percent rpm) at sea level; approximately full power (100 percent rpm) at 30,000 feet).

Figure 36.- Concluded.

(b) Power condition B (full power (100 percent rpm) at sea level).

Figure 37.- Pressure distribution over the top of the V-front canopy tested on the 1/5-scale model of the Republic XP-84 airplane.

(a) Power condition A (idling power (80 percent rpm) at sea level; approximately full power (100 percent rpm) at 30,000 feet).

FIGURE LEGENDS - Concluded

Figure 37.- Concluded.

(b) Power condition B (full power (100 percent rpm) at sea level).

Figure 38.- Pressure distribution over the nose of the entrance duct of the 1/5-scale model of the Republic XP-84 airplane.

(a) Power condition A (idling power (80 percent rpm) at sea level; approximately full power (100 percent rpm) at 30,000 feet).

Figure 38.- Concluded.

(b) Power condition B (full power (100 percent rpm) at sea level).

Figure 39.- Critical Mach numbers of two canopies for the Republic XP-84 airplane, as estimated from pressure-distribution tests of the 1/5-scale model. Power conditions A and B.

Figure 40.- Critical Mach numbers of the outside of the upper nose of the entrance duct of the Republic XP-84 airplane, as estimated from pressure-distribution tests of the 1/5-scale model.

1820 - 1

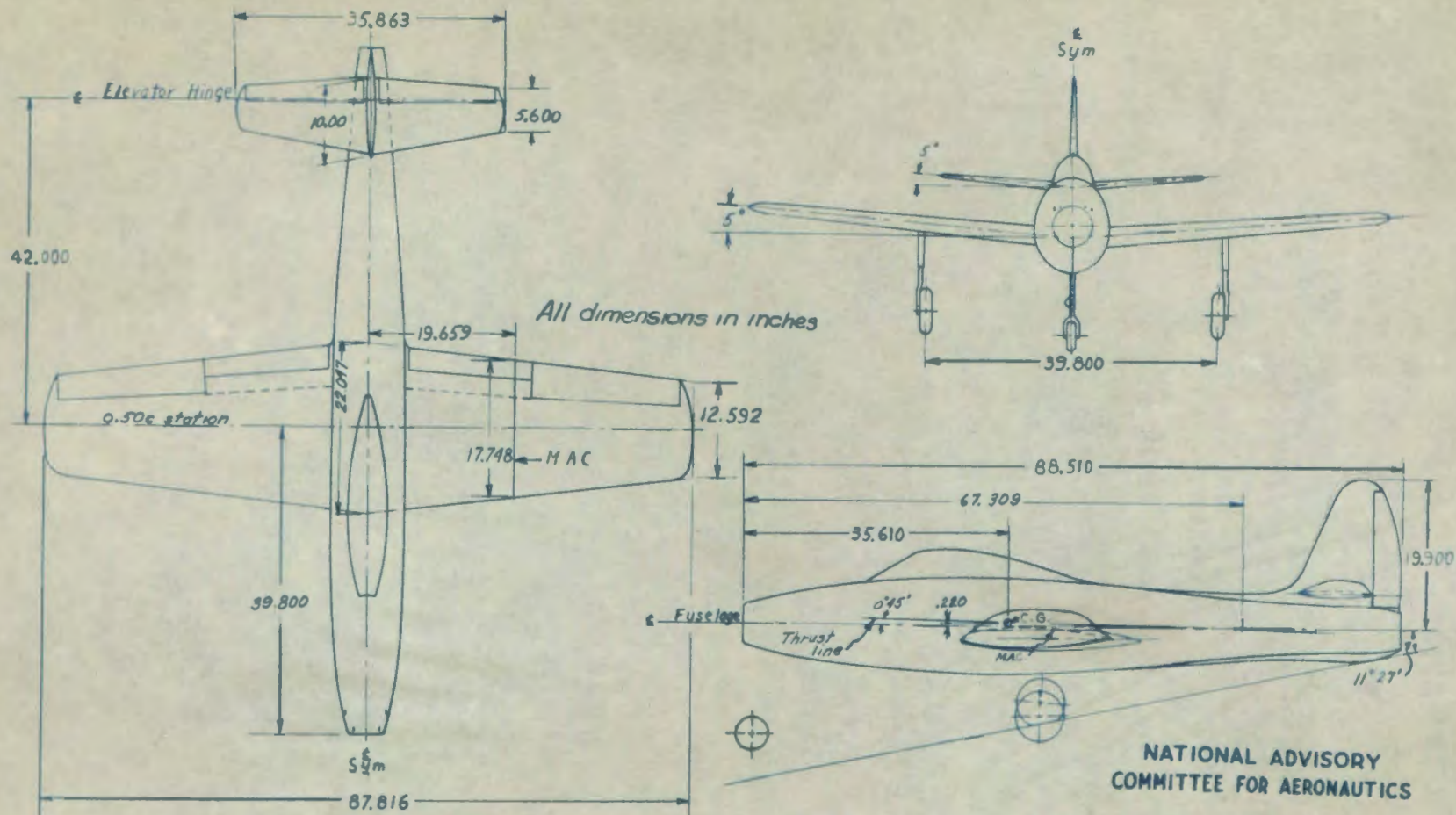
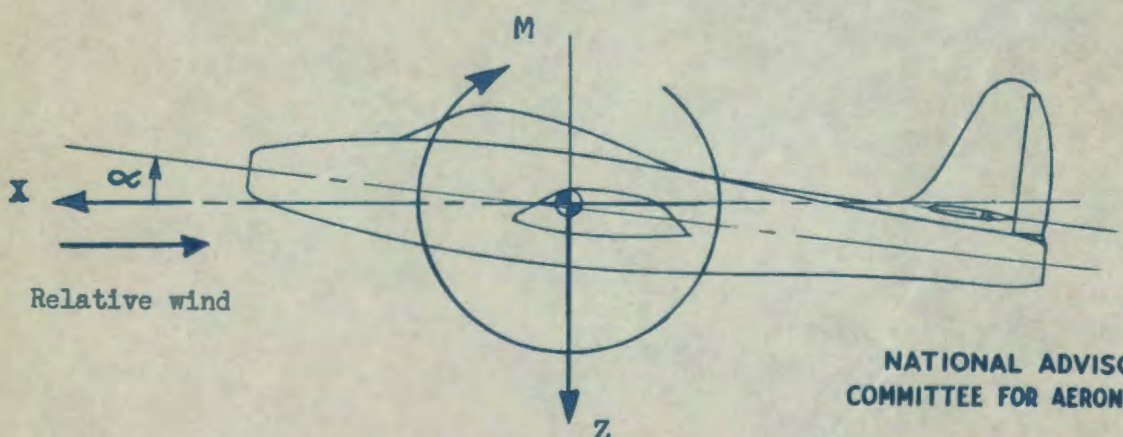
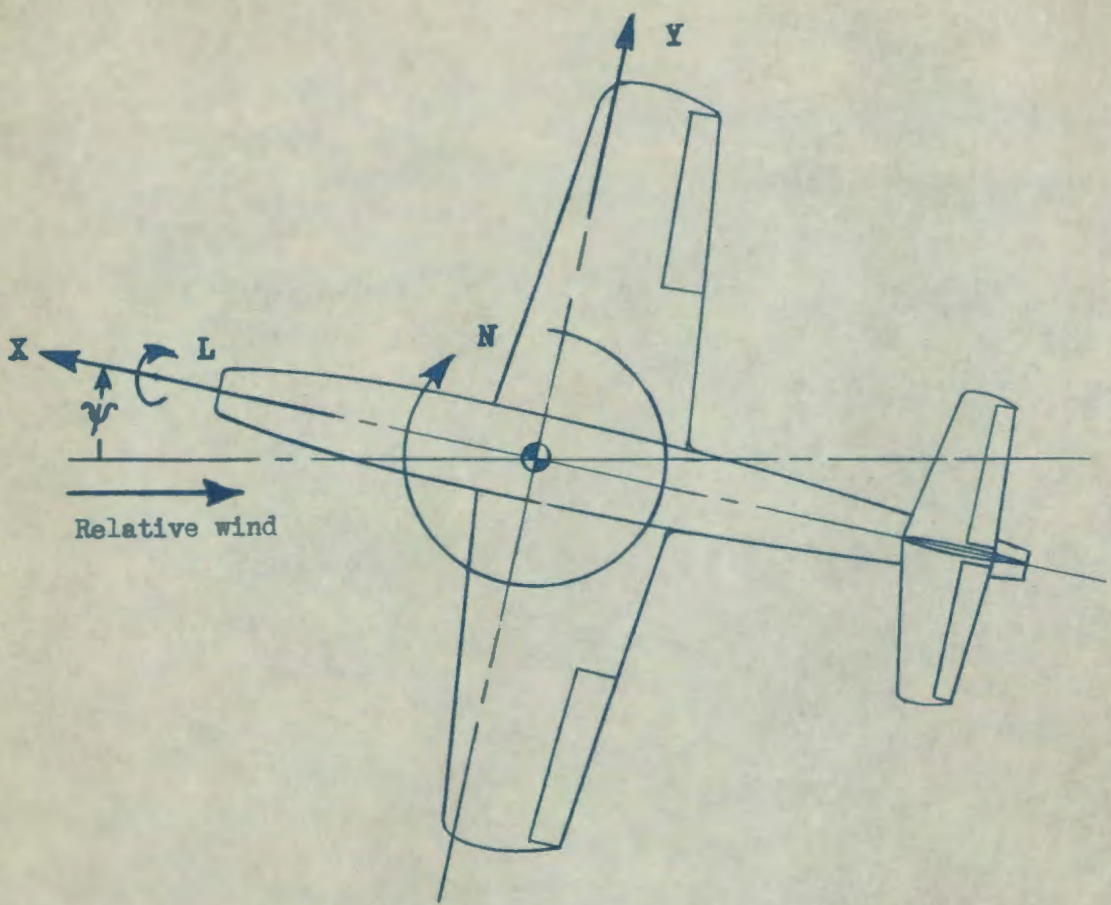


Figure 1.- Three-view drawing of the  $\frac{1}{5}$ -scale model of the Republic XP-84 airplane (Army Project MX-578) with original horizontal tail.

MR No. L6F25

2  
2  
0  
7

MR No. L6F25



NATIONAL ADVISORY  
COMMITTEE FOR AERONAUTICS

Figure 2.- System of axes. Positive values of forces, moments and angles are indicated by arrows.

1820-3

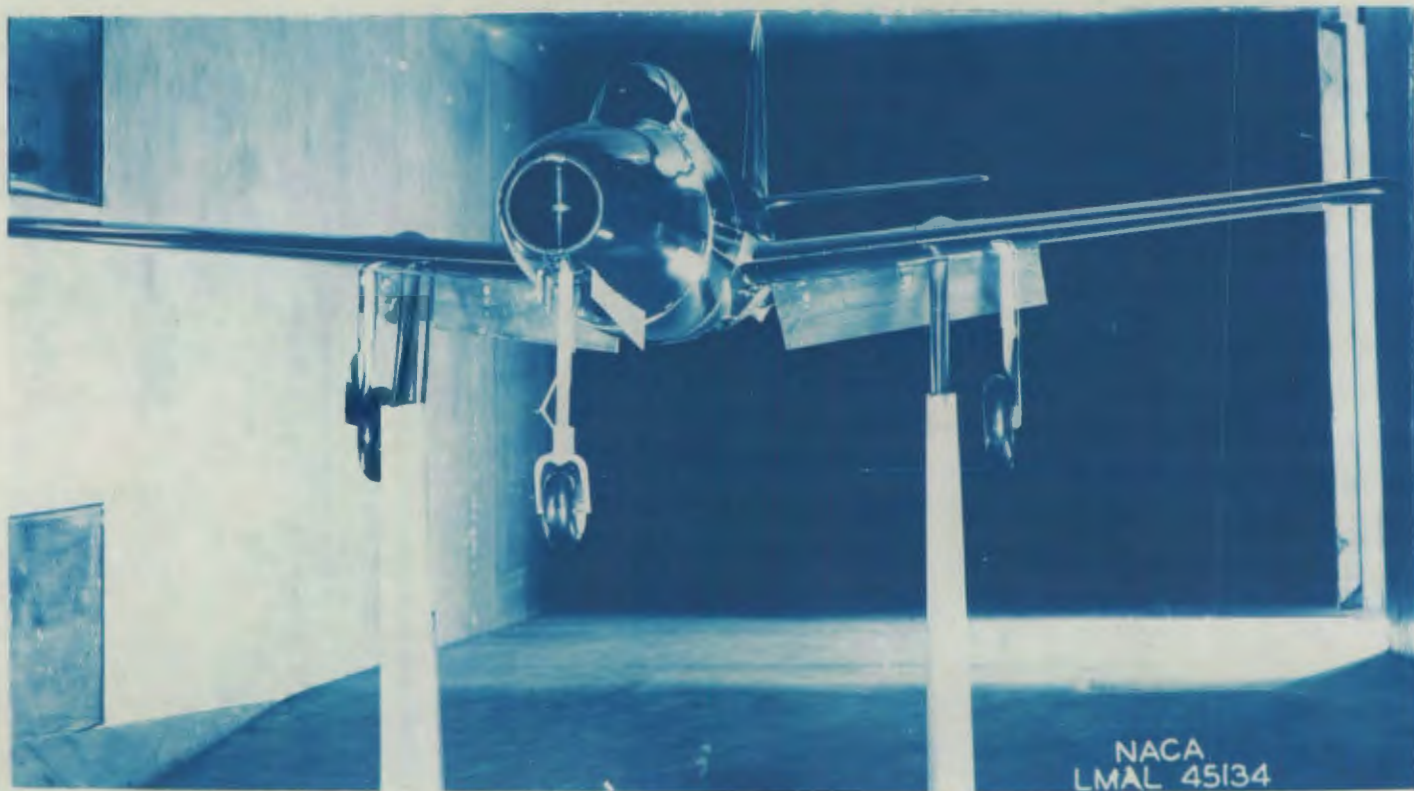


Figure 3.- The  $\frac{1}{5}$ -scale model of the Republic XP-84 airplane (Army Project MX-578)  
mounted in the 300 mph 7- by 10-foot tunnel.

MR NO. L6F25

NATIONAL ADVISORY COMMITTEE FOR AERONAUTICS  
LANGLEY MEMORIAL AERONAUTICAL LABORATORY - LANGLEY FIELD, VA.

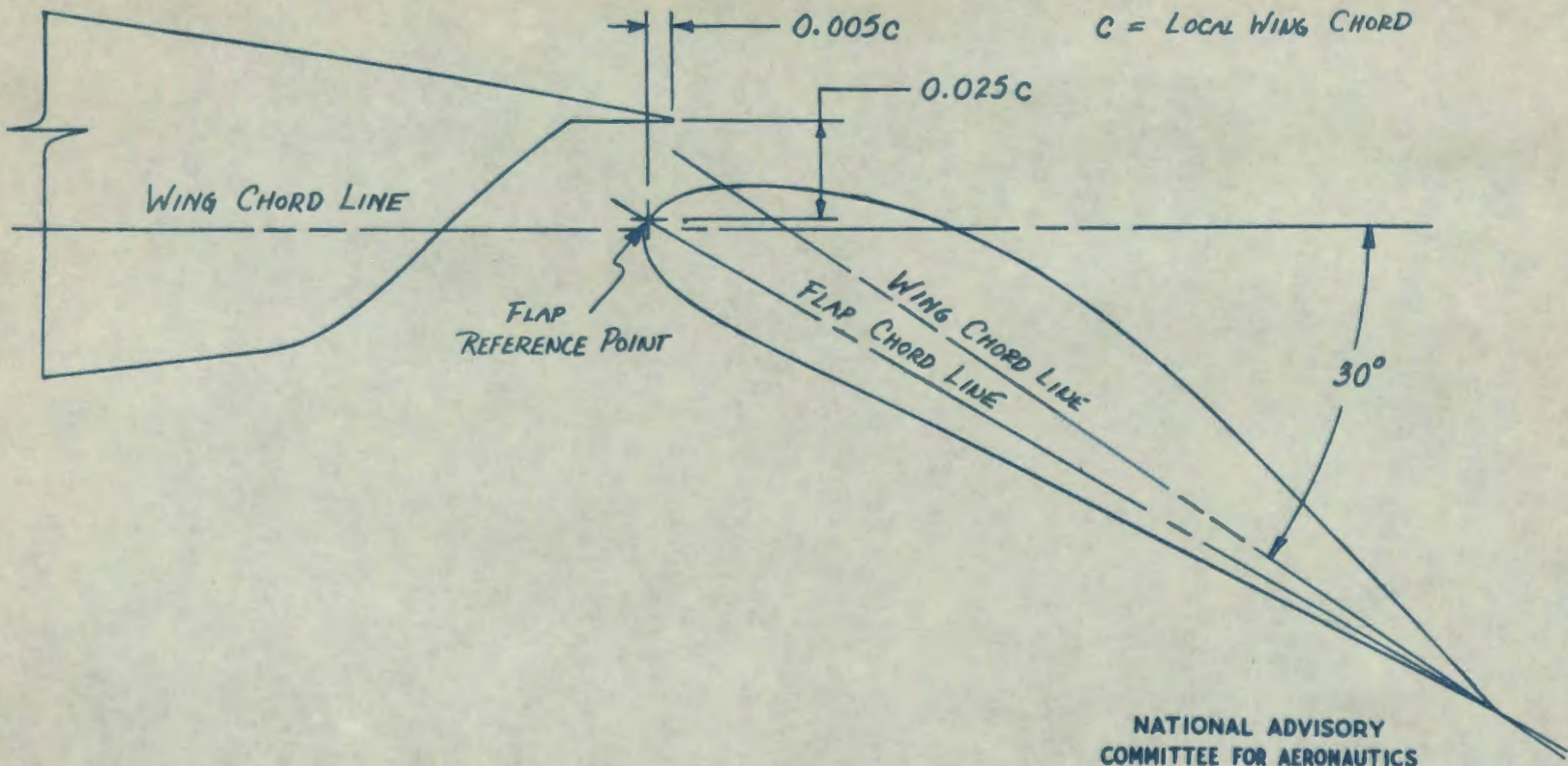


Figure 4.- Flap position for tests of 1/5-scale model of Republic XP-84 airplane (Army Project MX-578) with slotted flap deflected 30°.

All dimensions in inches

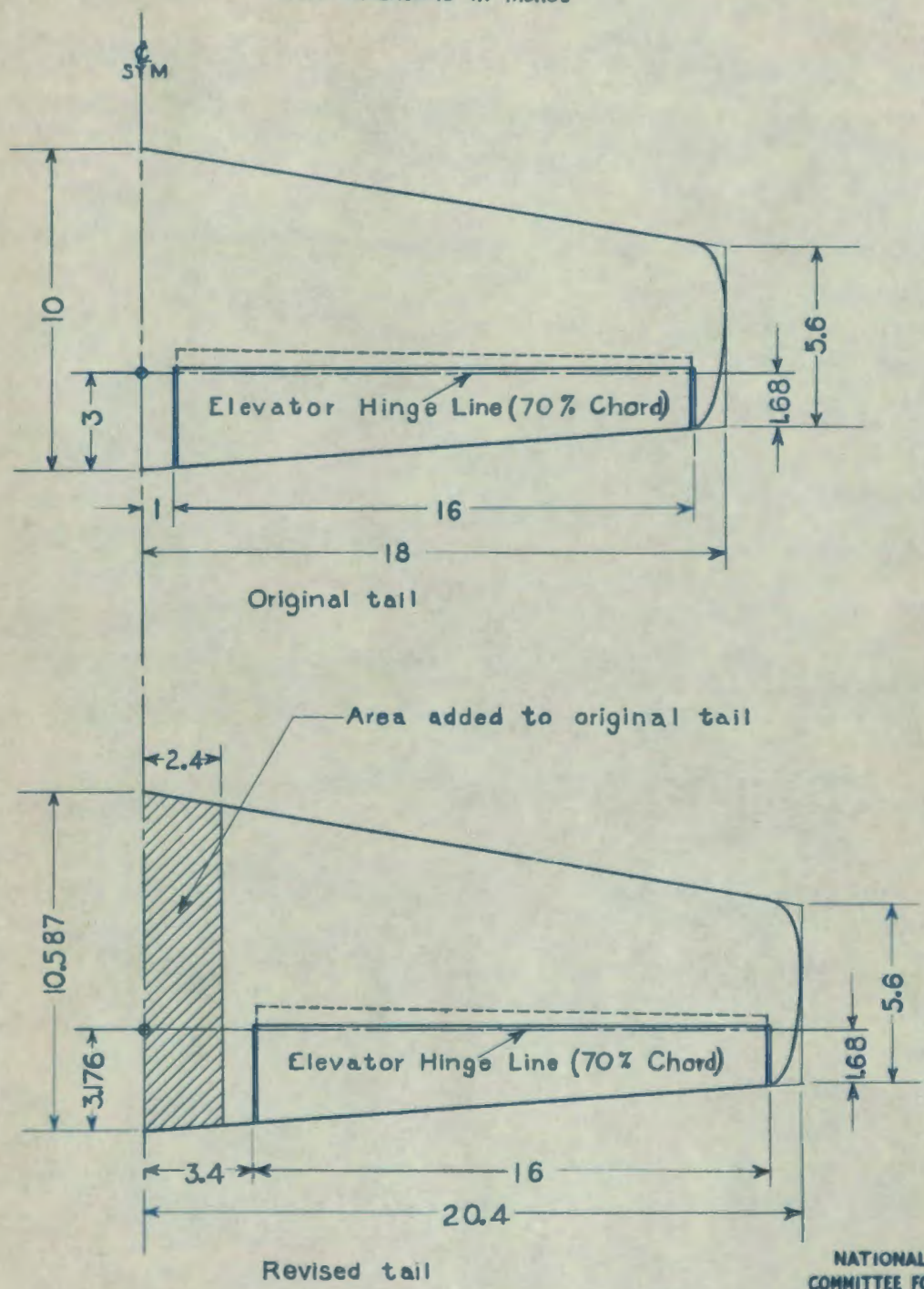


Figure 5.- Original and revised horizontal tails tested on the 1/5-scale model of the Republic XP-84 airplane (Army Project MX-578).

1620 6

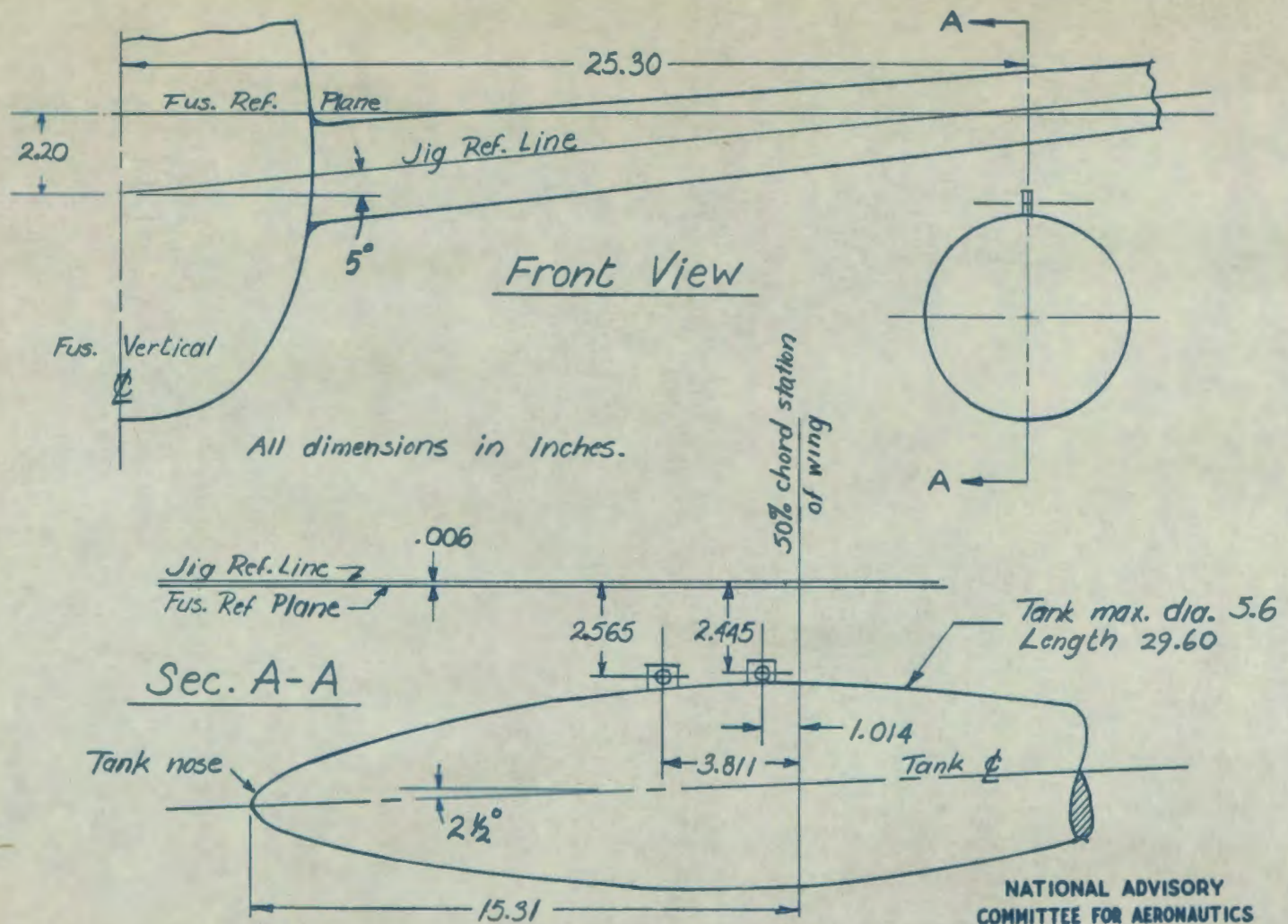


Figure 6.- Inboard position of fuel tank tested on the 1/5-scale model of the Republic XP-84 airplane (Army Project MX-578).

MR NO. L6F25

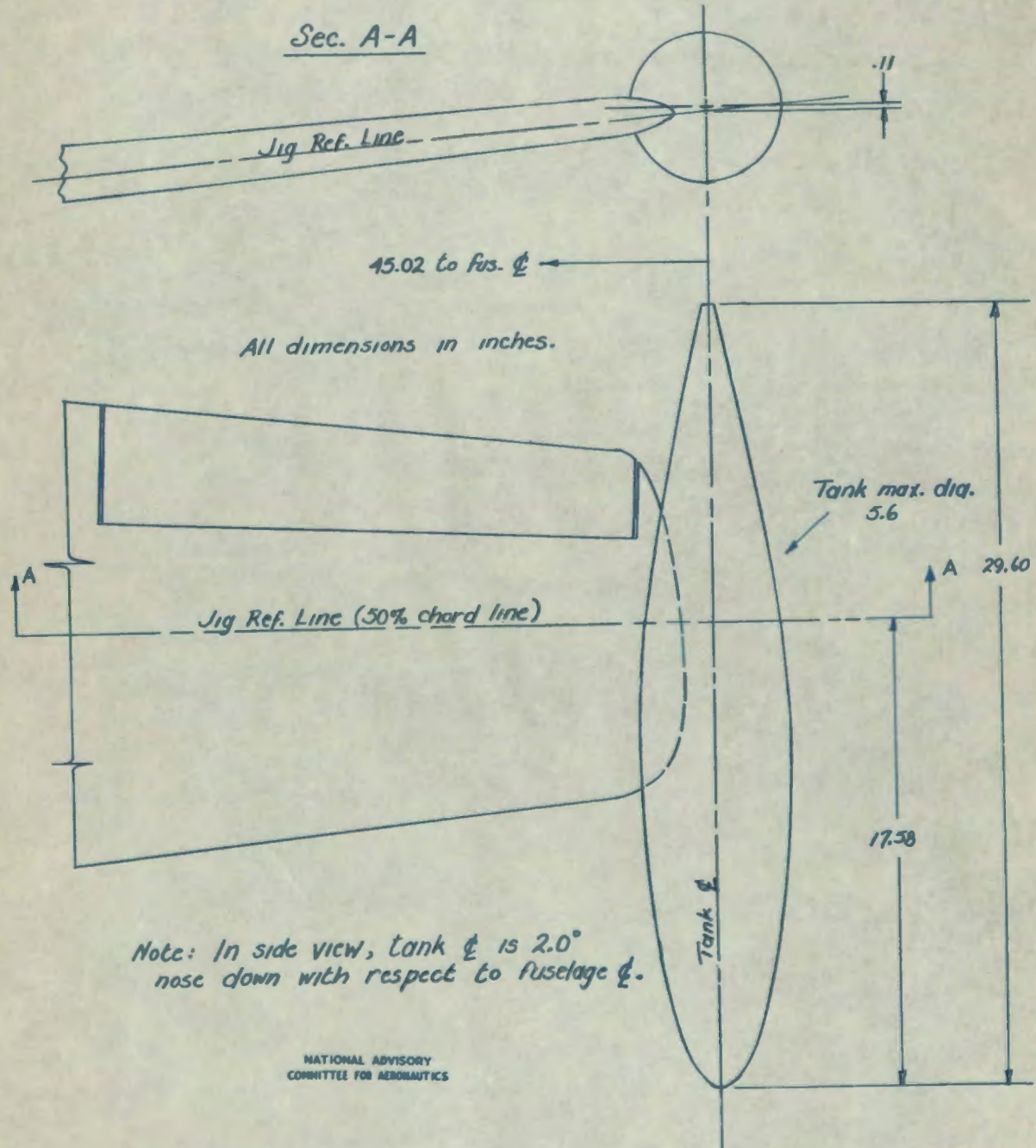


Figure 7.- Wing-tip position of fuel tank tested on the 1/5-scale model of the Republic XP-84 airplane (Army Project MX-578).

1820 6

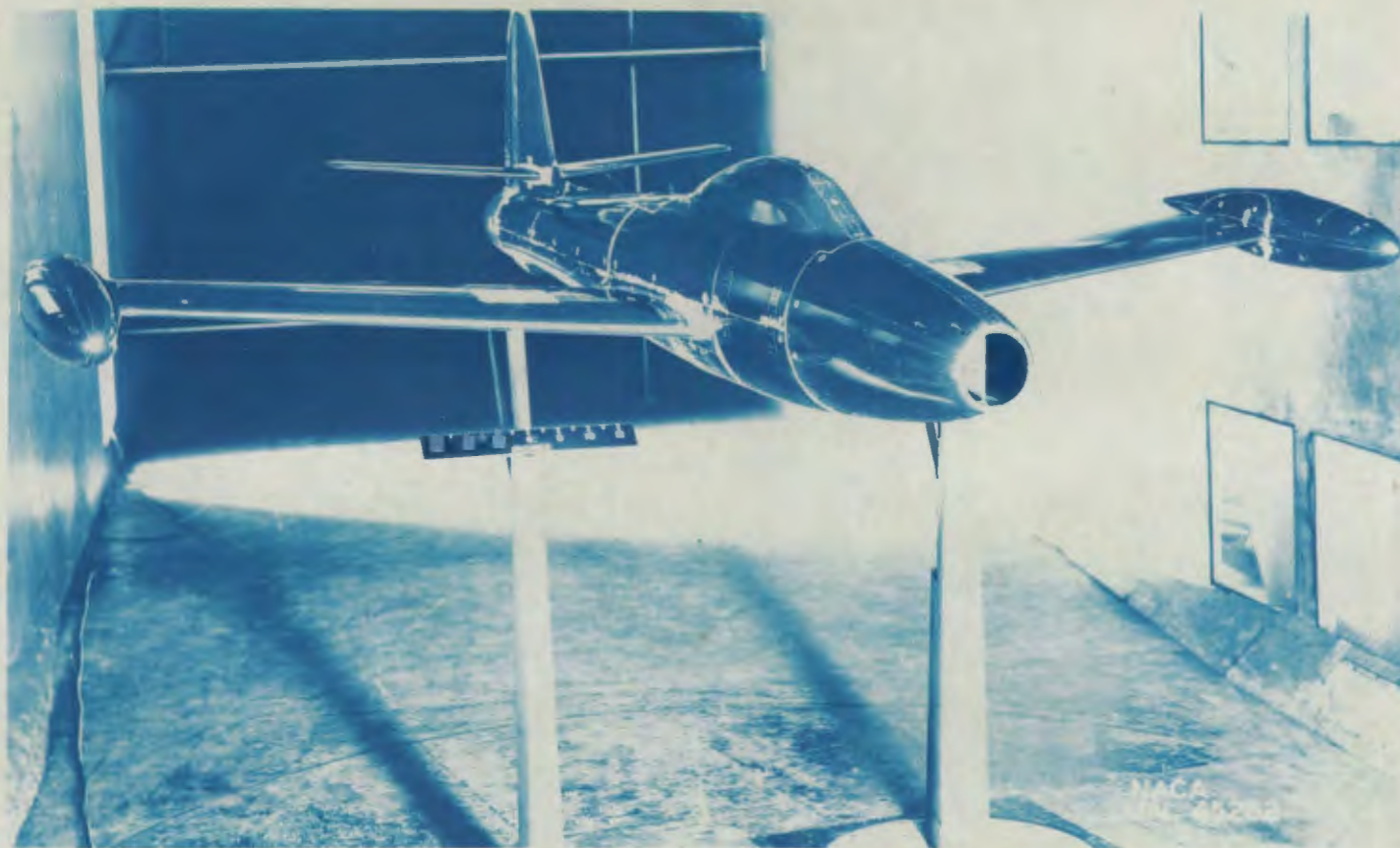


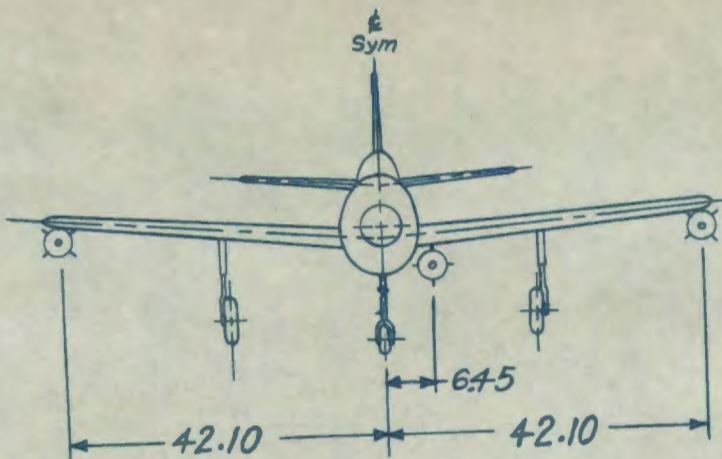
Figure 8.- Fuel tanks mounted at the wing tips of the  $\frac{1}{5}$ -scale model of the  
Republic XP-84 airplane (Army Project MX-578).

NATIONAL ADVISORY COMMITTEE FOR AERONAUTICS  
LANGLEY MEMORIAL AERONAUTICAL LABORATORY - LANGLEY FIELD, VA

MR No. L6F25

1820 9

All dimensions in inches.



Front view, showing spanwise locations of bombs. Note positions of fins.

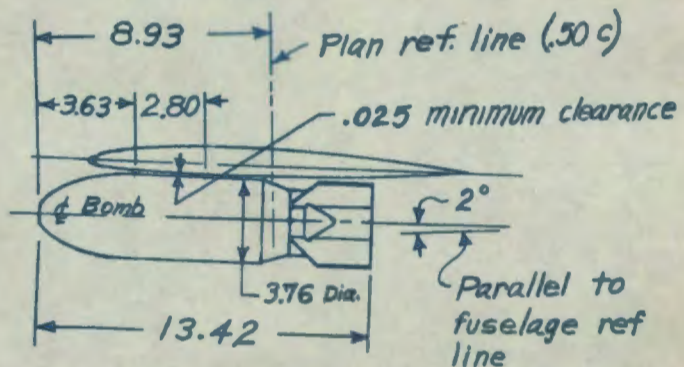
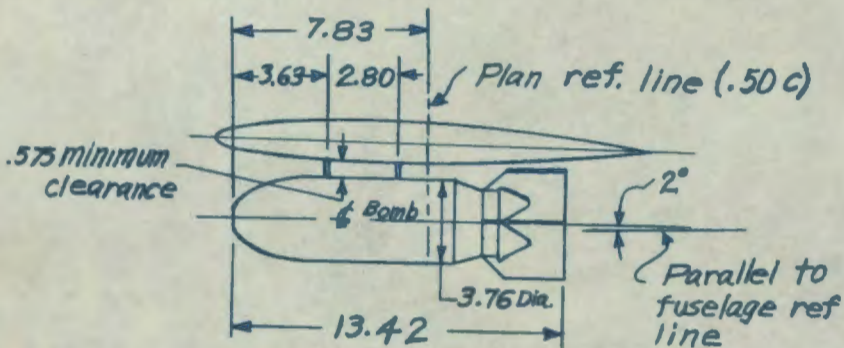


Figure 9.- Positions of bombs tested on the 1/5-scale model of the Republic XP-84 airplane (Army Project MX-578).

NATIONAL ADVISORY  
COMMITTEE FOR AERONAUTICS

MR No. L6F25

MR No. L6F25

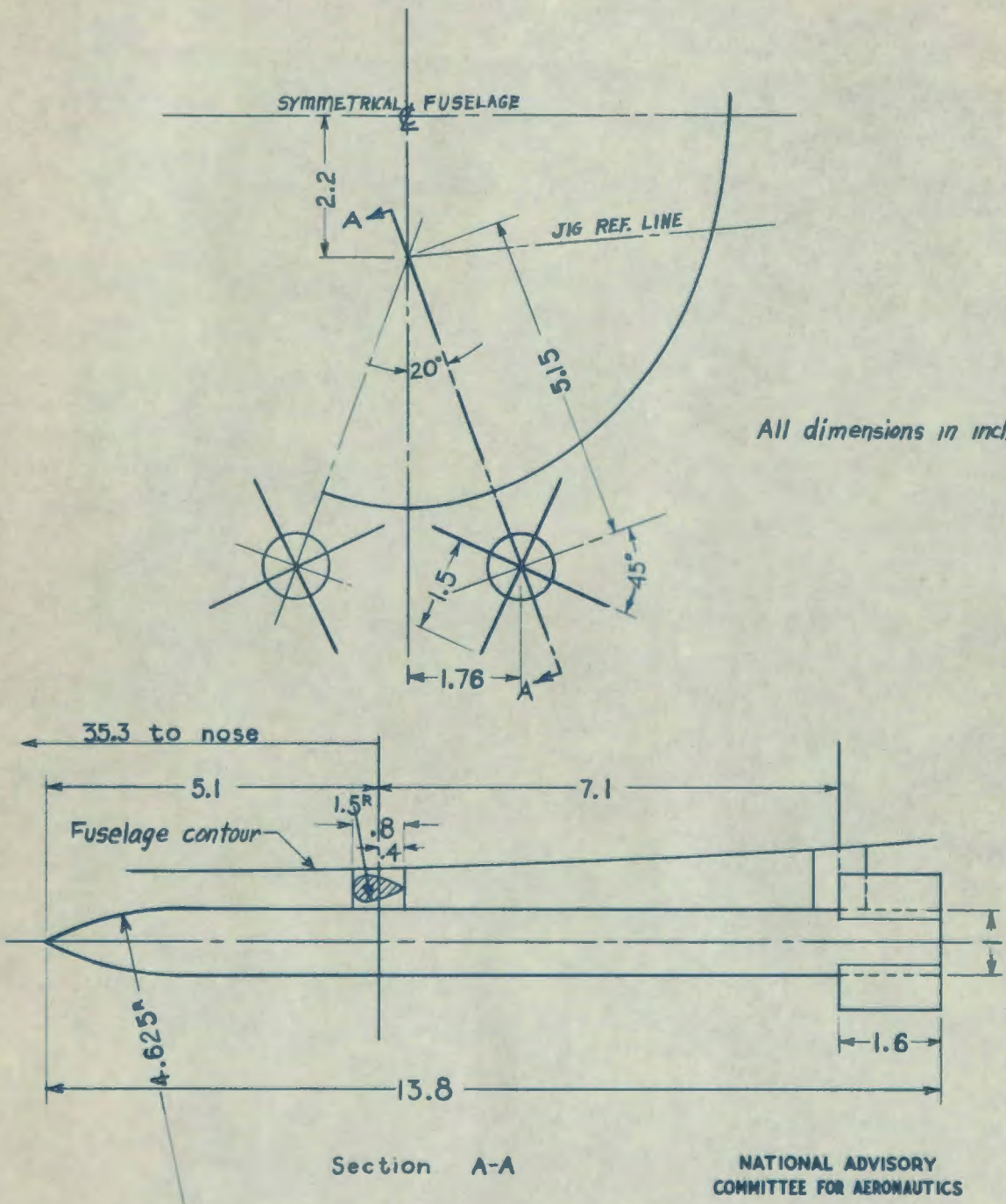


Figure 10.- Details of rockets tested on the 1/5-scale model of the Republic XP-84 airplane (Army Project MX-578).

182011

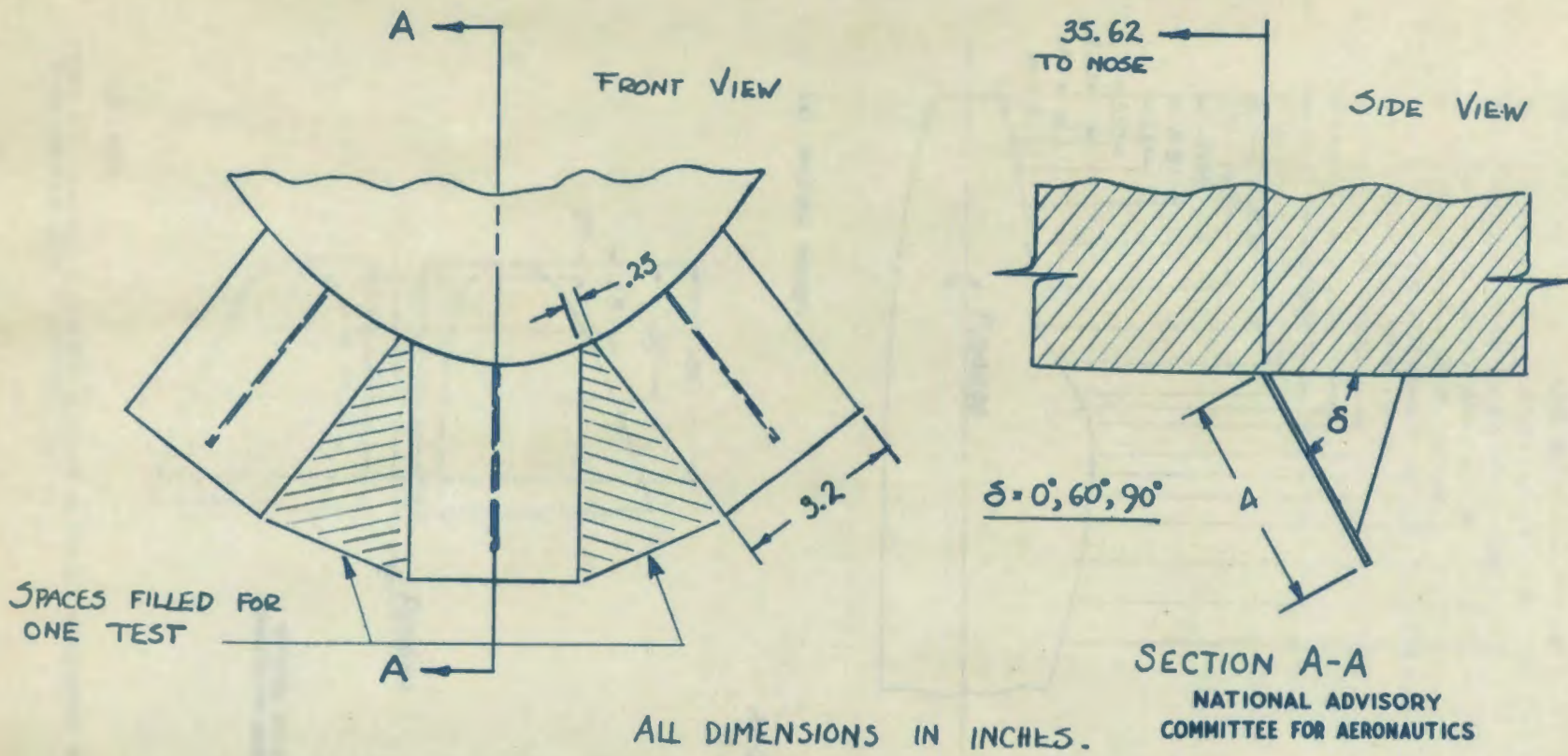


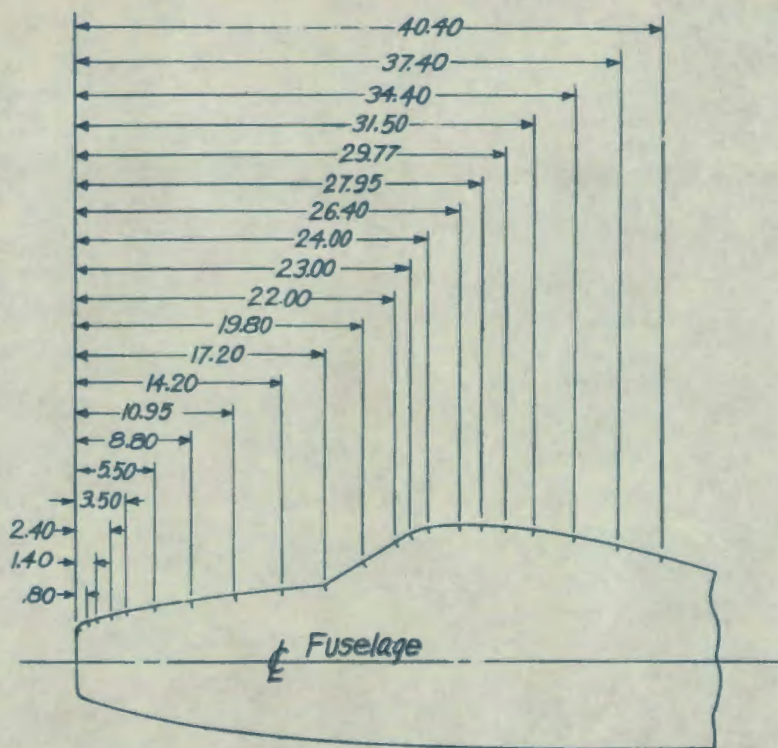
Figure 11.- Fuselage dive brakes tested on the 1/5-scale model of the Republic XP-84 airplane (Army Project MX-578).

NATIONAL ADVISORY  
COMMITTEE FOR AERONAUTICS

MR. NO. L6P25

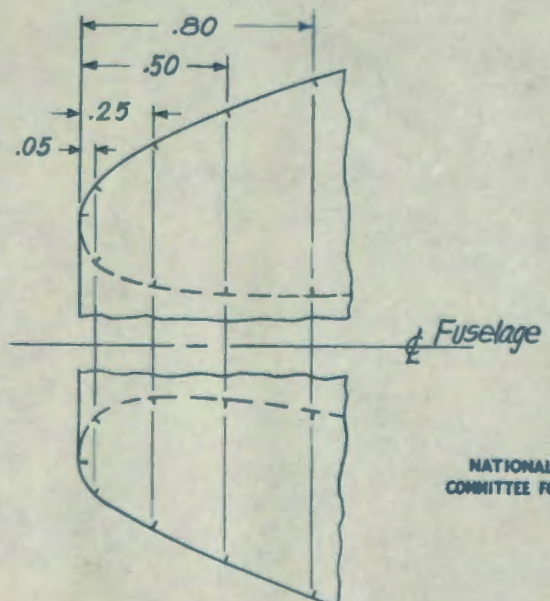
24  
24  
24  
24

MR No. L6F25



(a) Original canopy.

All dimensions  
in inches

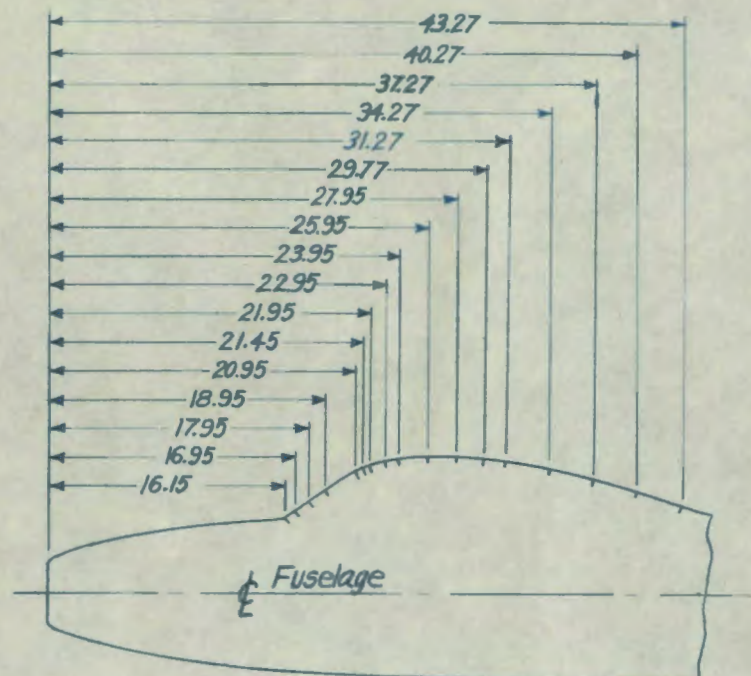


NATIONAL ADVISORY  
COMMITTEE FOR AERONAUTICS

(b) Nose.

Figure 12.- Location of pressure orifices on the 1/5-scale model of the Republic XP-84 airplane (Army Project MX-578).

MR No. L6F25



NATIONAL ADVISORY  
COMMITTEE FOR AERONAUTICS

*All dimensions in inches*

(c) V-front canopy.

Figure 12.- Concluded.

X	Design Nose				Actual Nose			
	$Y_{U_0}$	$Y_{U_L}$	$Y_{L_0}$	$Y_{L_L}$	$Y_{U_0}$	$Y_{U_L}$	$Y_{L_0}$	$Y_{L_L}$
0	2.200	2.200	2.200	2.200	2.20	2.20	2.20	2.20
.40	—	1.980	—	2.020	2.57	1.95	2.56	2.00
.80	2.714	1.945	2.714	2.045	2.74	1.93	2.72	2.02
1.40	2.911	1.900	2.911	2.100	2.95	—	2.93	—
2.40	3.173	—	3.173	—	3.22	—	3.18	—

Note: Difference in ordinates too small to be shown accurately in sketch below.

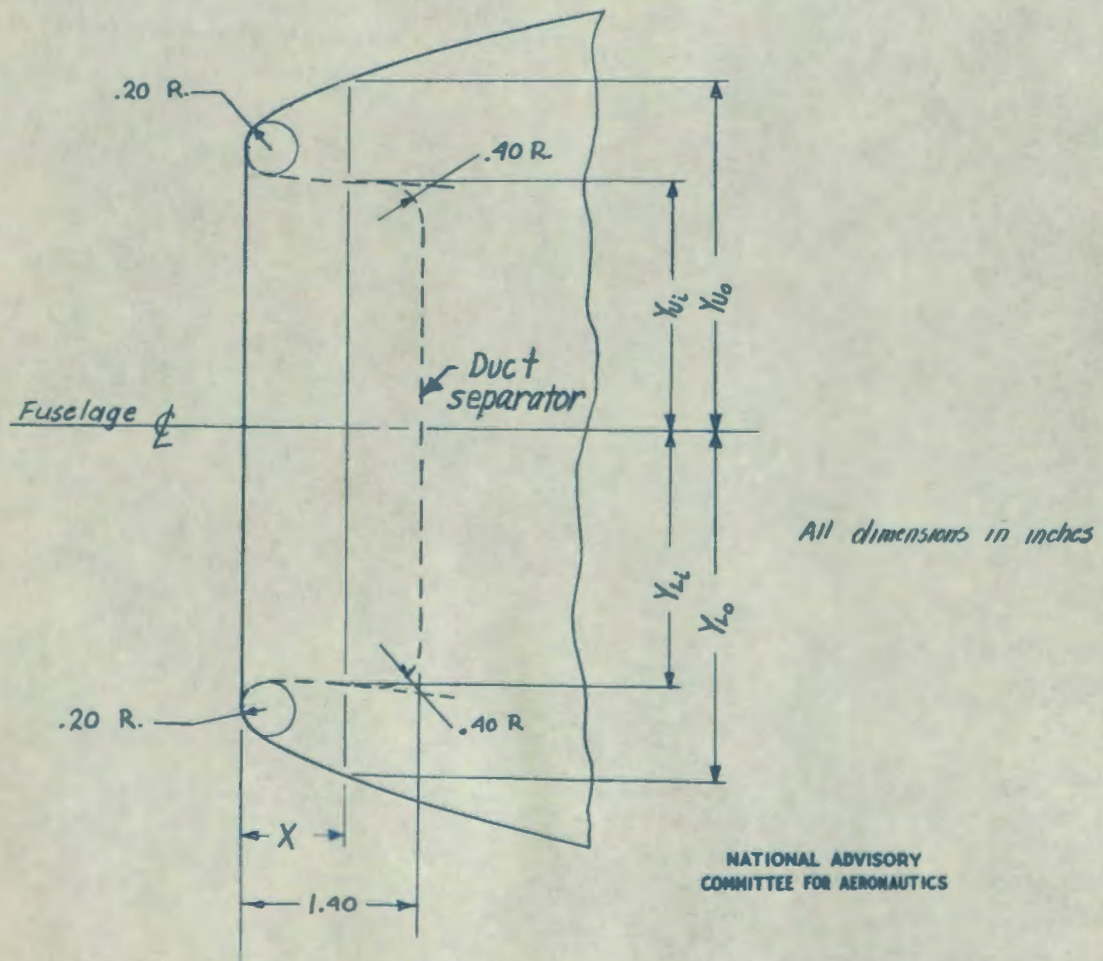
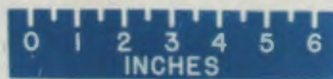


Figure 13.- A comparison of ordinates for the design nose and the actual nose as tested on the 1/5-scale model of the Republic XP-84 airplane (Army Project MX-578).

MR No. L6F25



Front view.



Three-quarters view.



Side view.

Figure 14.- The original canopy tested on the  $\frac{1}{5}$ -scale model of the Republic XP-84 airplane (Army Project MX-578)

MX-578)

CONFIDENTIAL

NATIONAL ADVISORY COMMITTEE FOR AERONAUTICS  
LANGLEY MEMORIAL AERONAUTICAL LABORATORY - LANGLEY FIELD, VA.

10  
74  
2  
04  
80  
77

MR No. L6F25



Front view.



Three-quarters view.



Side view.

Figure 15.- The V-front canopy tested on the  $\frac{1}{5}$ -scale model of the Republic XP-84 airplane (Army Project MX-578).

CONFIDENTIAL

NATIONAL ADVISORY COMMITTEE FOR AERONAUTICS  
LANGLEY MEMORIAL AERONAUTICAL LABORATORY - LANGLEY FIELD, VA.

182014

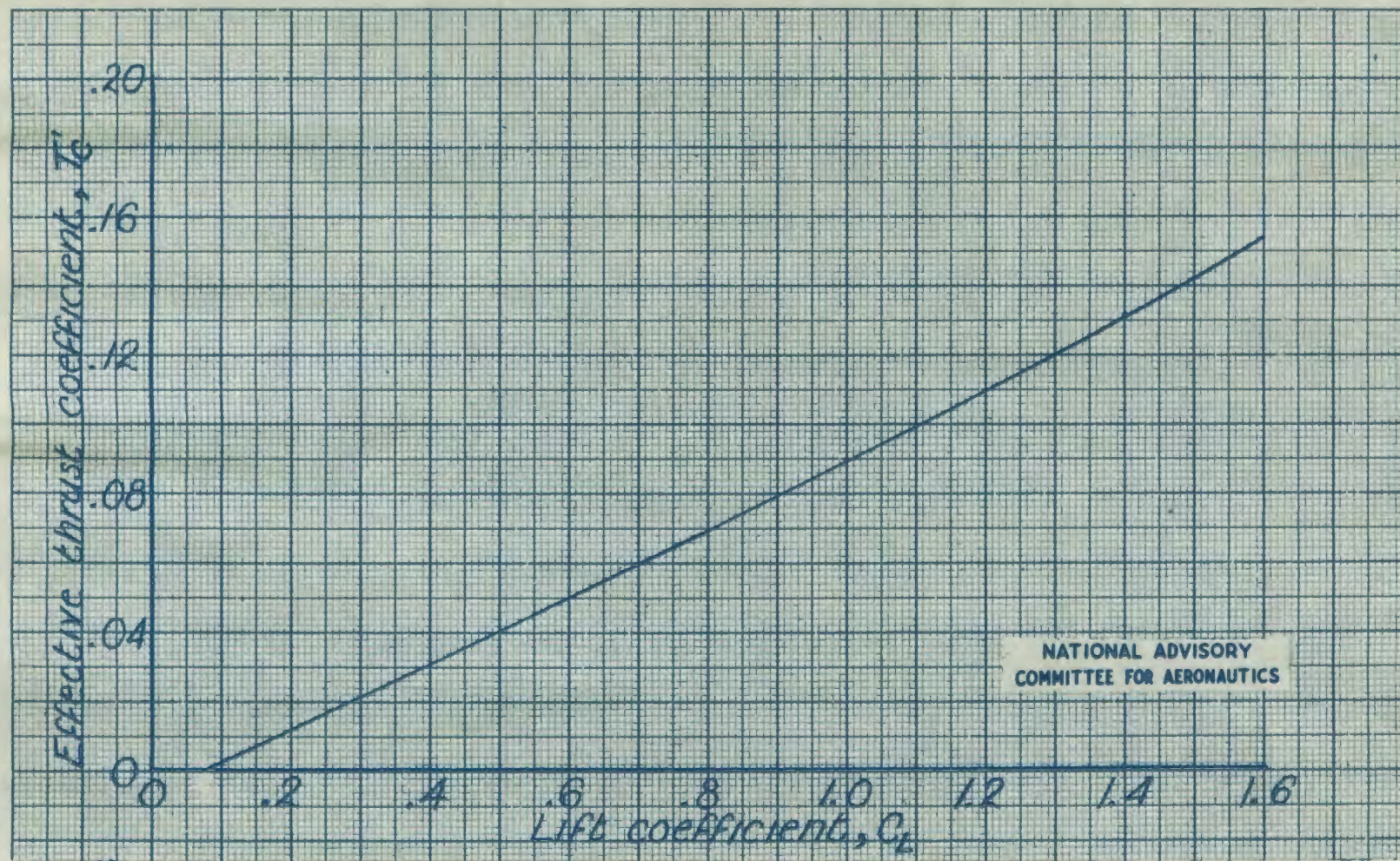


Figure 16.- Variation of effective thrust coefficient with lift coefficient for the Republic XP-84 airplane (Army Project MX-578)  
Idling power (80 percent rpm) at sea level (power condition A);  
gross weight = 12,500 lb.

MR NO L6F25

162017

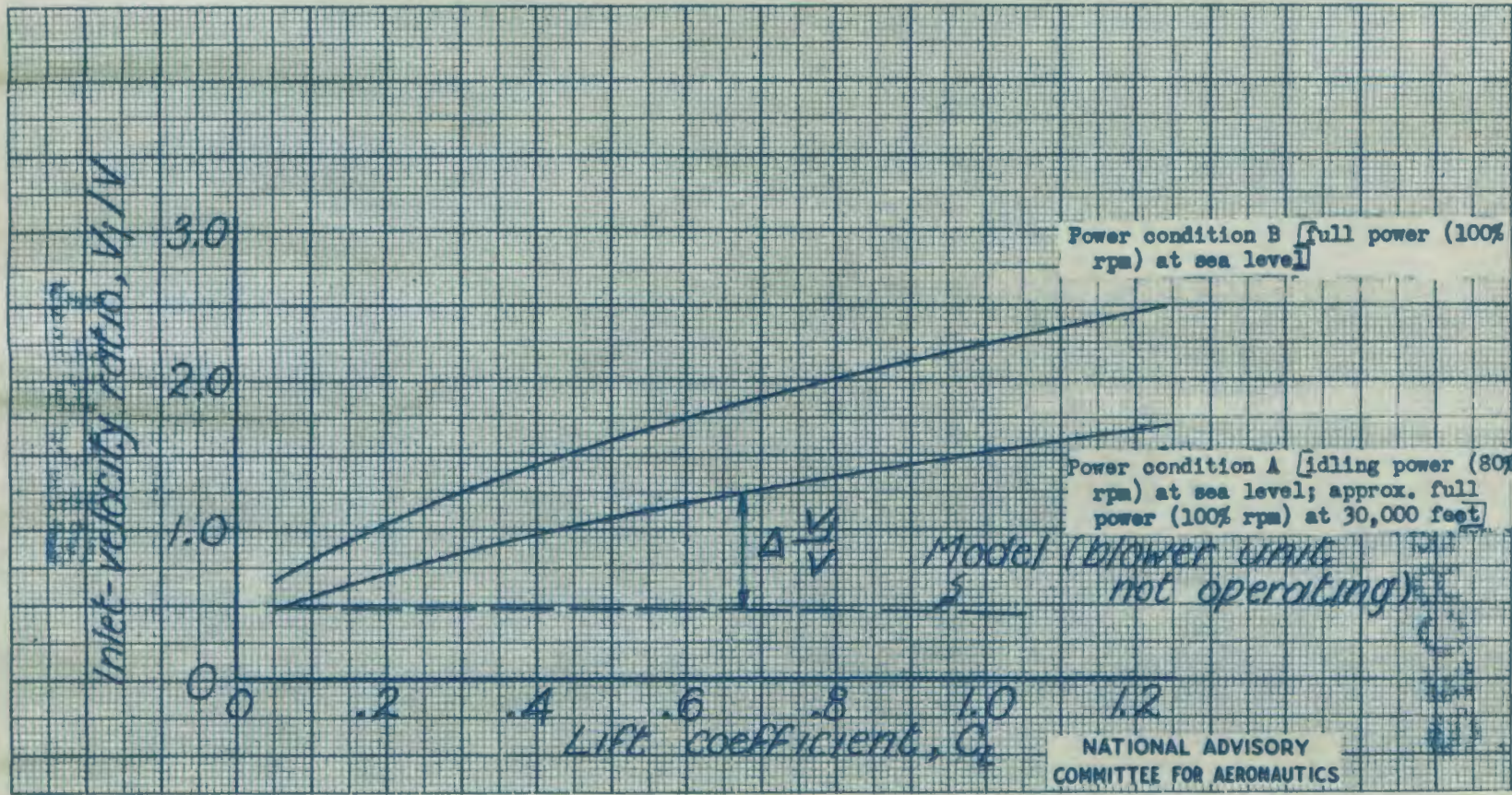


Figure 17.- Variation of inlet-velocity ratio with lift coefficient for the Republic XP-84 airplane (Army Project MX-578). Gross weight = 12,500 lb.

MR No. L6F25

MR No. L6F25

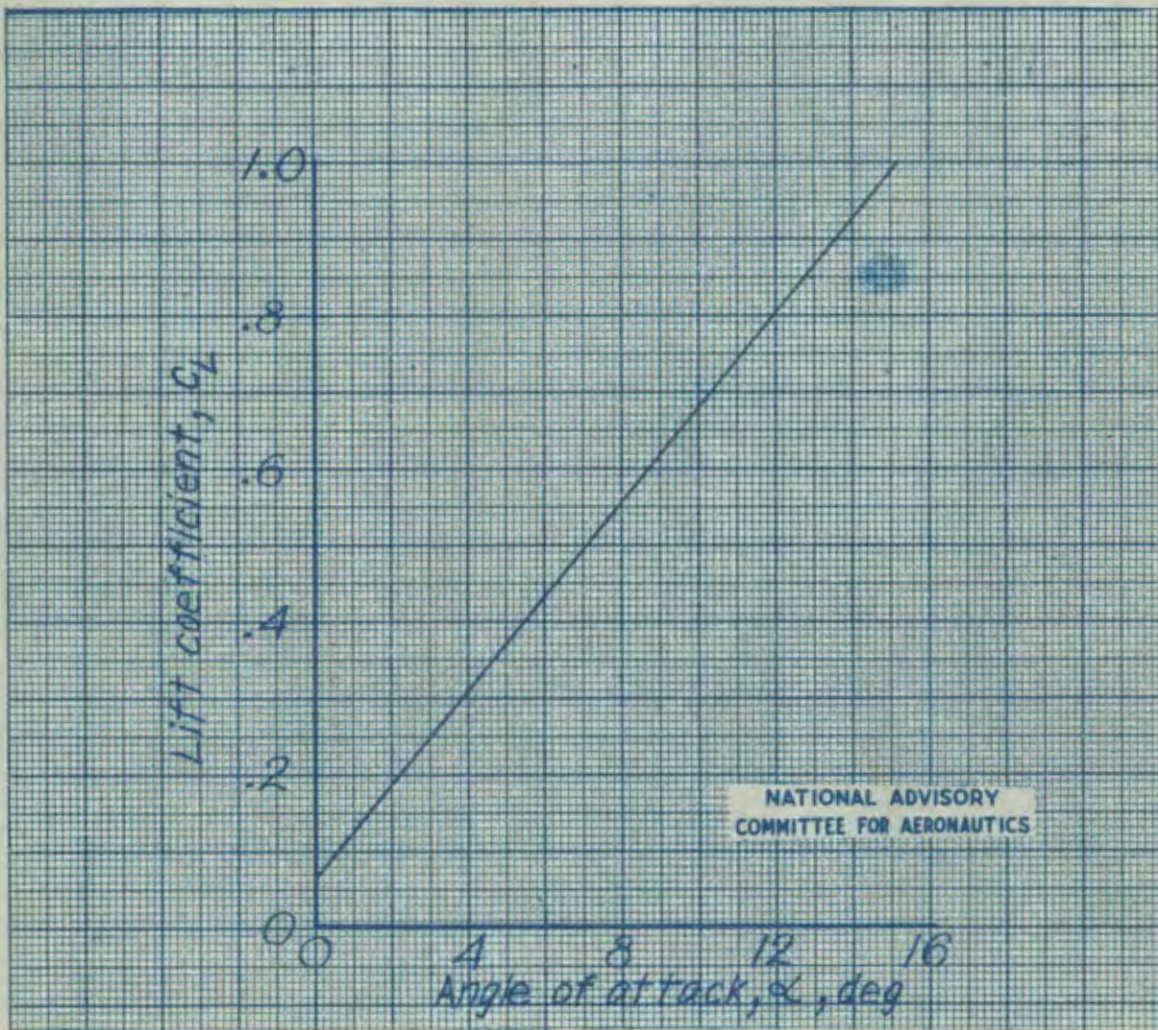
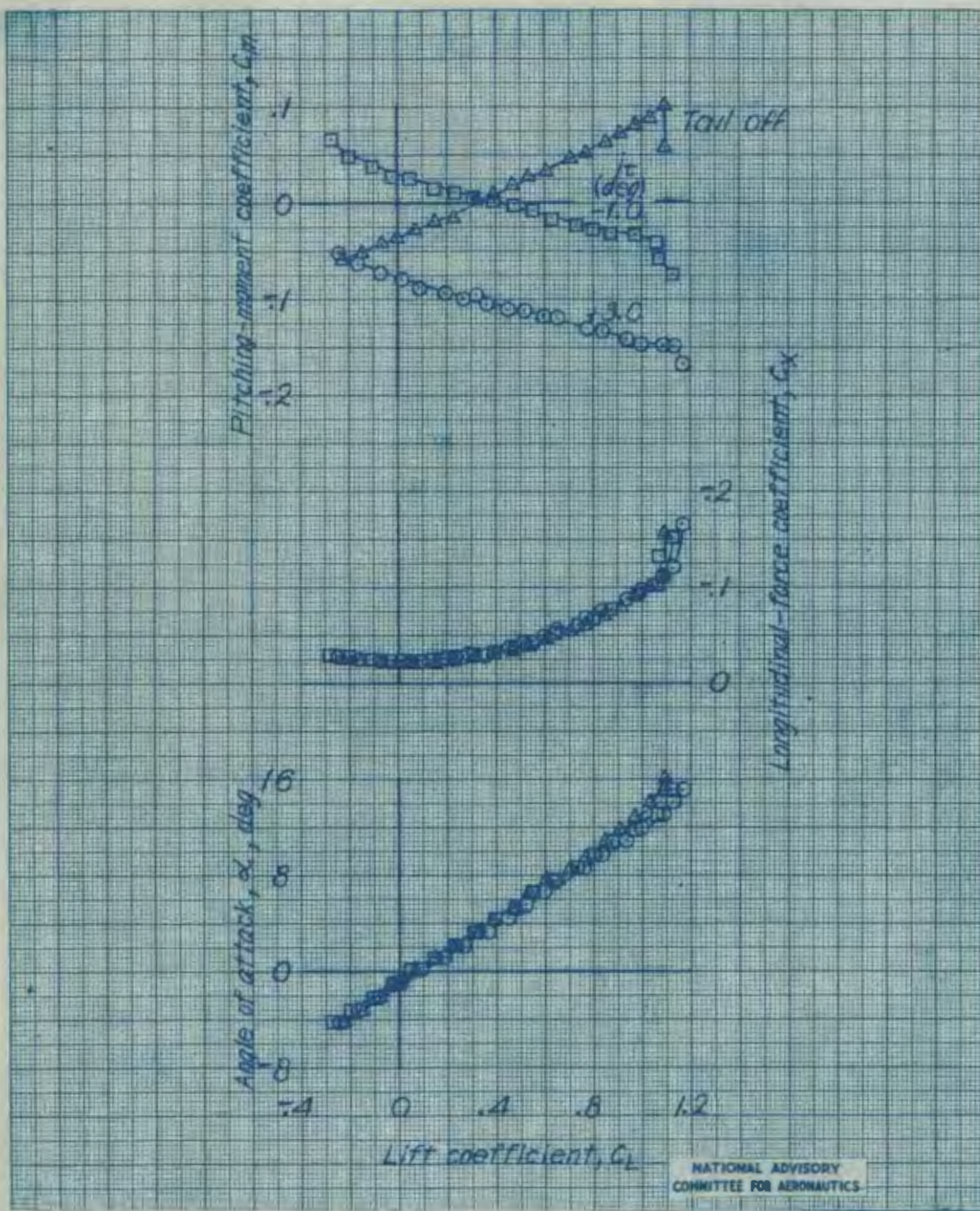


Figure 18.- Variation of trim lift coefficient with angle of attack used making pressure-distribution tests on the 1/5-scale model of the Republic XP-84 airplane (Army Project MX-578). Cruising configuration.

183019

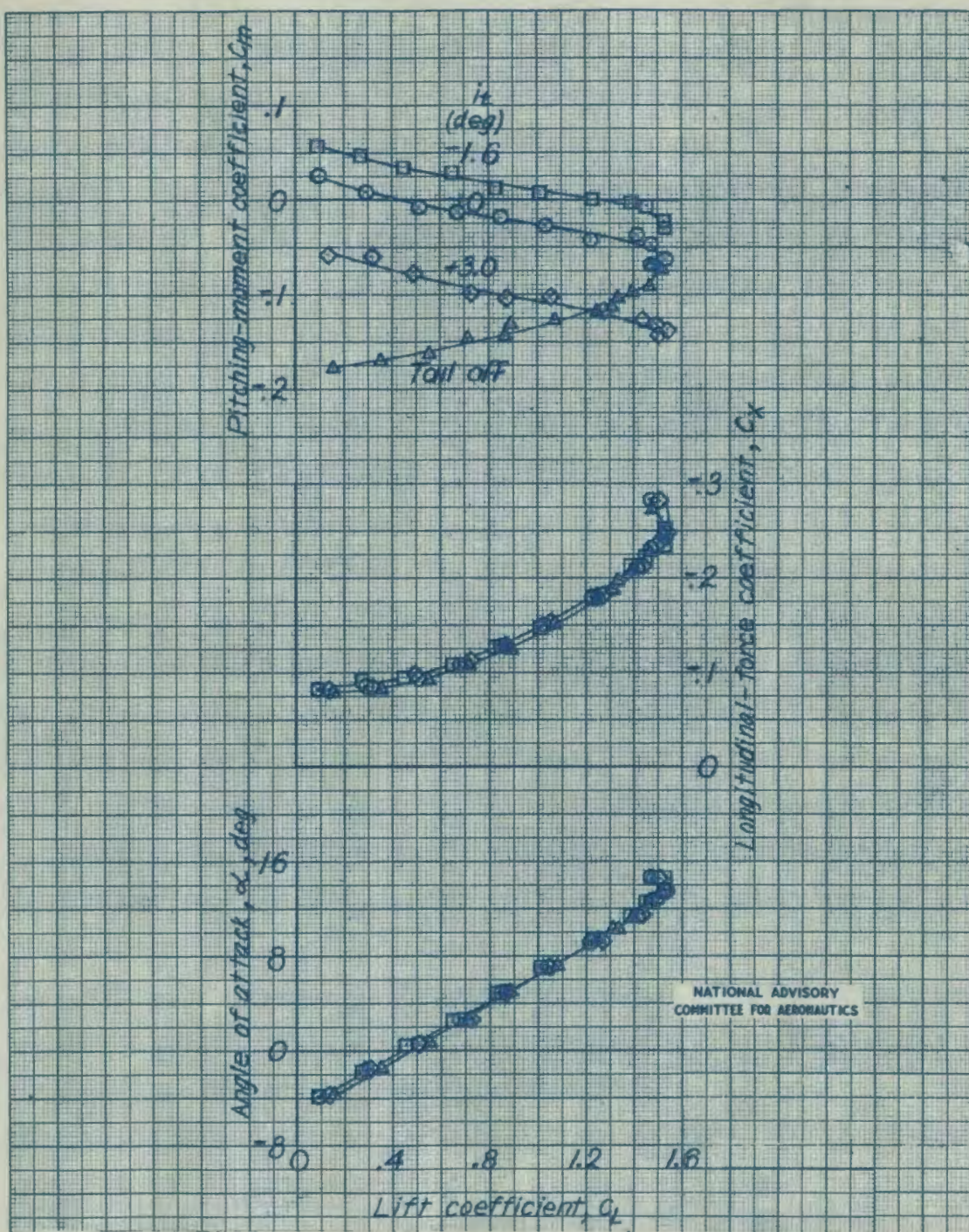
MR No. L6F25



(a) Cruising configuration.

Figure 19.- Effect of stabilizer on the aerodynamic characteristics in pitch of the 1/5-scale model of the Republic XP-84 airplane with original horizontal tail. Idling power.

MR No. L6F25



(b) Landing configuration (slotted flaps deflected  $30^\circ$ ).

Figure 19.- Continued.

1822013

MR No. L6F25

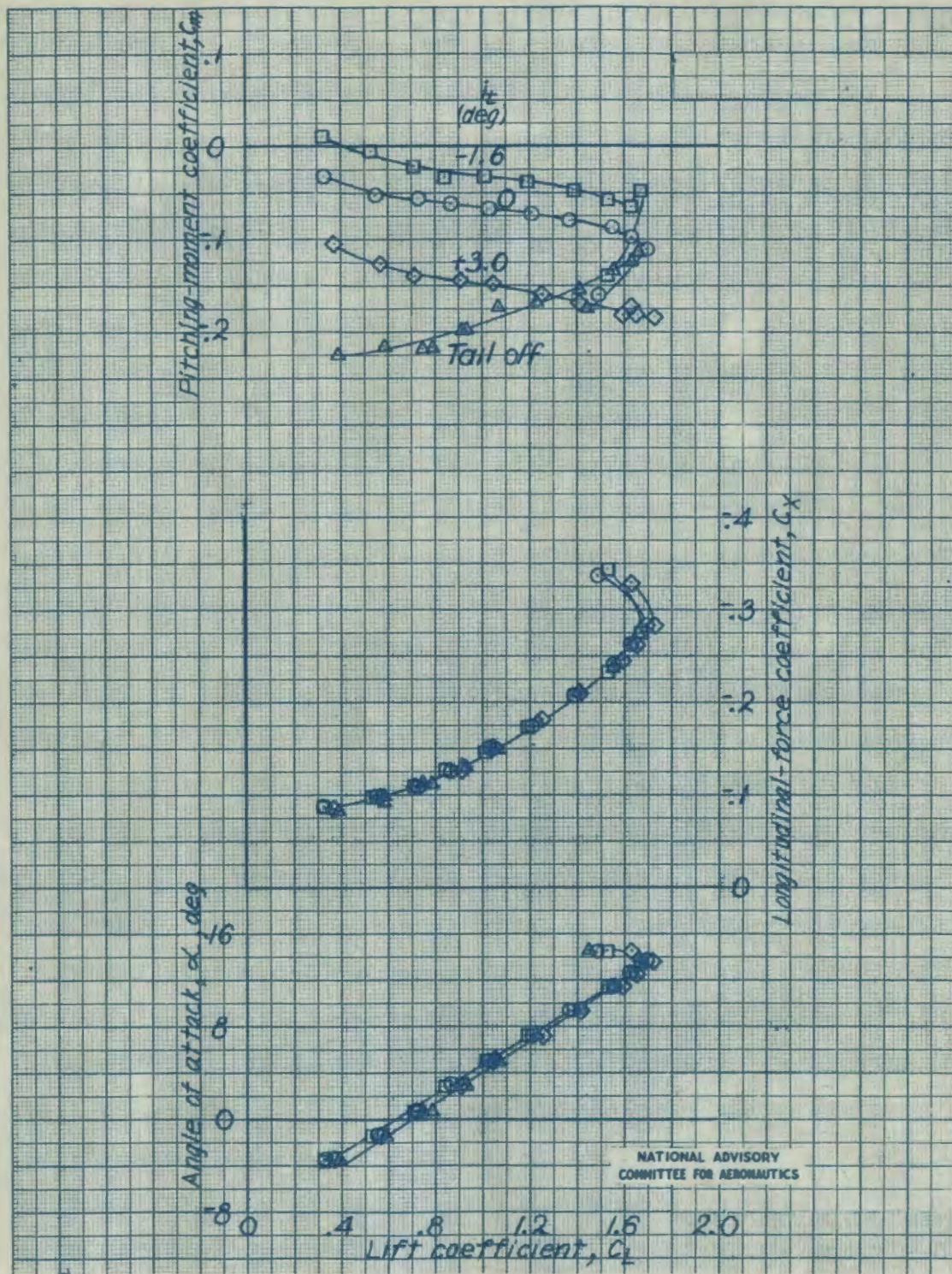
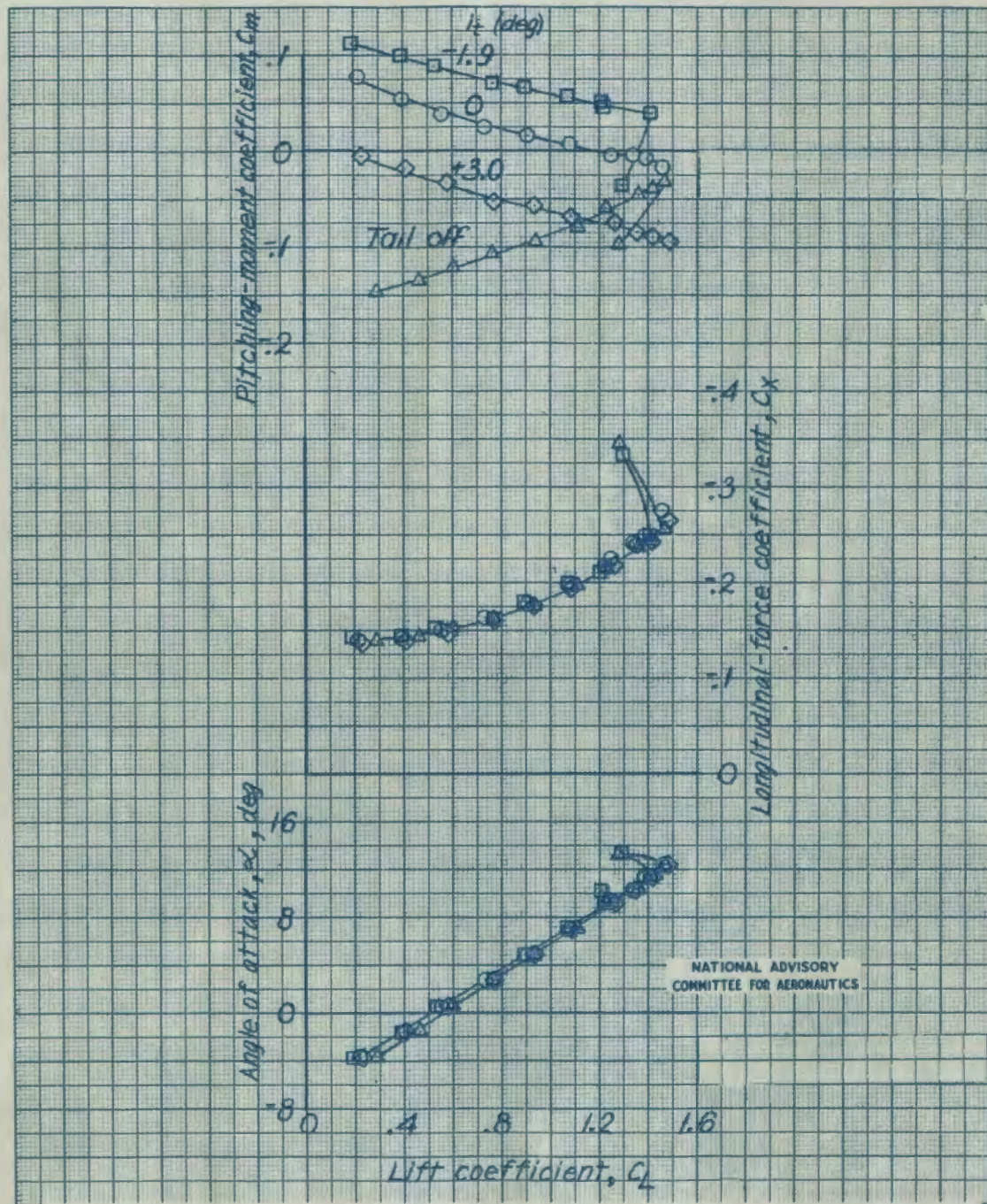


Figure 19.- Continued.

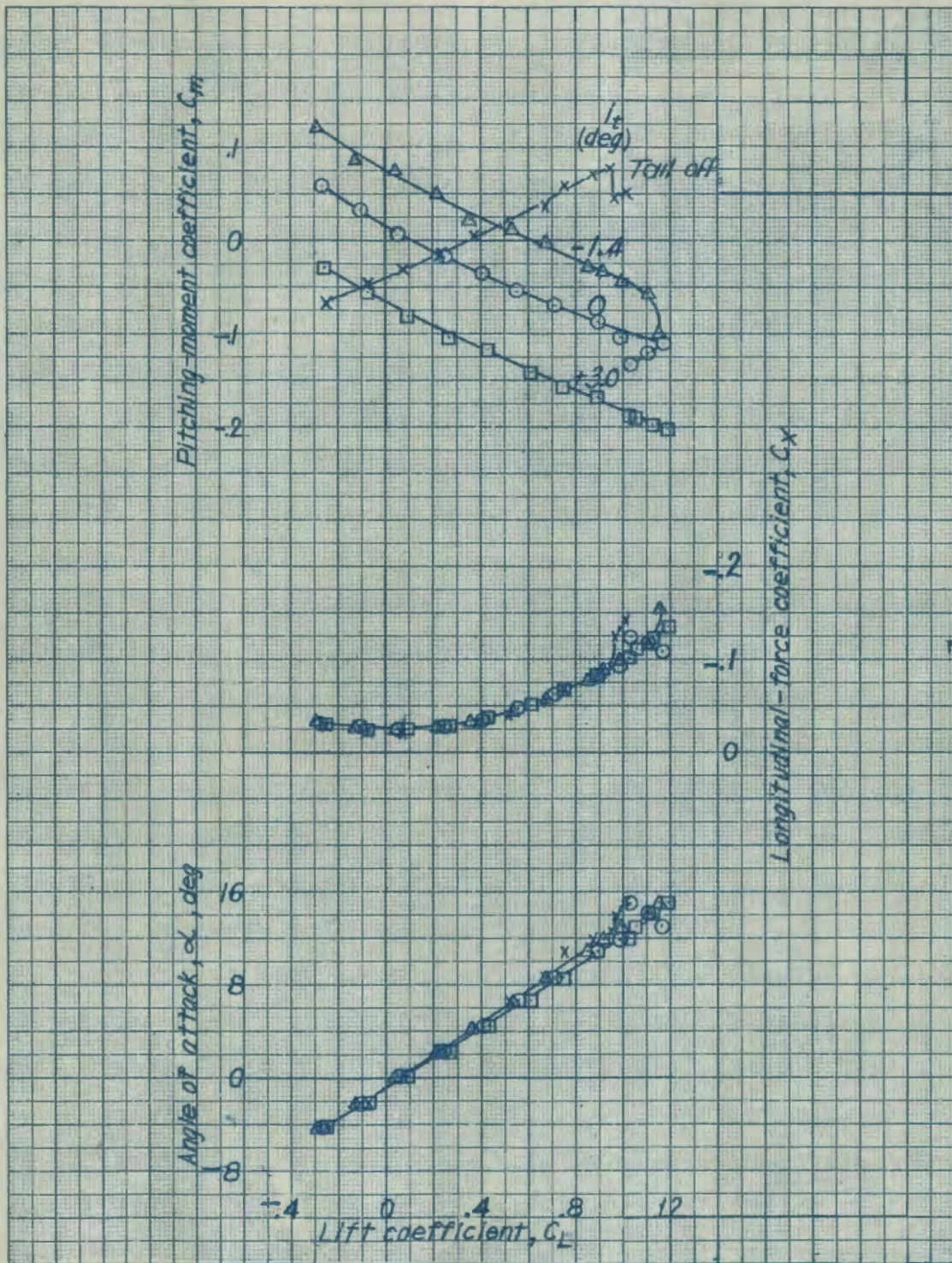
182010

MR No. L6F25



(d) Landing configuration (split flaps deflected 80°).

Figure 19.- Concluded.



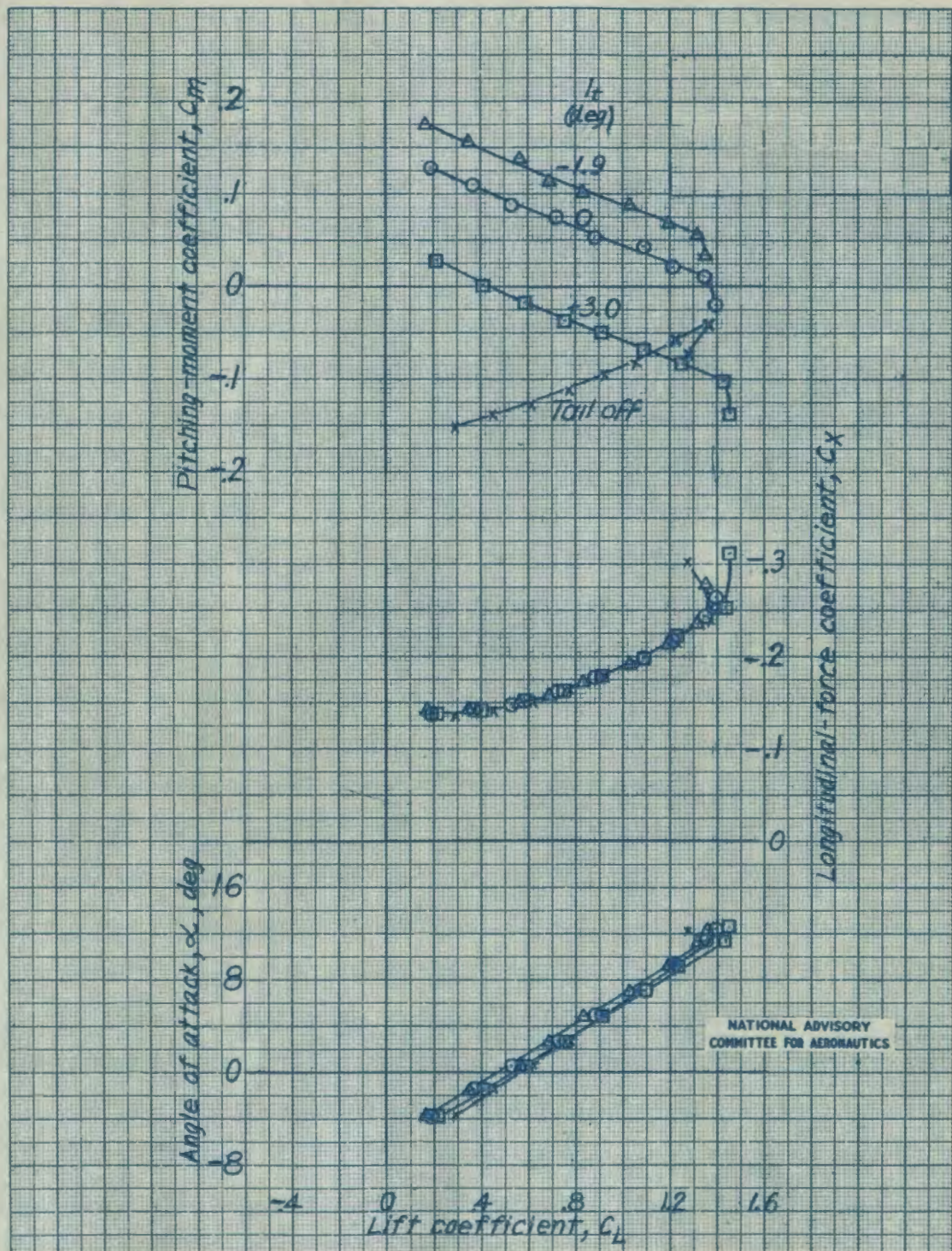
(a) Cruising configuration.

NATIONAL ADVISORY  
COMMITTEE FOR AERONAUTICS.

Figure 20.- Effect of stabilizer on the aerodynamic characteristics in pitch of the 1/5-scale model of the Republic XP-84 airplane with revised horizontal tail. Idling power.

1320320

MR No. L6F25

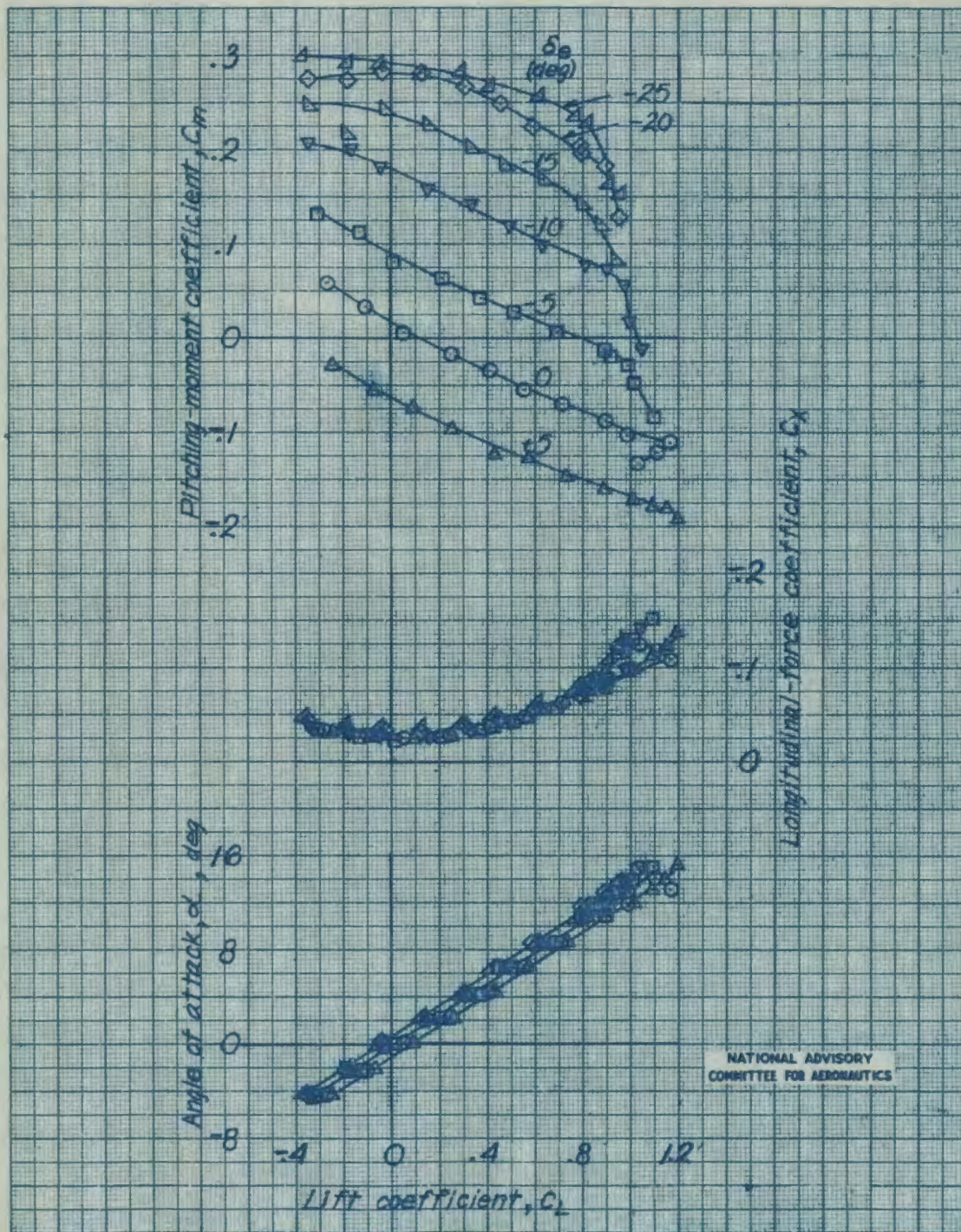


(b) Landing configuration (split flaps deflected 60°).

Figure 20.- Concluded.

102031

MR No. L6P25

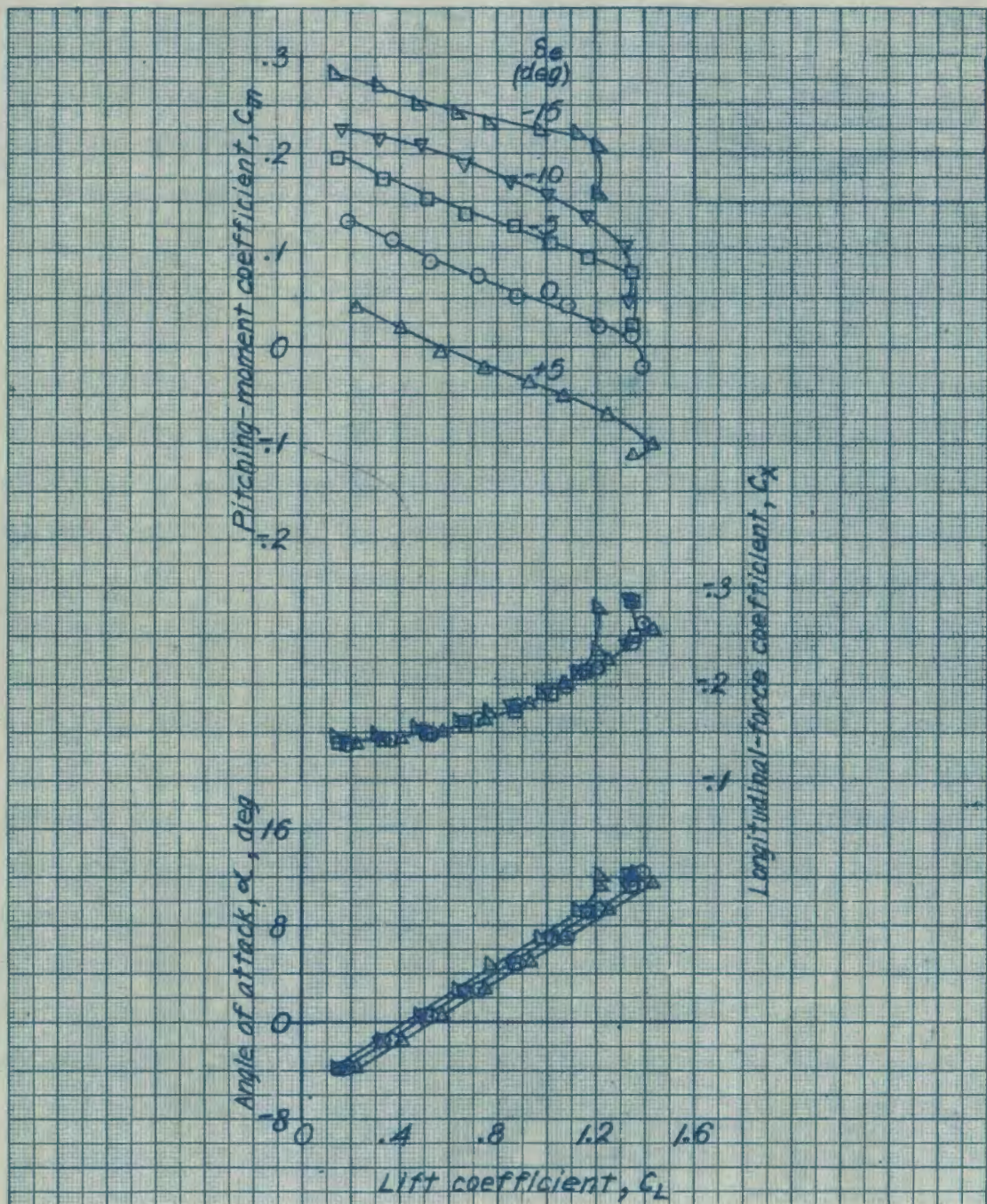


(a) Cruising configuration.

Figure 21.- Effect of elevator deflection on the aerodynamic characteristics in pitch of the 1/5-scale model of the Republic XP-84 airplane with revised horizontal tail. Idling power;  $\alpha_t = 0^\circ$ .

13202

MR No. L6F25



(b) Landing configuration (split flaps deflected 60°).

Figure 21.- Concluded.

NATIONAL ADVISORY  
COMMITTEE FOR AERONAUTICS

182022

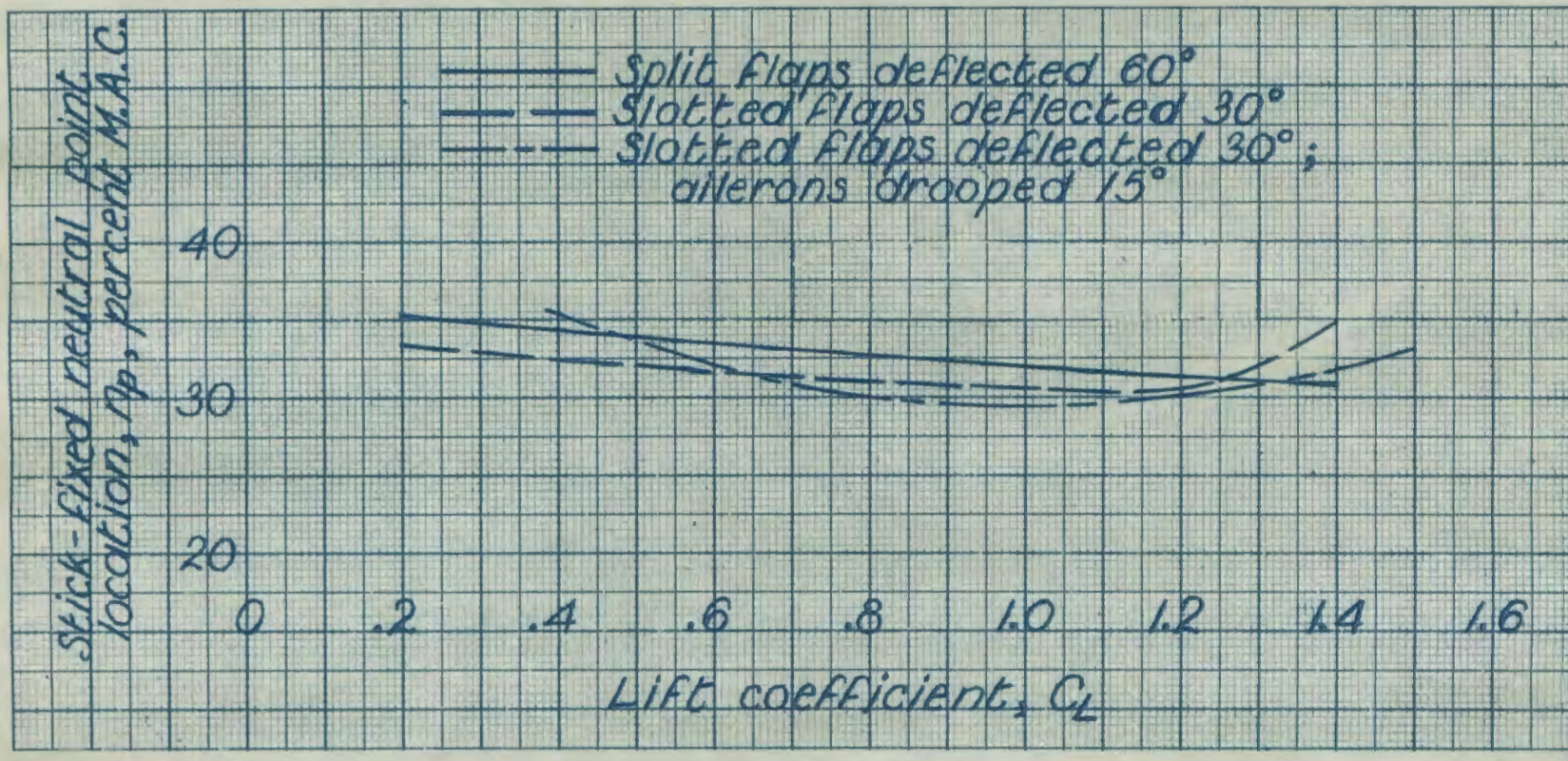


Figure 22.- Stick-fixed neutral points of the Republic XP-84 airplane with original horizontal tail, as determined from tests of the 1/5-scale model. Idling power, landing configuration.

MR No. L6F25

NATIONAL ADVISORY  
COMMITTEE FOR AERONAUTICS.

182023

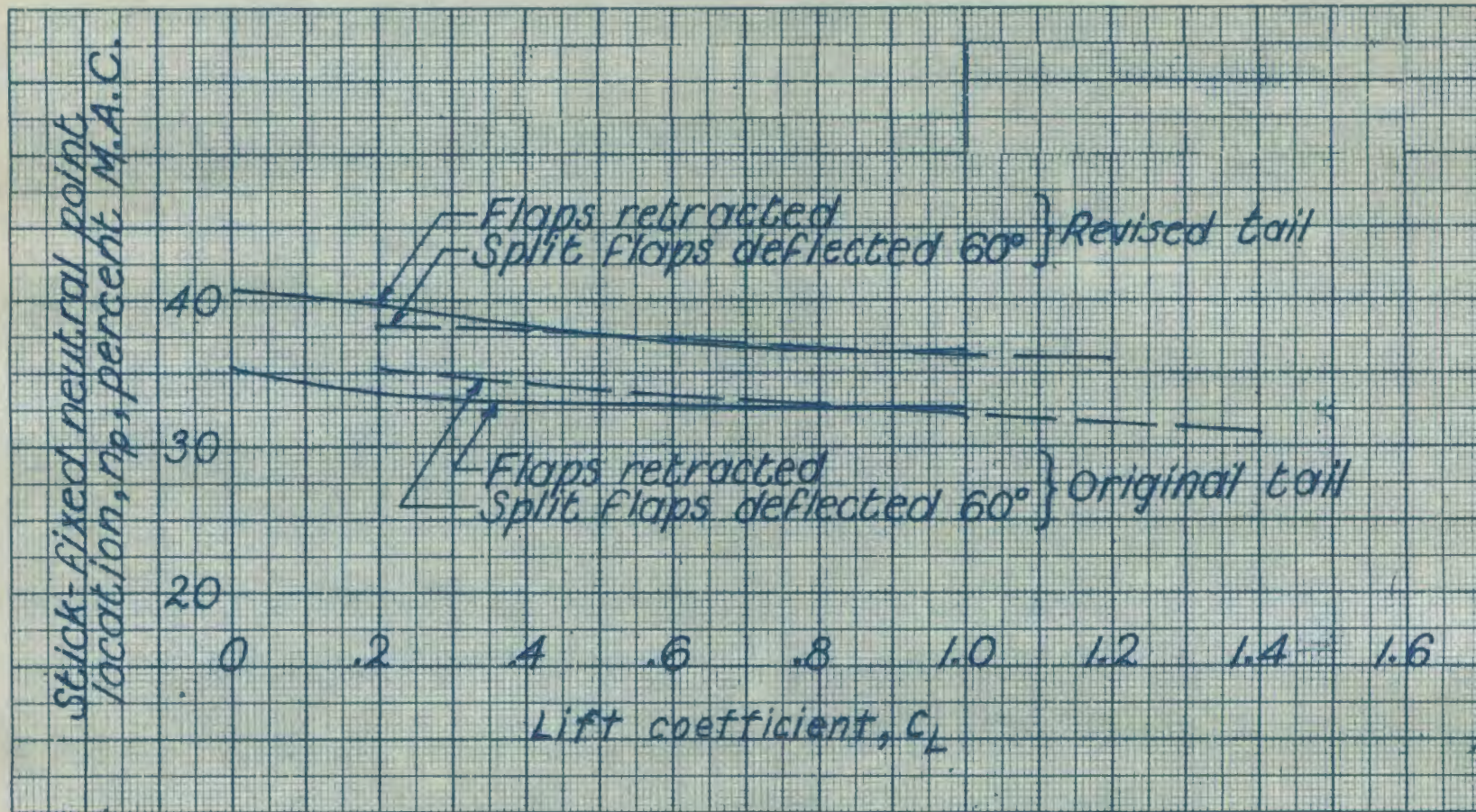


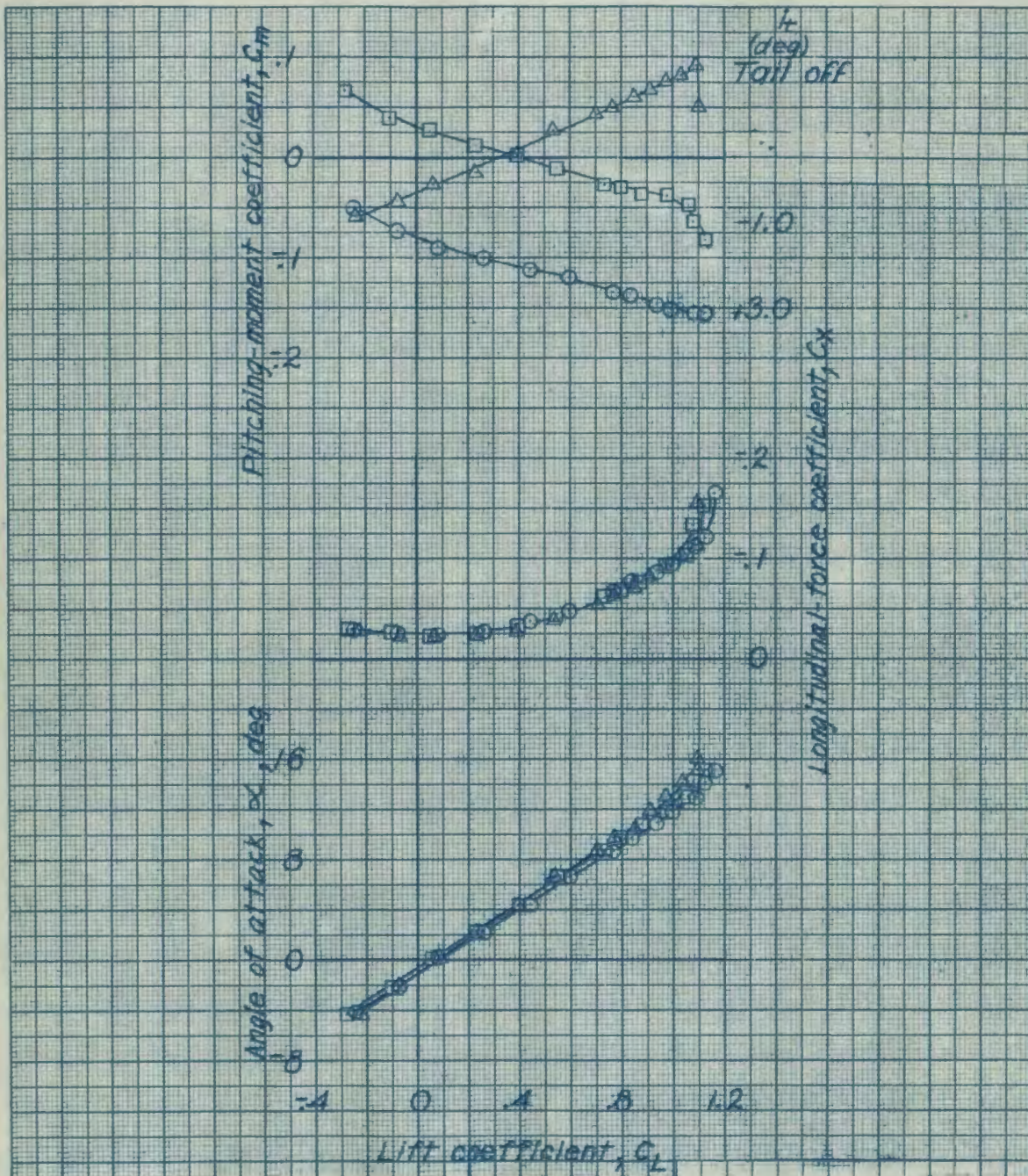
Figure 23.- Effect of revised horizontal tail on the stick-fixed neutral points of the Republic XP-84 airplane, as determined from tests of the 1/5-scale model. Idling power.

NATIONAL ADVISORY  
COMMITTEE FOR AERONAUTICS

MR No. L6F25

132024

MR No. L6F25

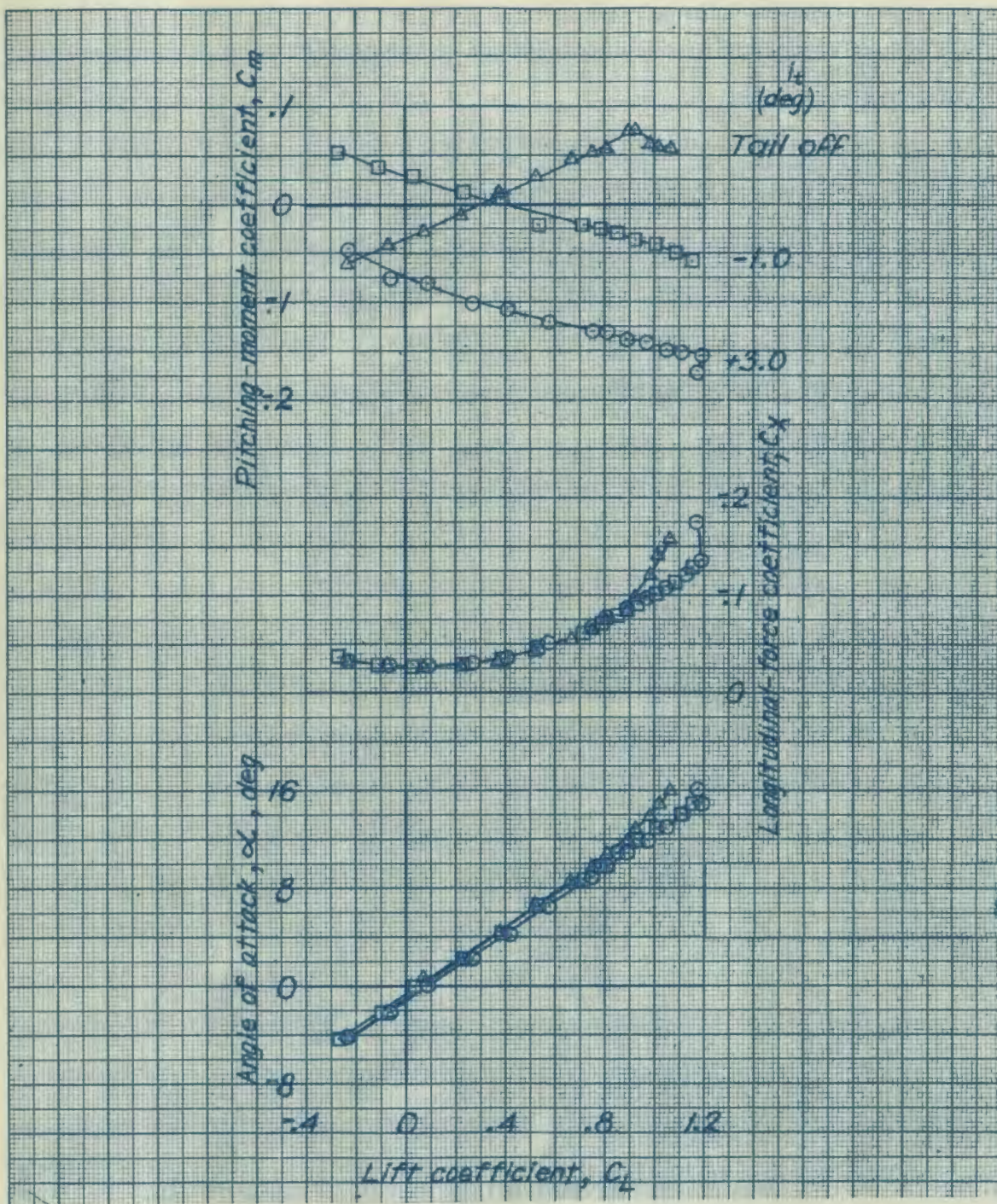


(a) Tanks off; bombs off.

Figure 24.- Effect of external fuel tanks and bombs on the aerodynamic characteristics in pitch of the 1/5-scale model of the Republic XP-84 airplane with original horizontal tail. Power off; cruising configuration.

130024

MR No. L6F25



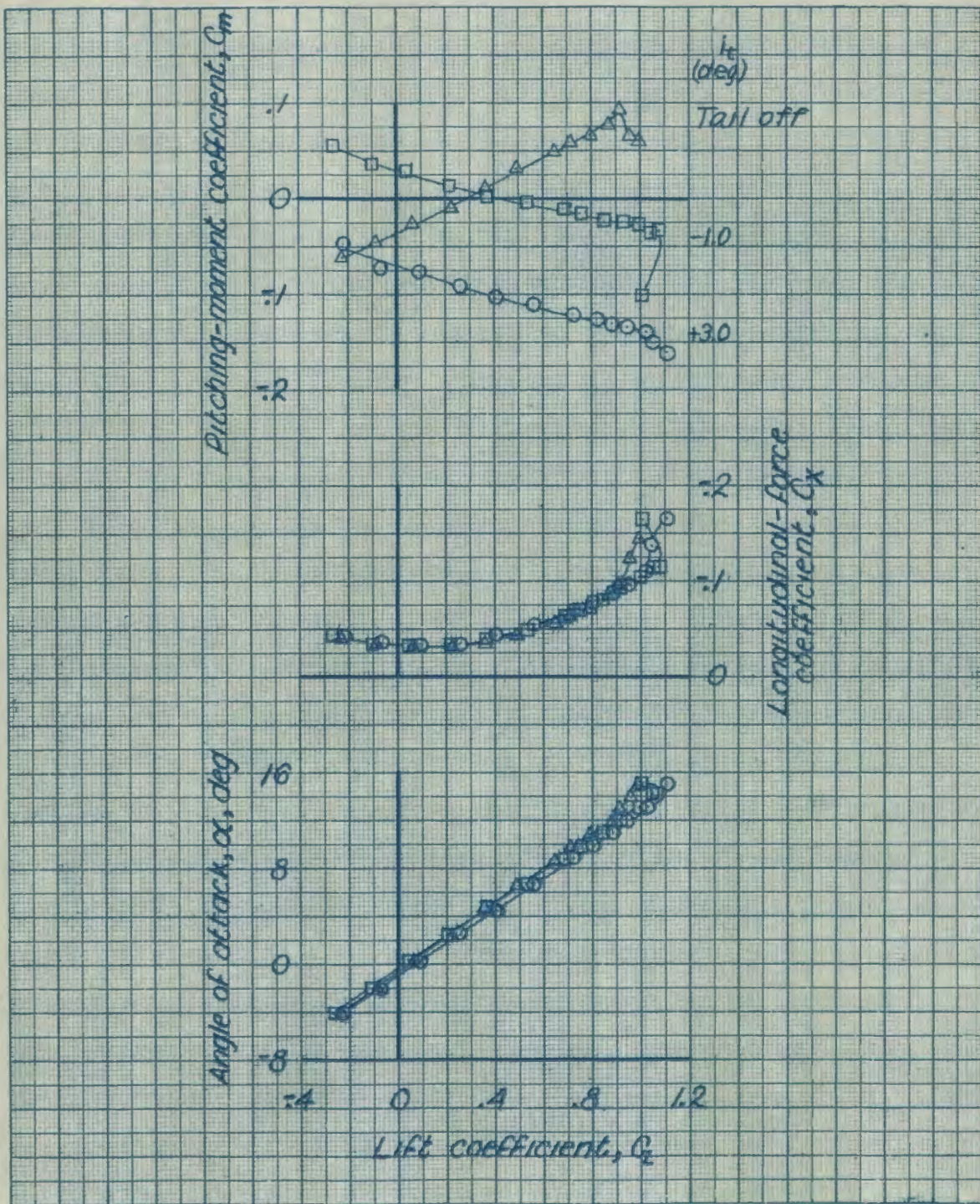
(b) Right tank in inboard position; left tank off; bombs off.

Figure 24.- Continued.

NATIONAL ADVISORY  
COMMITTEE FOR AERONAUTICS

132024

MR No. L6F25



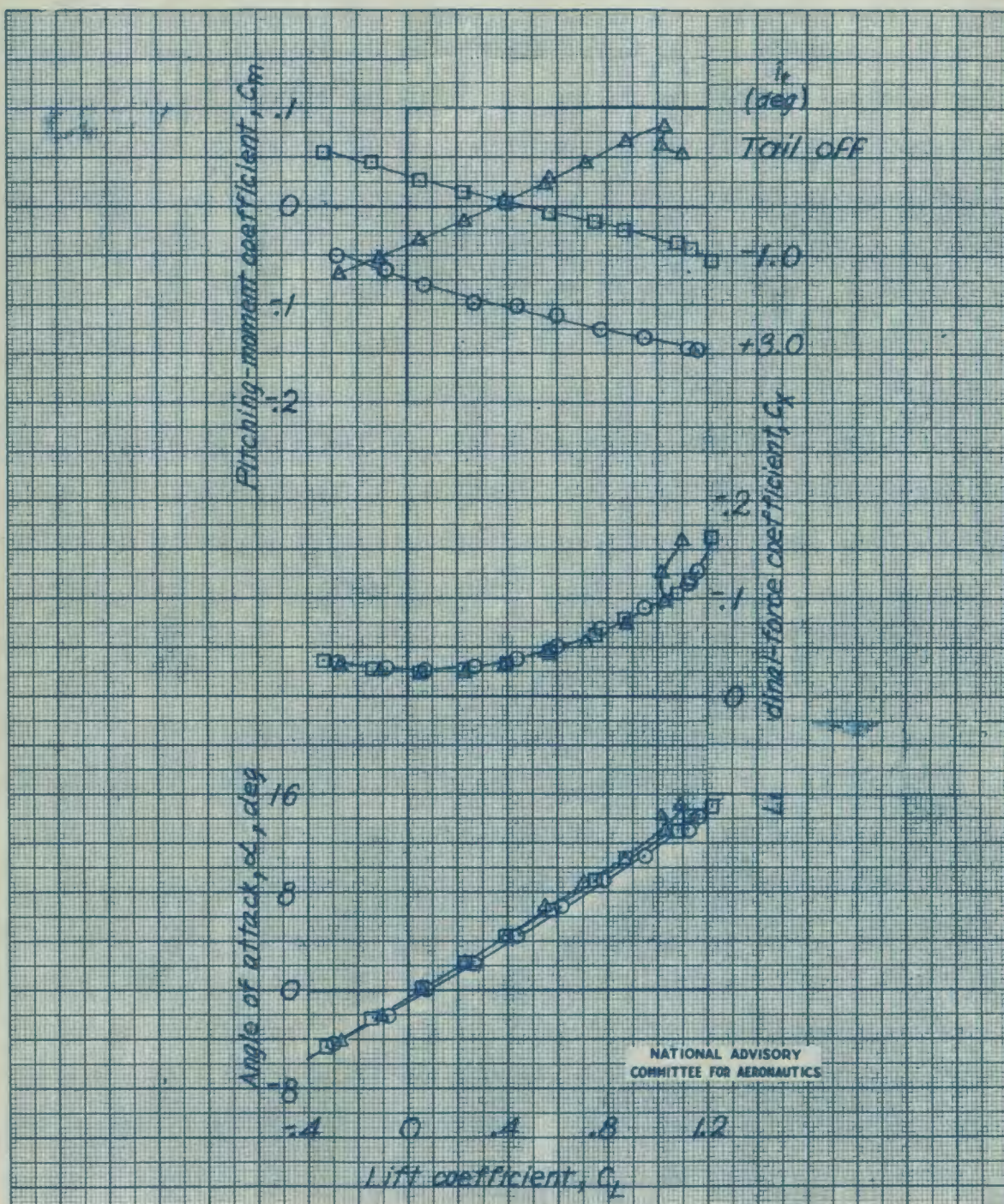
(c) Both tanks in inboard position; bombs off.

Figure 24.- Continued.

NATIONAL ADVISORY  
COMMITTEE FOR AERONAUTICS.

132024

MR No. L6F25

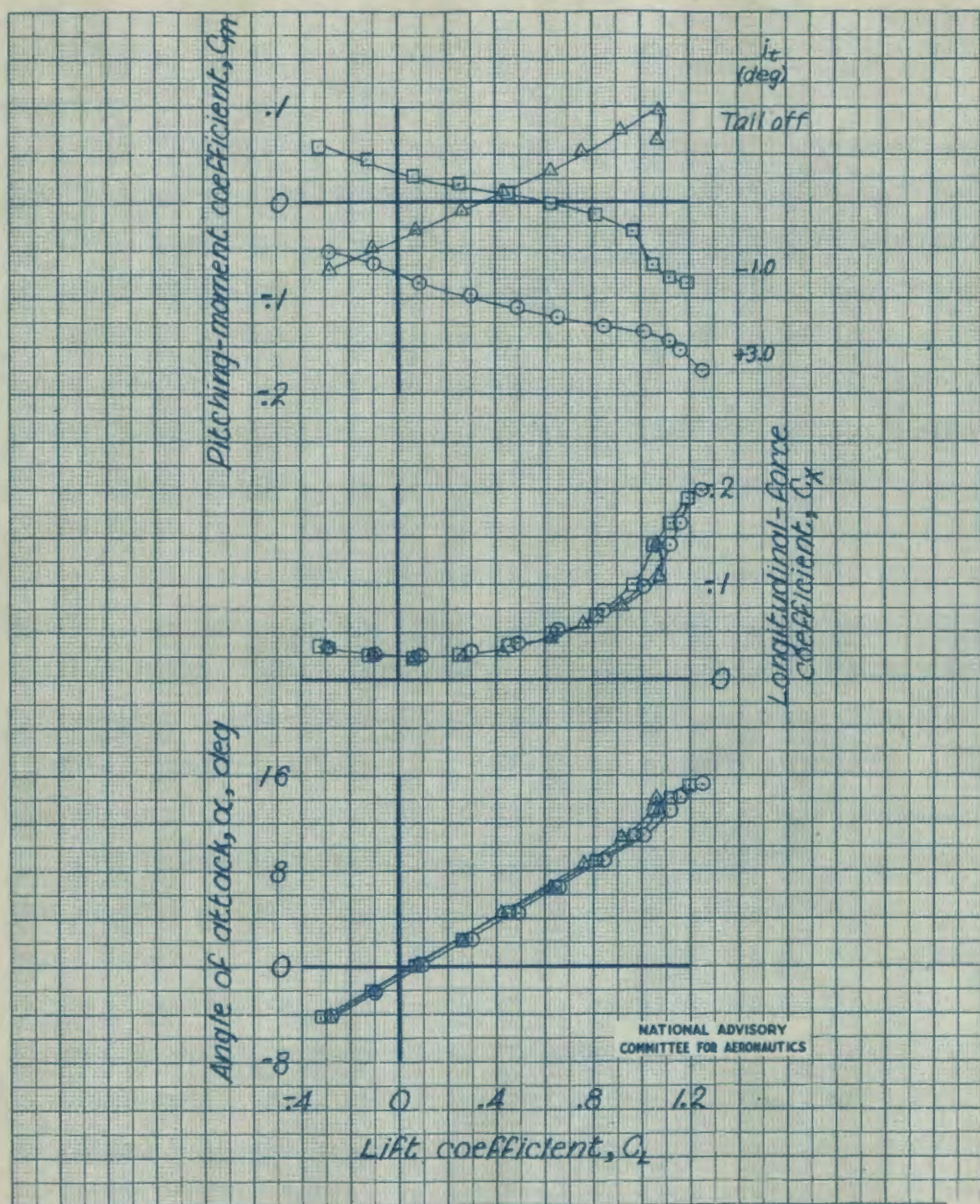


(d) Right tank in tip position; left tank off; bombs off.

Figure 24.- Continued.

182024

MR No. L6F25

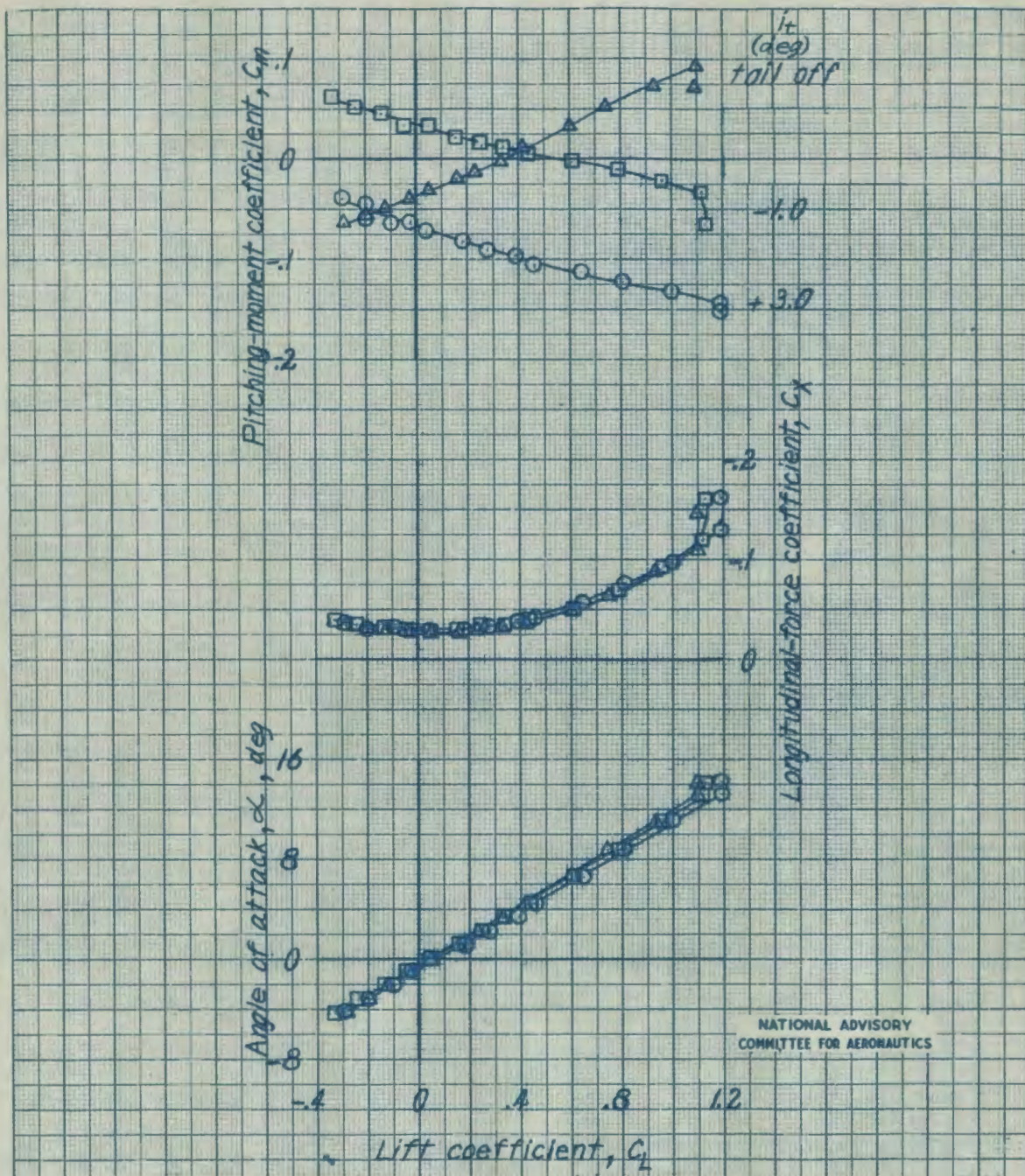


(e) Both tanks in tip position; bombs off.

Figure 24.- Continued.

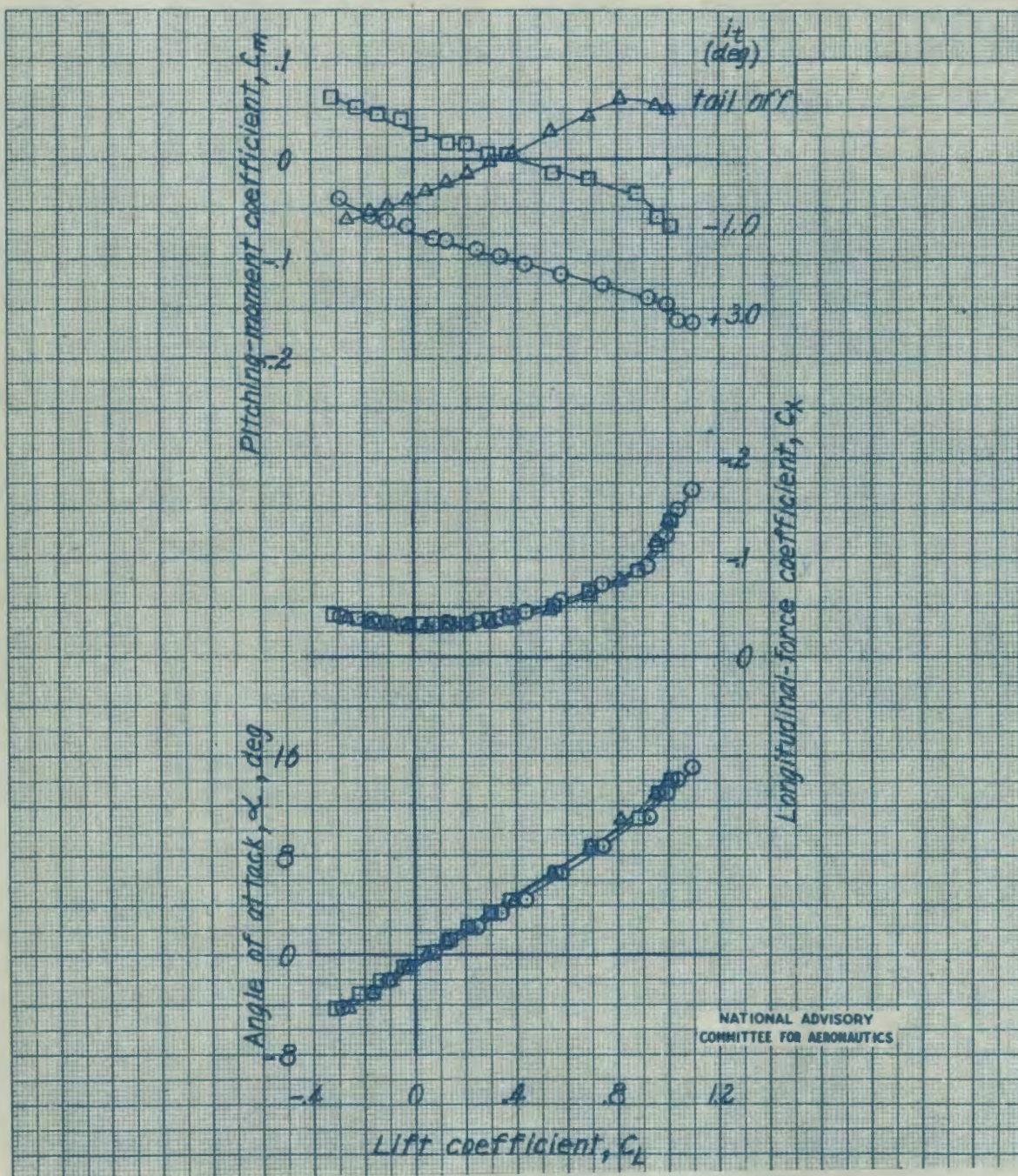
1820234

MR No. L6F25



(f) Both tanks in tip position; left inboard bomb on,  
tip bombs off.

Figure 24.- Continued.



(g) Tanks off; left inboard bomb on, tip bombs on.

Figure 24.- Concluded.

162025

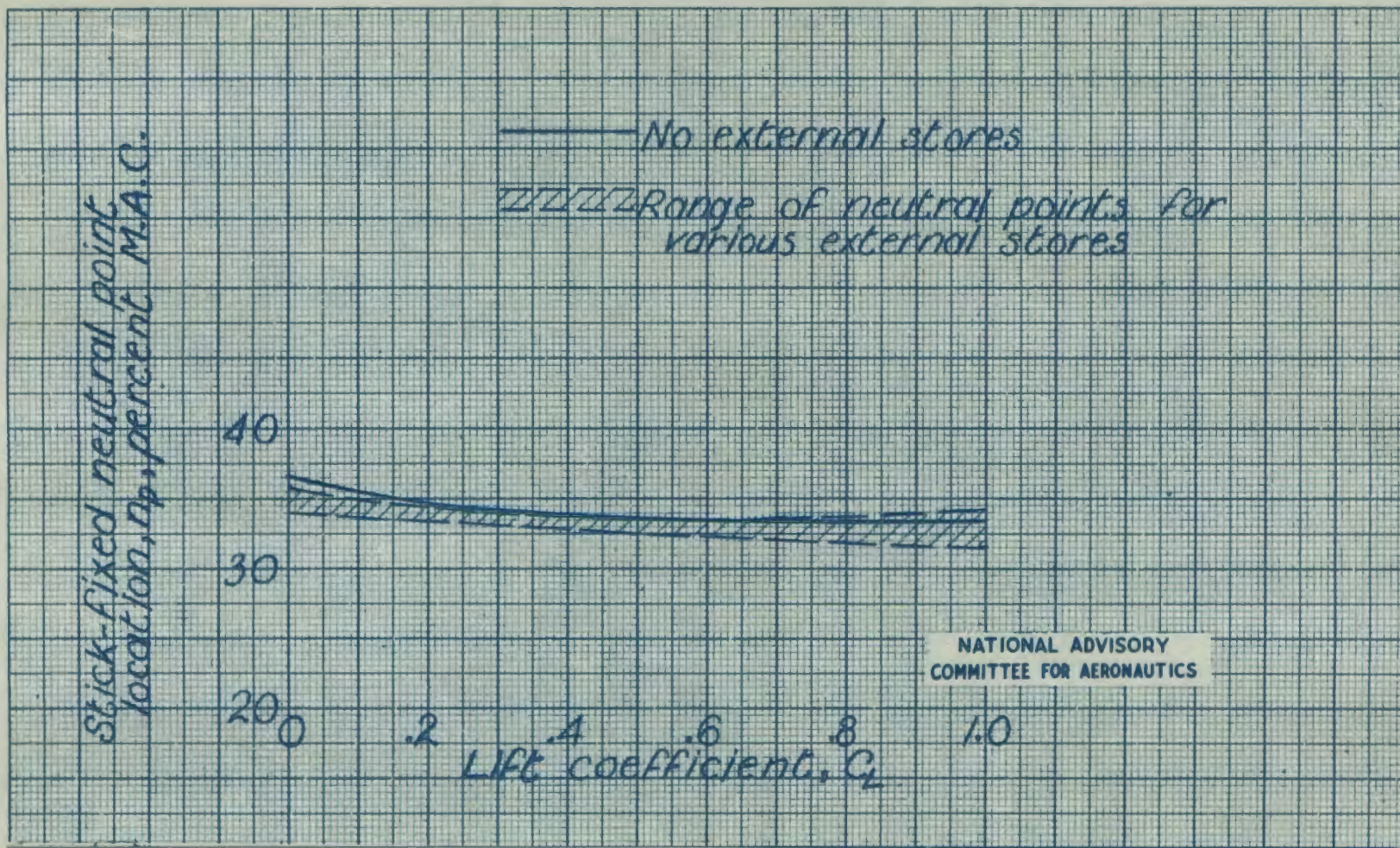
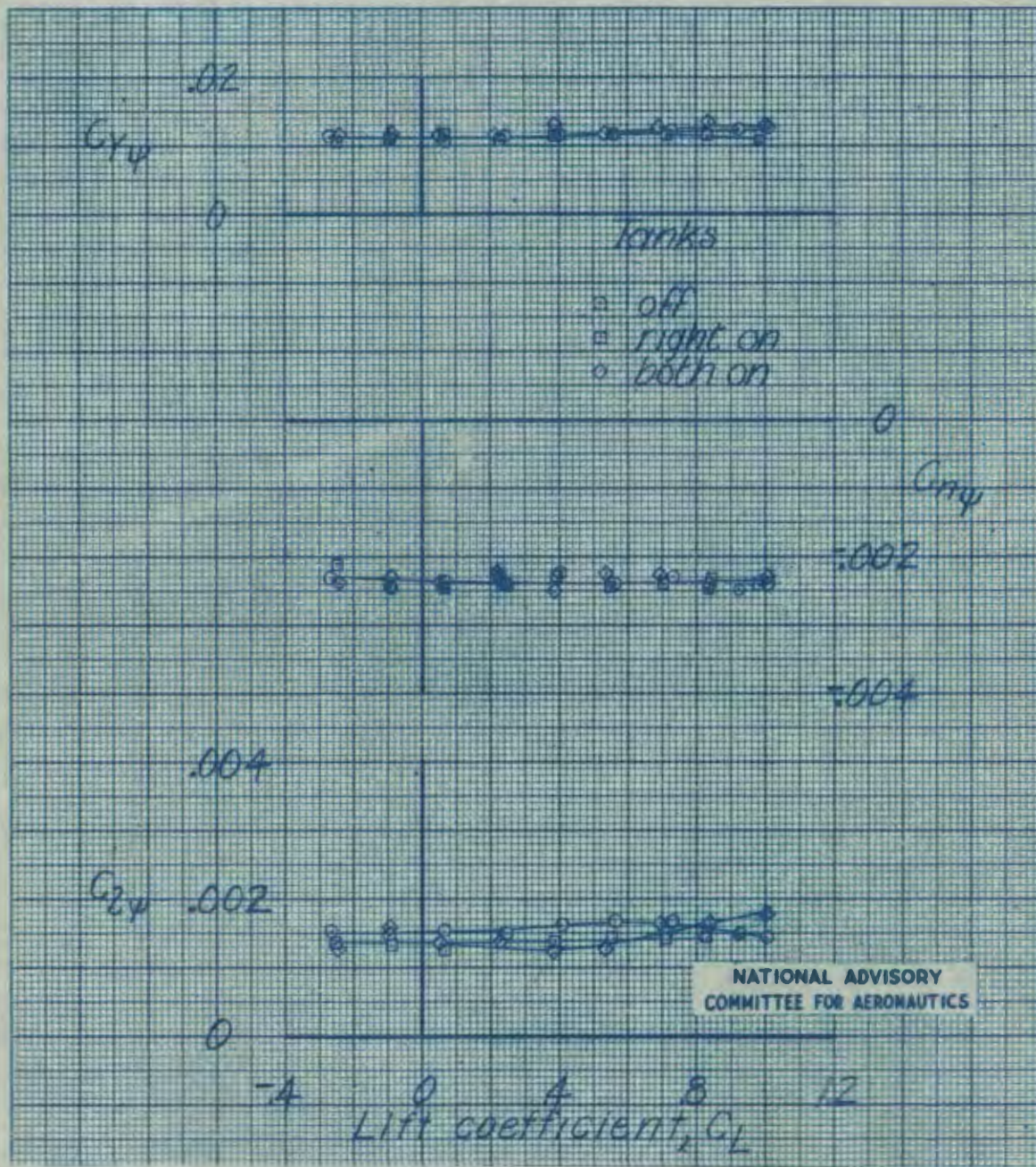


Figure 25.- Effect of external fuel tanks and bombs on the stick-fixed neutral points of the Republic XP-84 airplane, as determined from tests of the 1/5-scale model. Power off; cruising configuration.

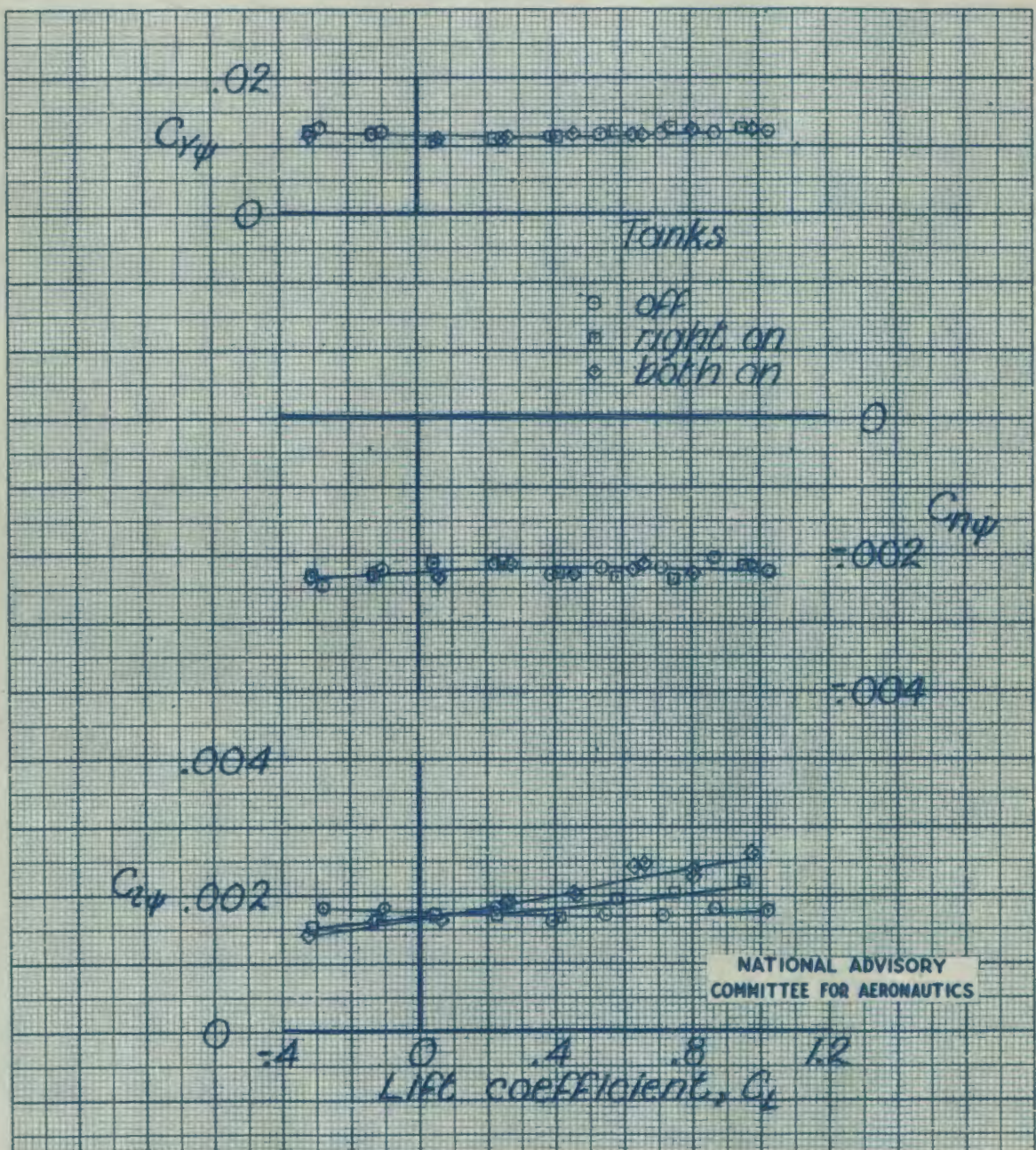
MR No. L6F25



(a) Inboard tanks.

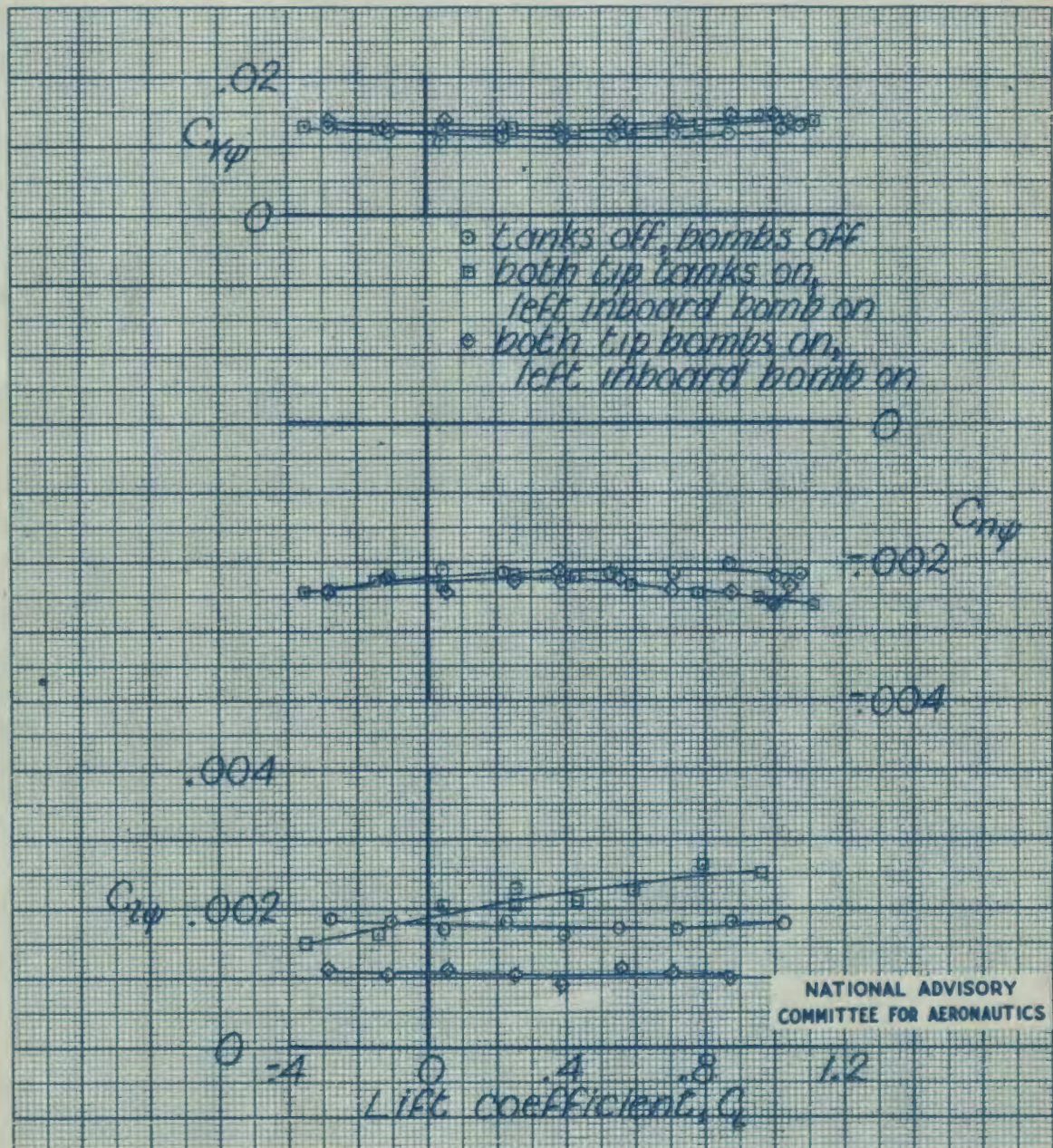
Figure 28.- Effect of external fuel tanks and bombs on the lateral-stability derivatives at small angles of yaw of the 1/5-scale model of the Republic XP-84 airplane. Power off; cruising configuration;  $i_t = 0^\circ$ .

MR No. L6F25



(b) Tip tanks.

Figure 26.- Continued.



(c) Tanks and bombs.

Figure 26.- Concluded.

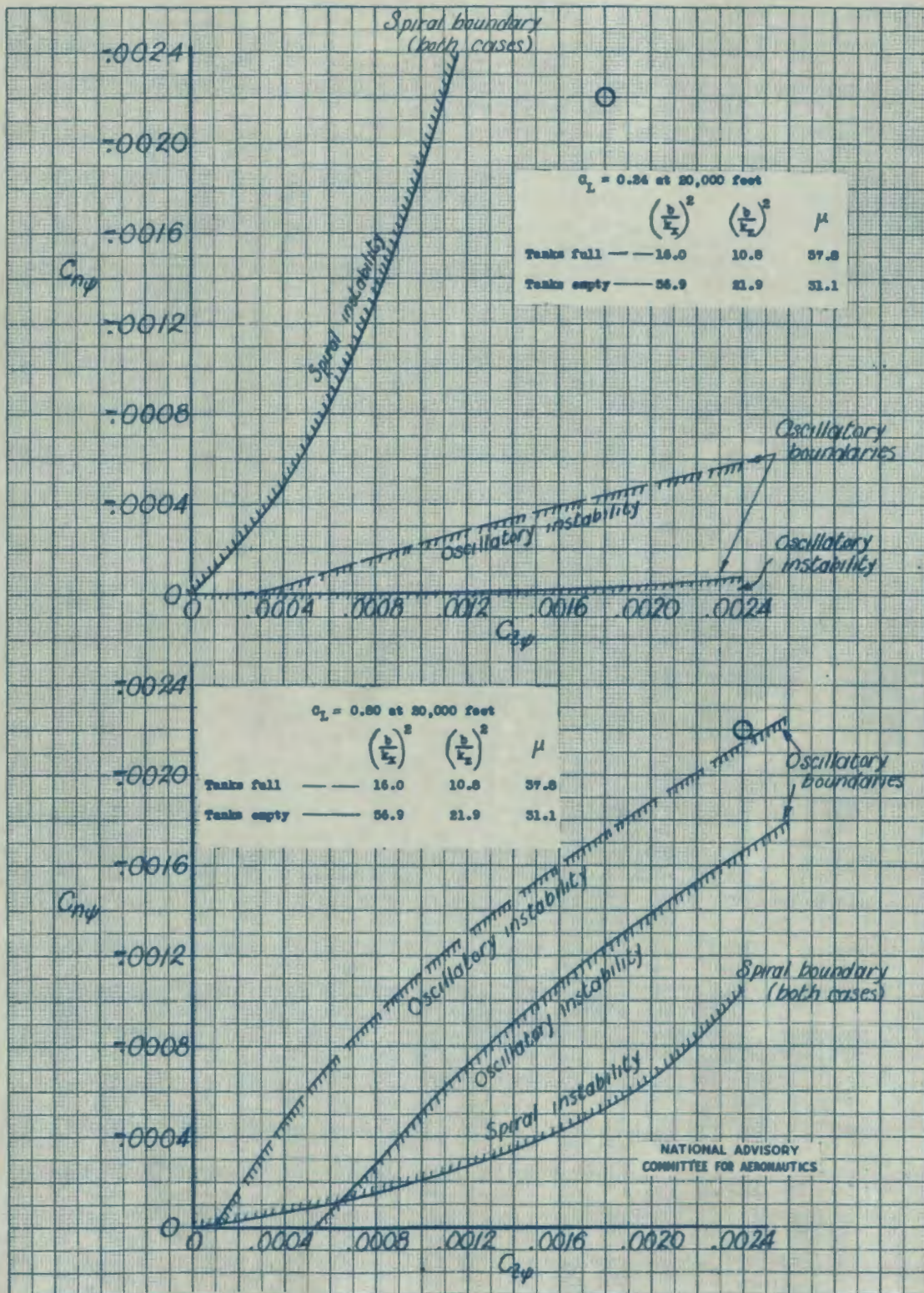


Figure 27 -- Effect of carrying fuel in the wing tip tanks on the dynamic lateral-stability boundaries of the XP-84 airplane. Cruising configuration.

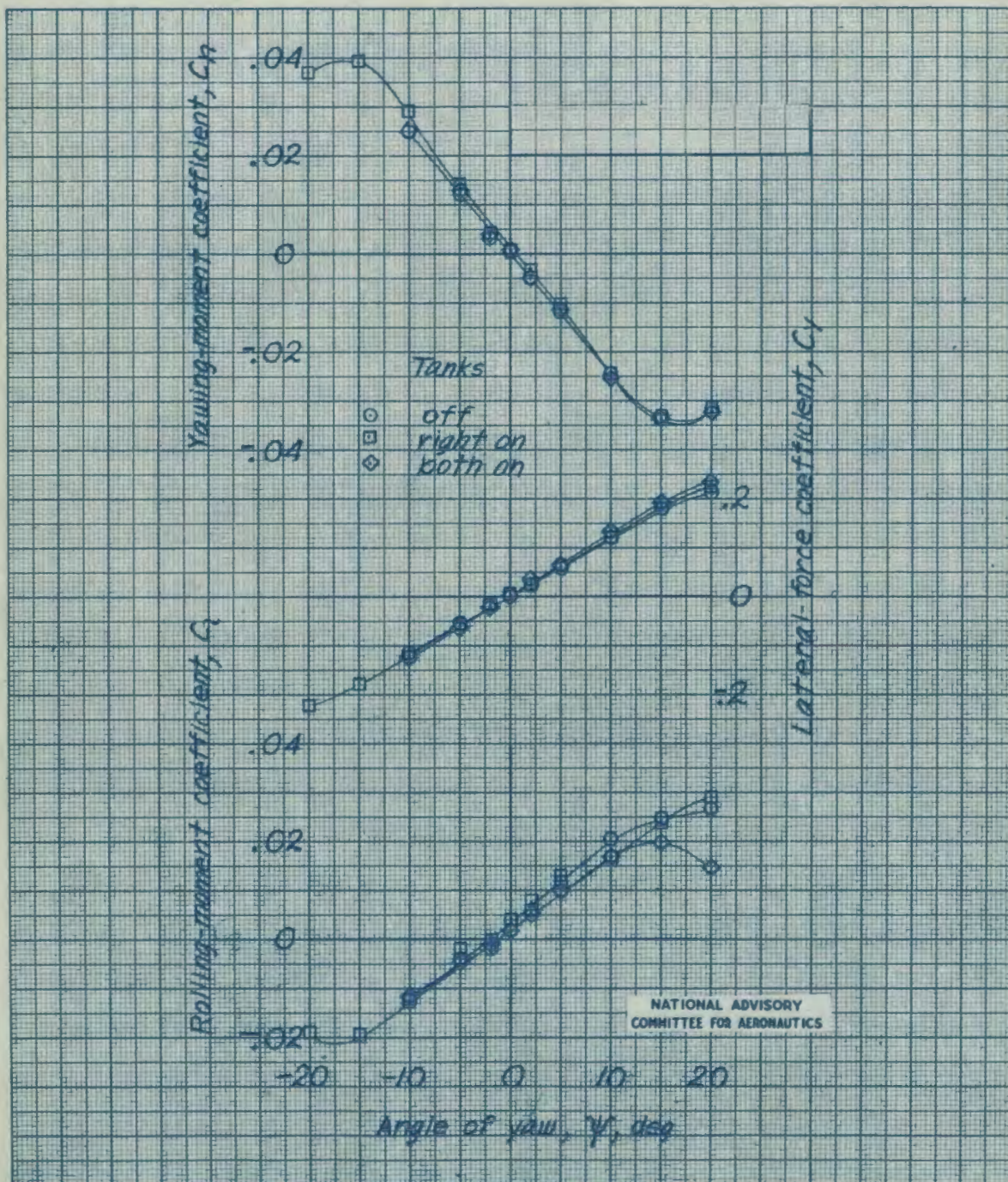
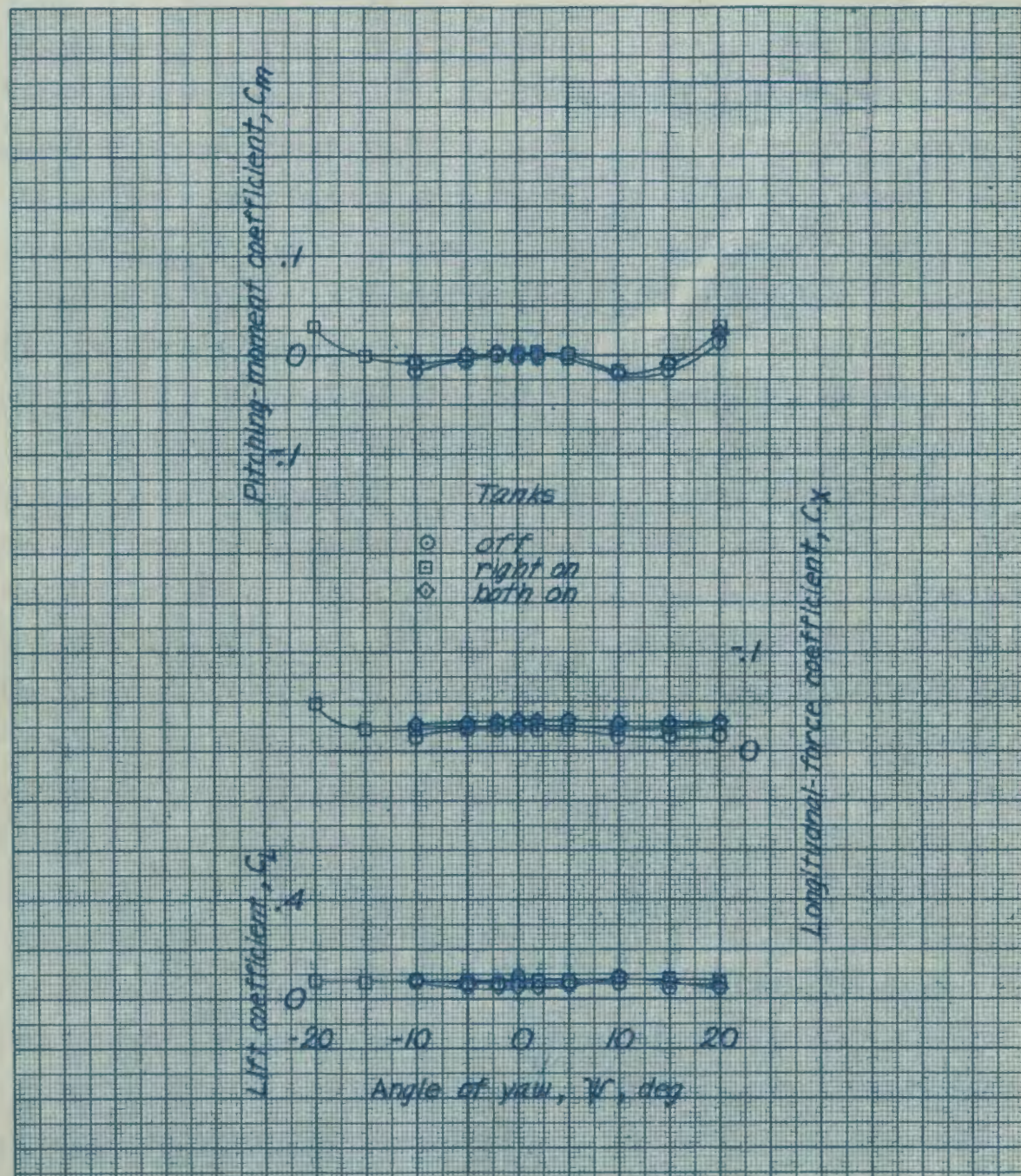
(a)  $\alpha = 0.1^\circ$ .

Figure 28.- Effect of inboard fuel tanks on the aerodynamic characteristics in yaw of the 1/5-scale model of the Republic XP-84 airplane. Power off; cruising configuration;  $it = 0^\circ$ .

132020

MR No. L6F25



(a) Concluded.

Figure 28. Continued.

1322028

MR No. L6F25

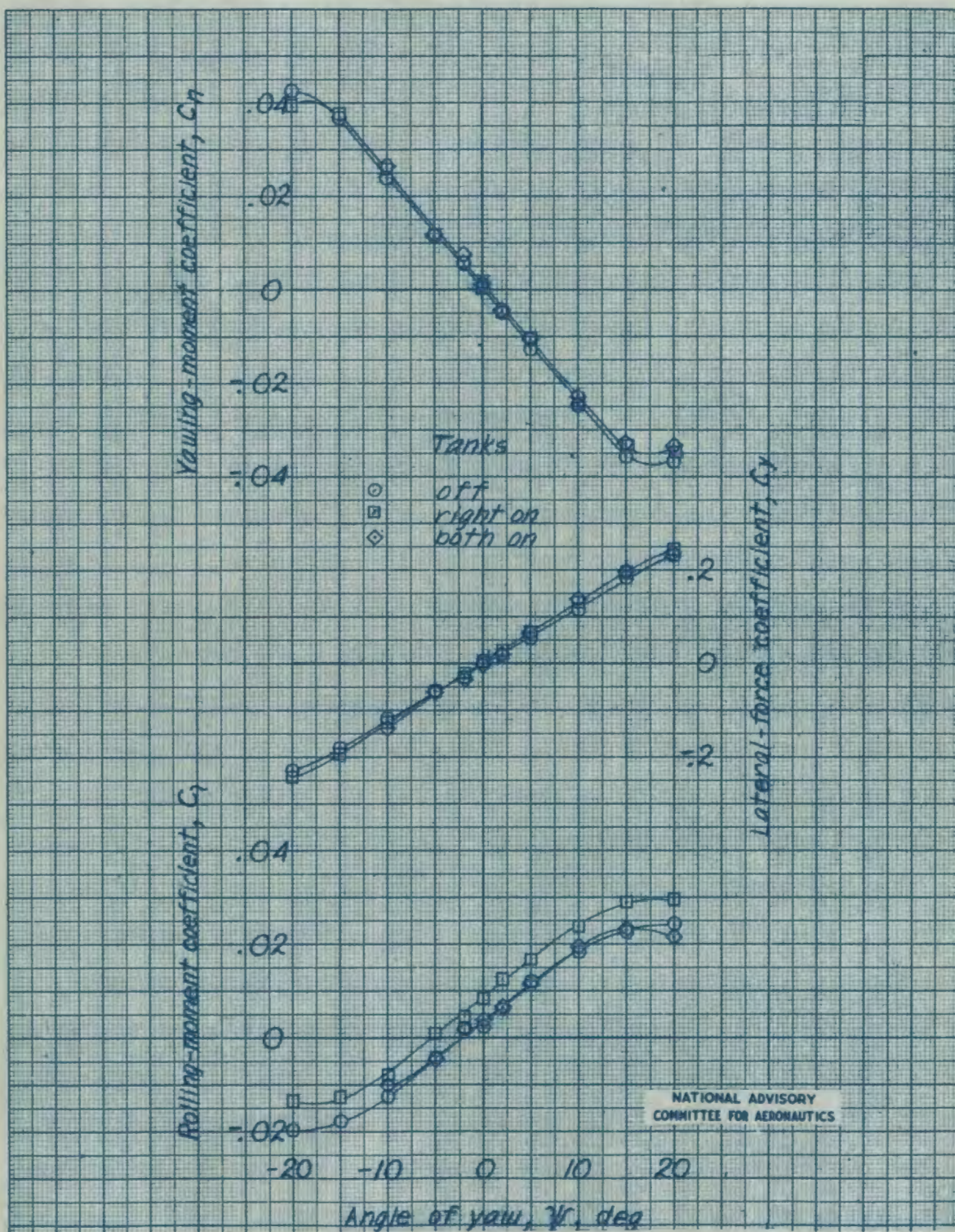
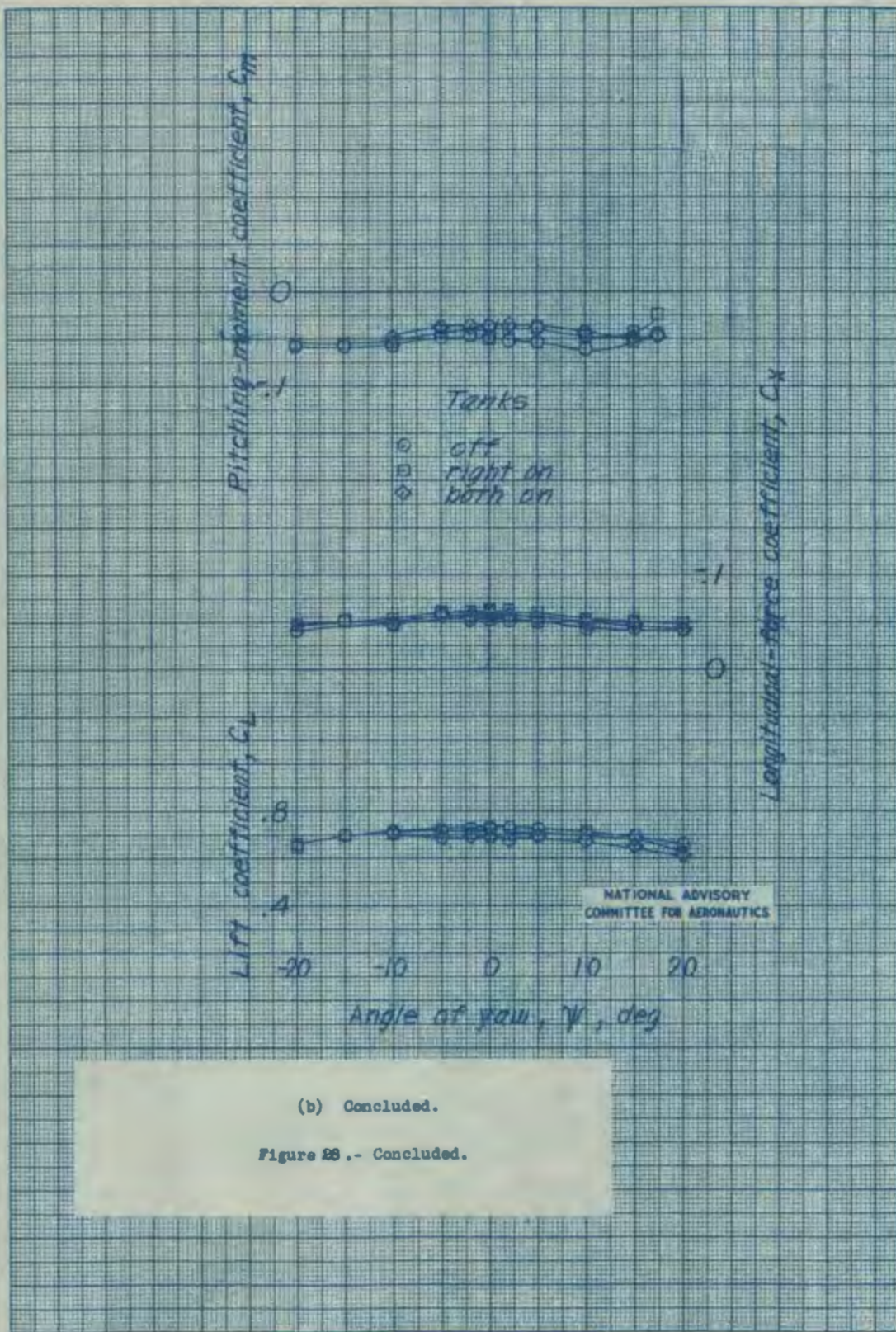
(b)  $\alpha = 8.7^\circ$ .

Figure 28. Continued.

182026

MR No. L6F25



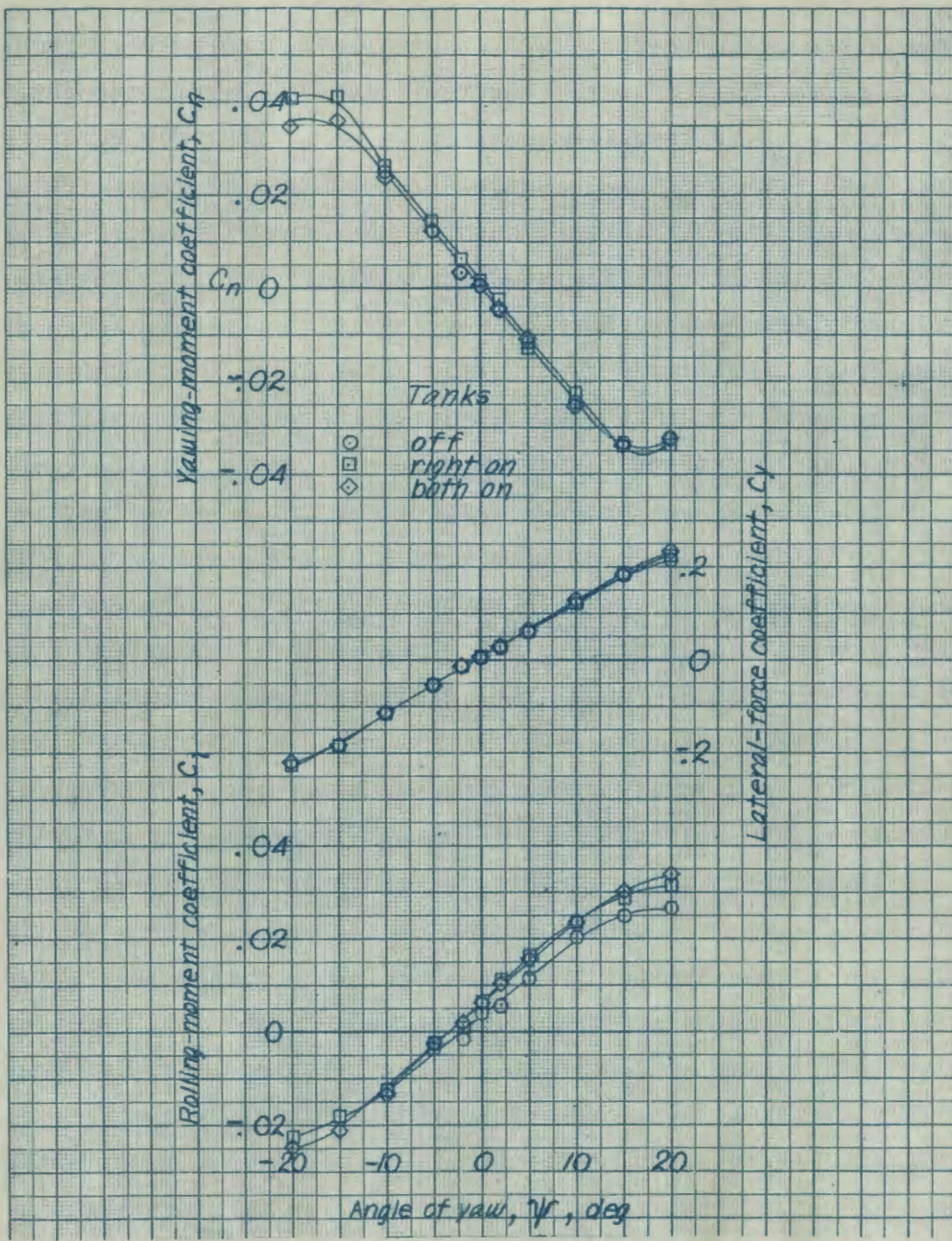
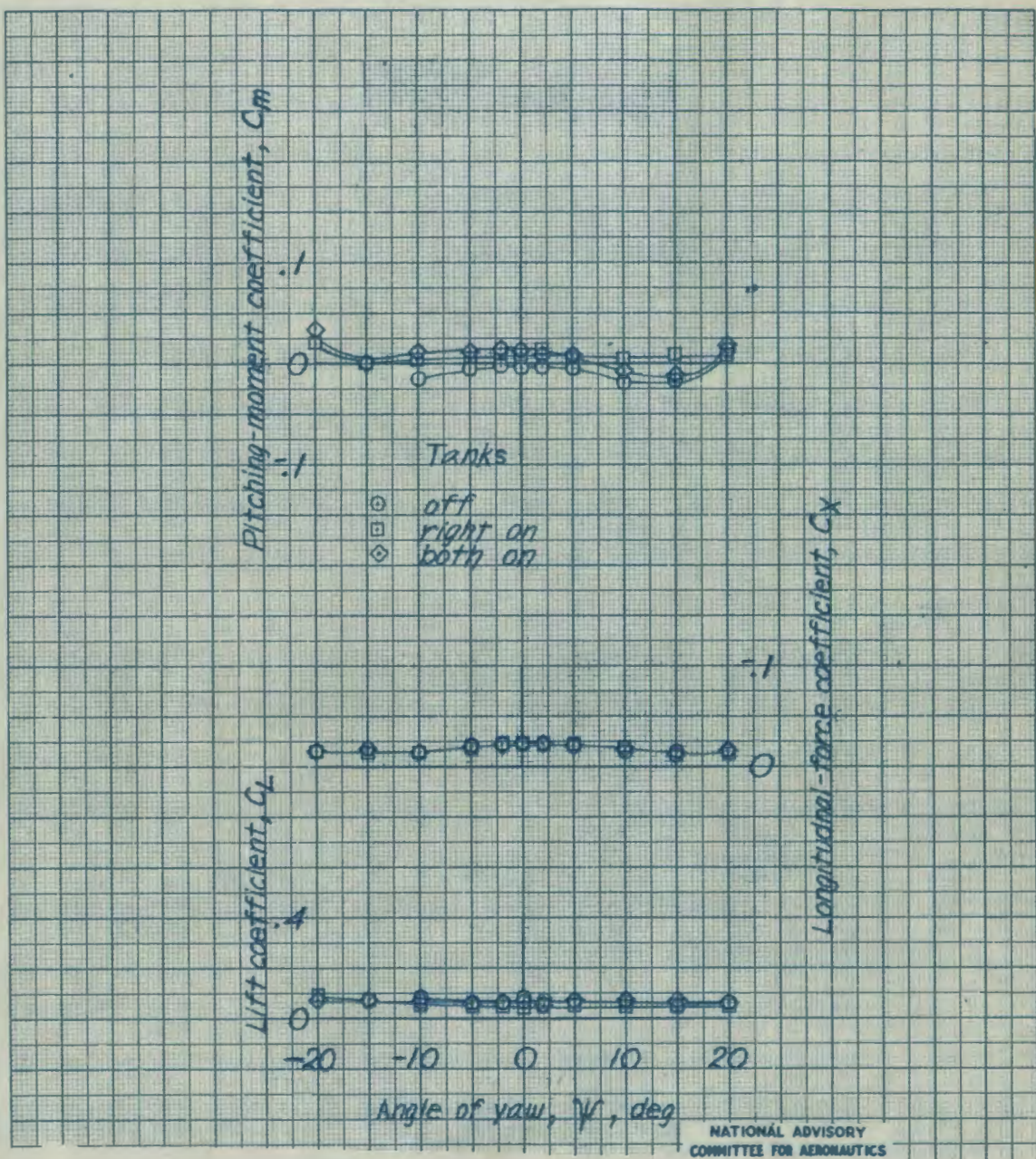
(a)  $\alpha = 0.1^\circ$ .NATIONAL ADVISORY  
COMMITTEE FOR AERONAUTICS

Figure 29.- Effect of tip-mounted fuel tanks on the aerodynamic characteristics in yaw of the 1/5-scale model of the Republic XP-84 airplane. Power off, cruising configuration;  $\delta_t = 0^\circ$ .



(a) Concluded.

Figure 29 -- Continued.

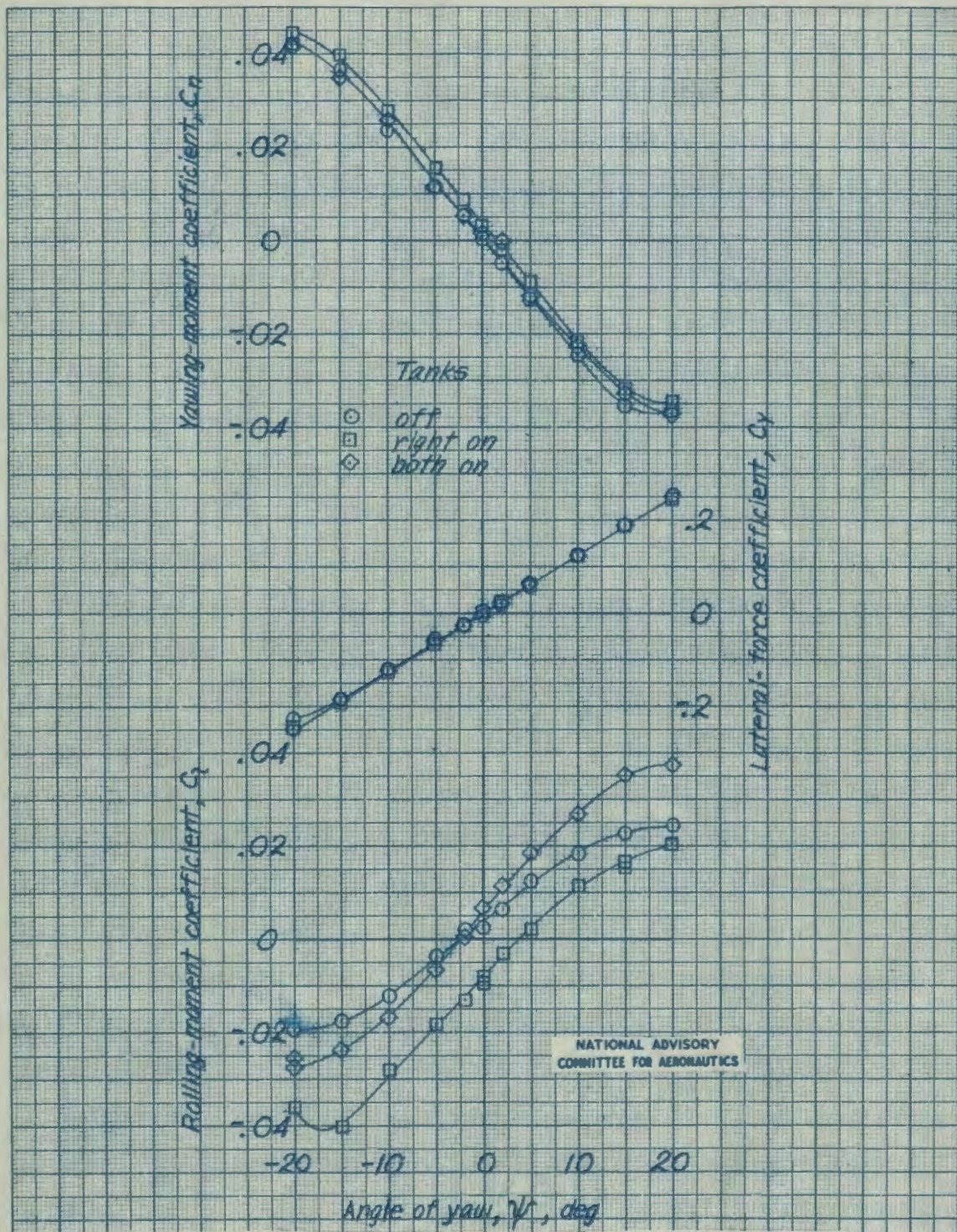
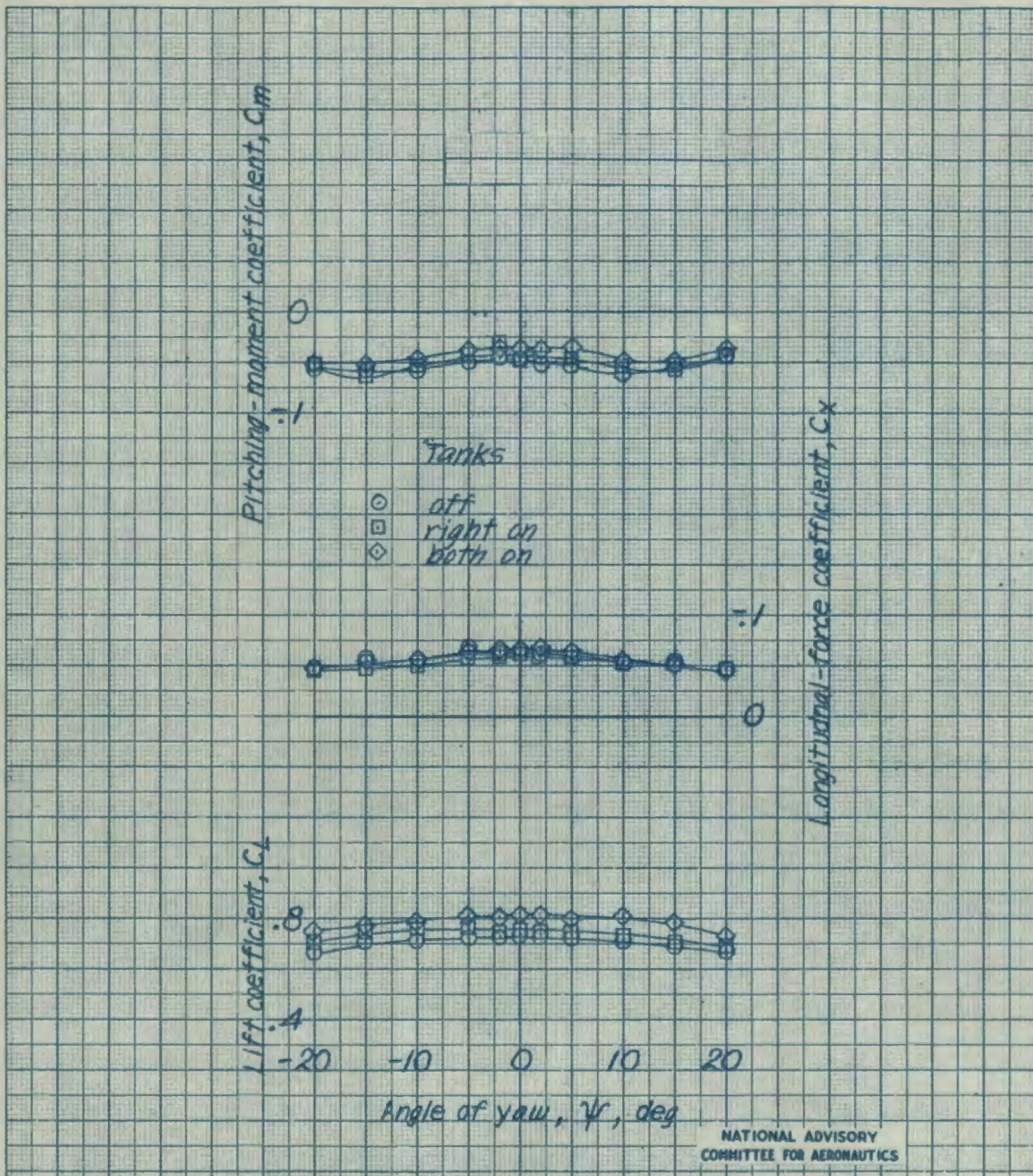


Figure 29 .- Continued.

182028

MR No. L6F25



(b) Concluded.

Figure 29.- Concluded.

182030

MR No. L6F25

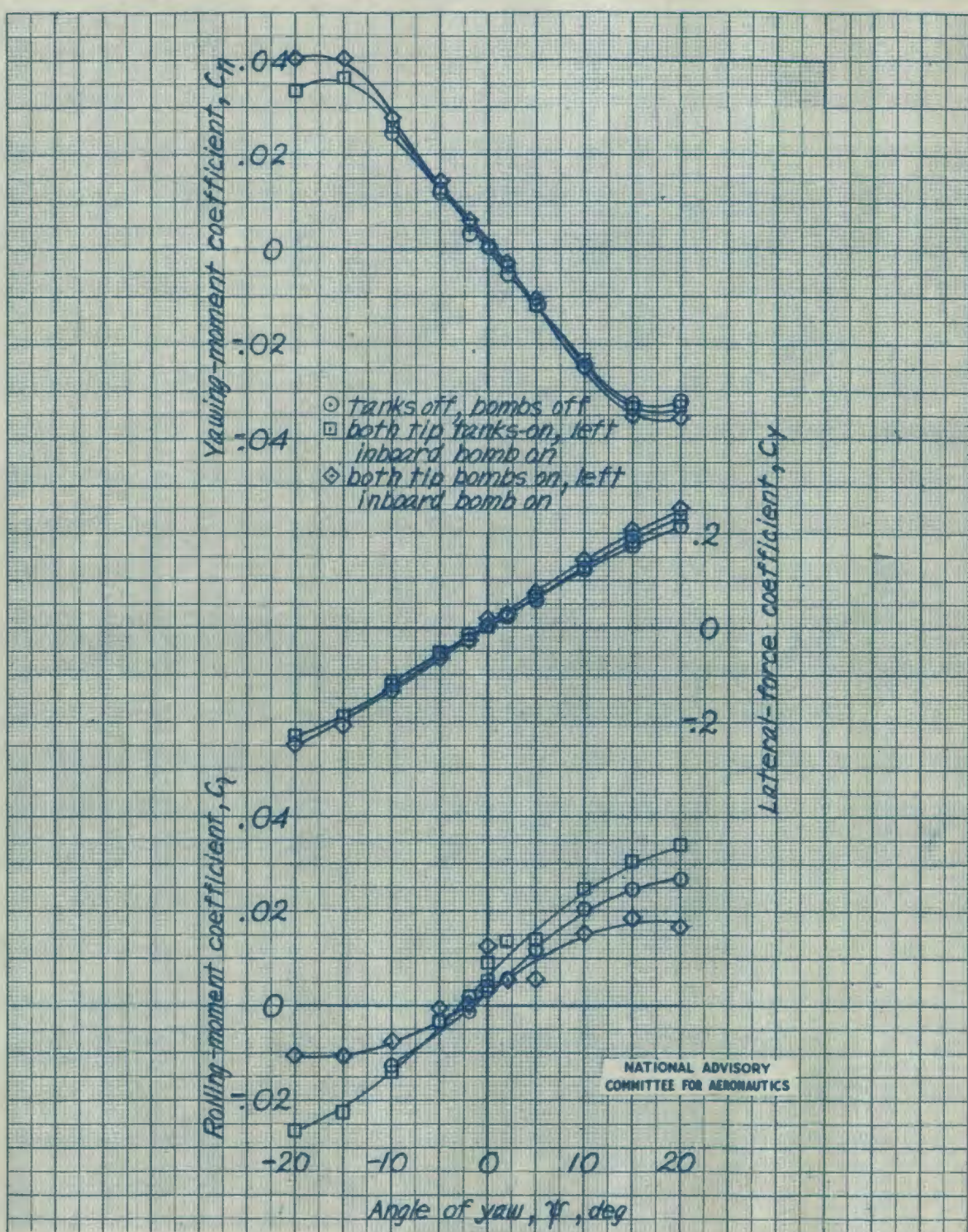
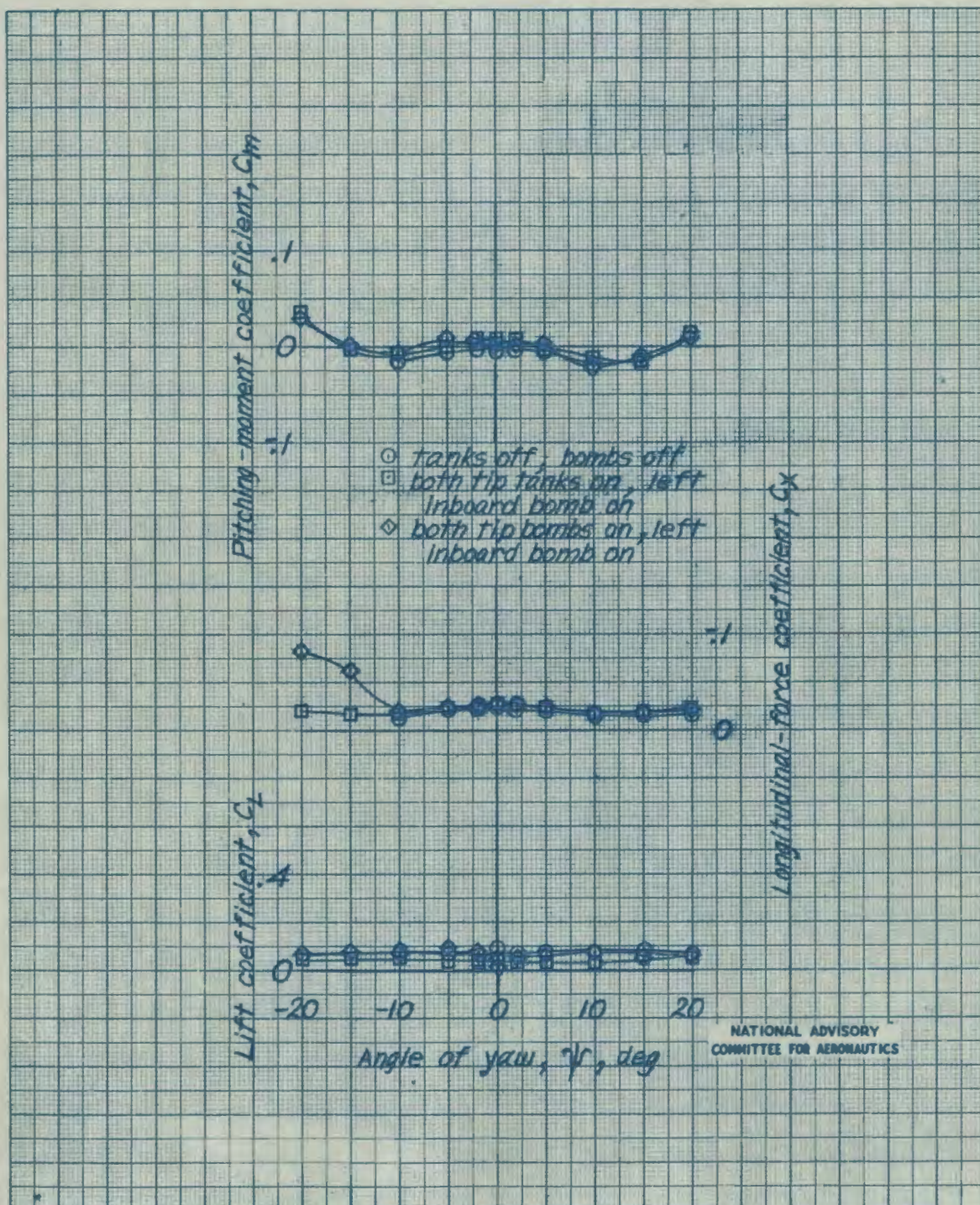
(a)  $\alpha = 0.1^\circ$ .

Figure 30 - Effect of fuel tanks and bombs on the aerodynamic characteristics in yaw of the 1/5-scale model of the Republic XP-84 airplane. Power off, cruising configuration;  $\dot{t}_t = 0^\circ$ .



(a) Concluded.

Figure 30.- Continued.

132330

MR No. L6F25

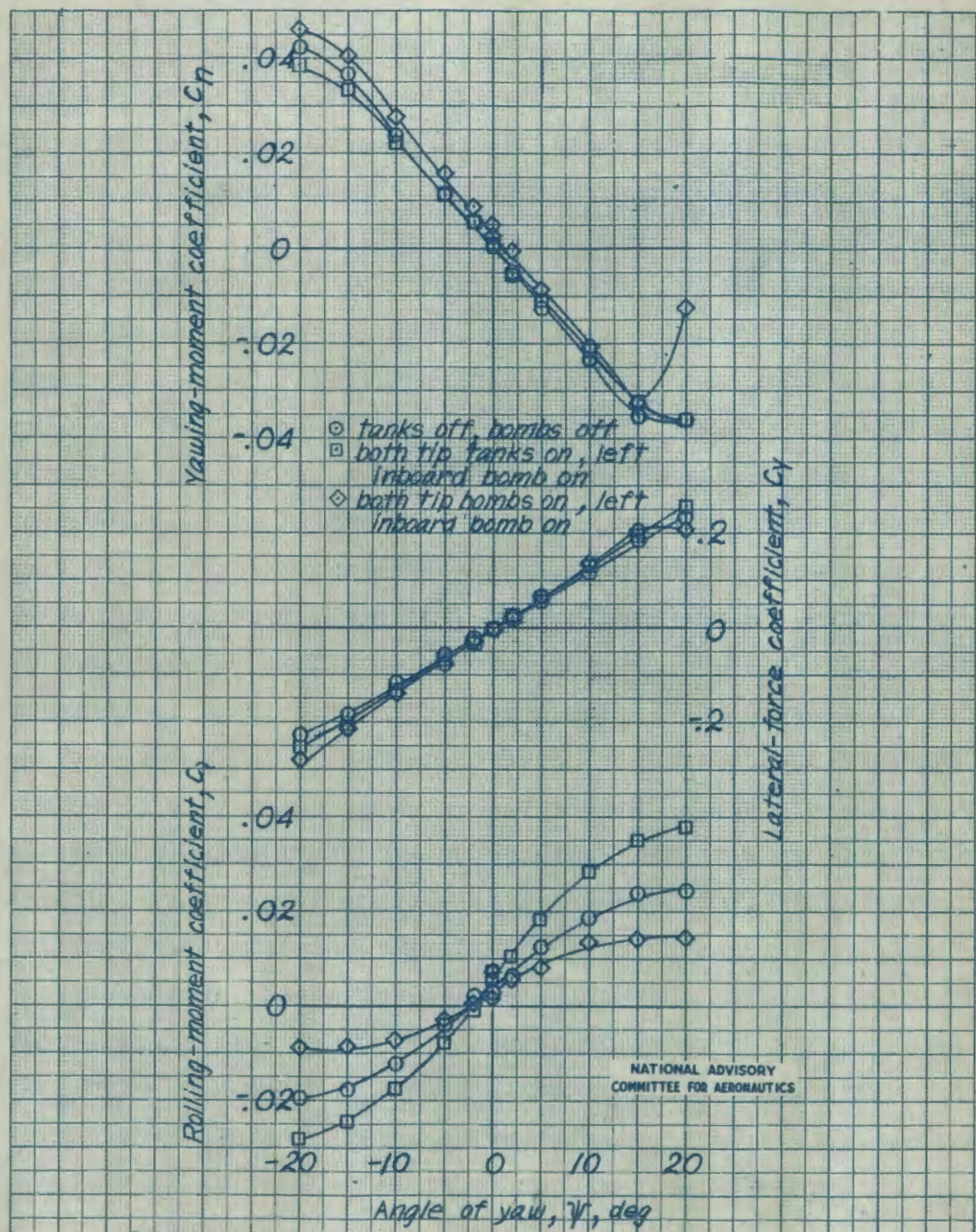
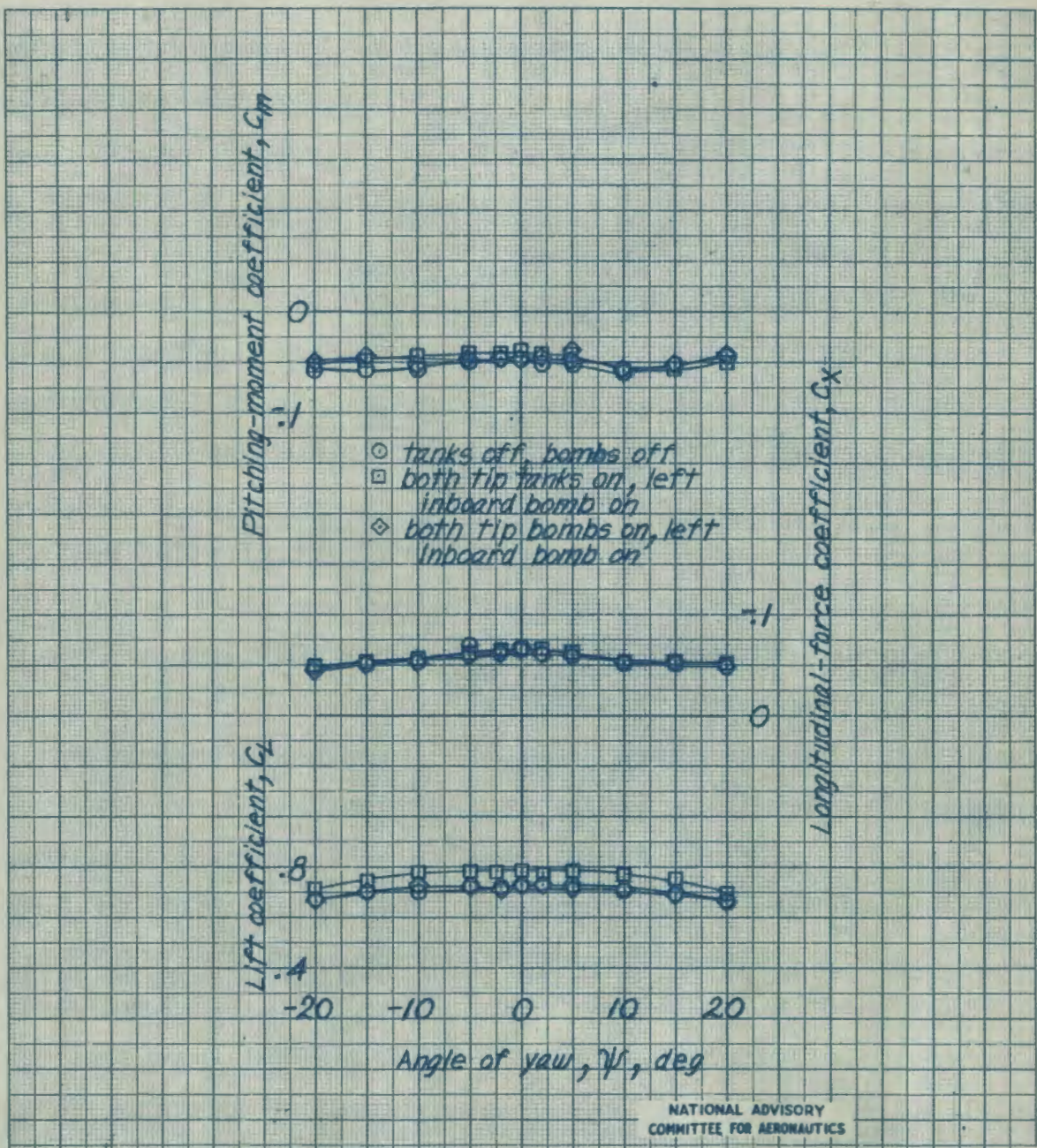
(b)  $\alpha = 8.7^\circ$ .

Figure 80. - Continued.

132000

MR No. L6F25



(b) Concluded.

Figure 30.- Concluded.

18203

MR No. L6F25

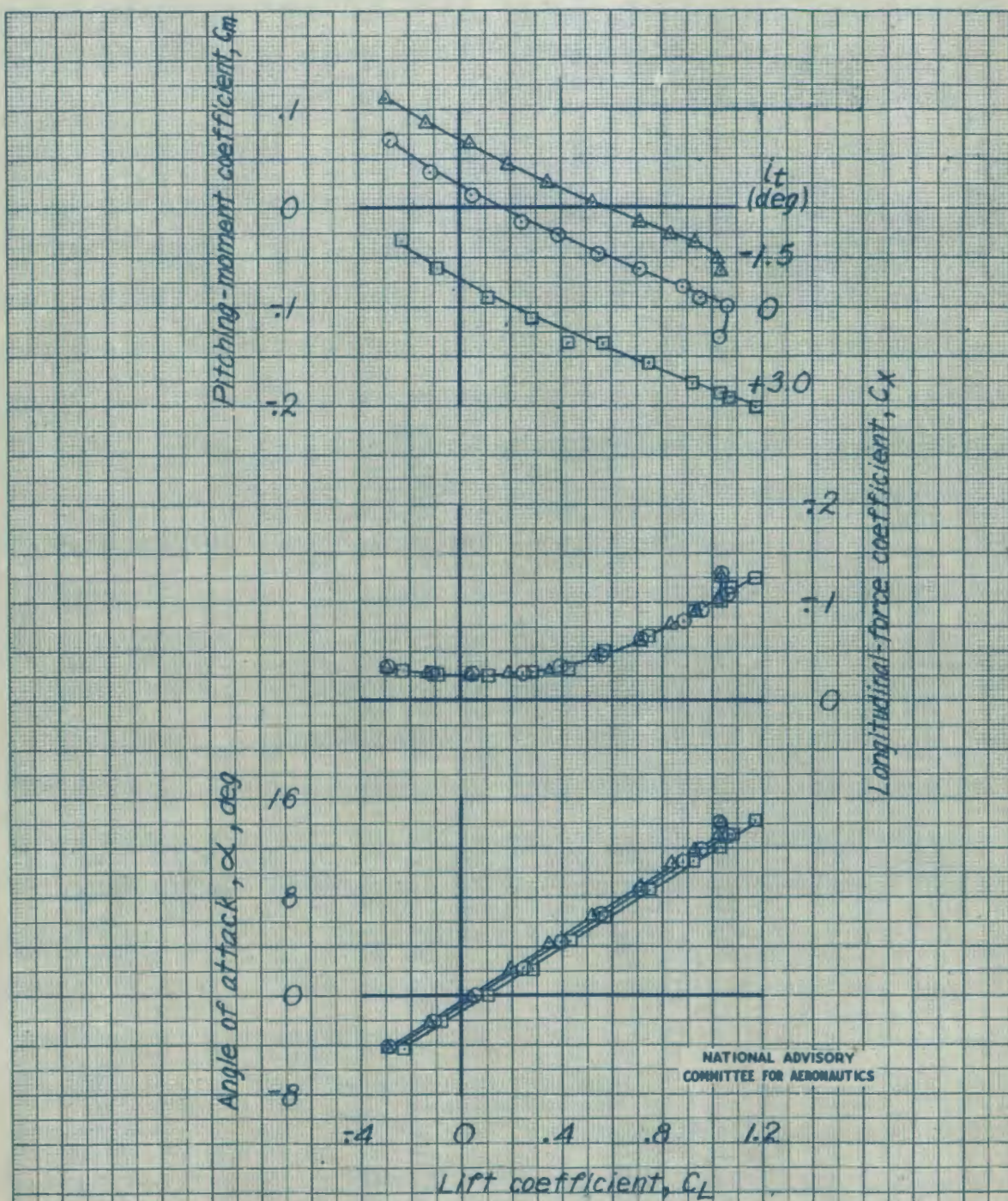


Figure 31.- Effect of stabilizer on the aerodynamic characteristics in pitch of the 1/5-scale model of the Republic XP-84 airplane with revised horizontal tail. Idling power; cruising configuration. Two rockets beneath fuselage.

132032

MR No. L6F25

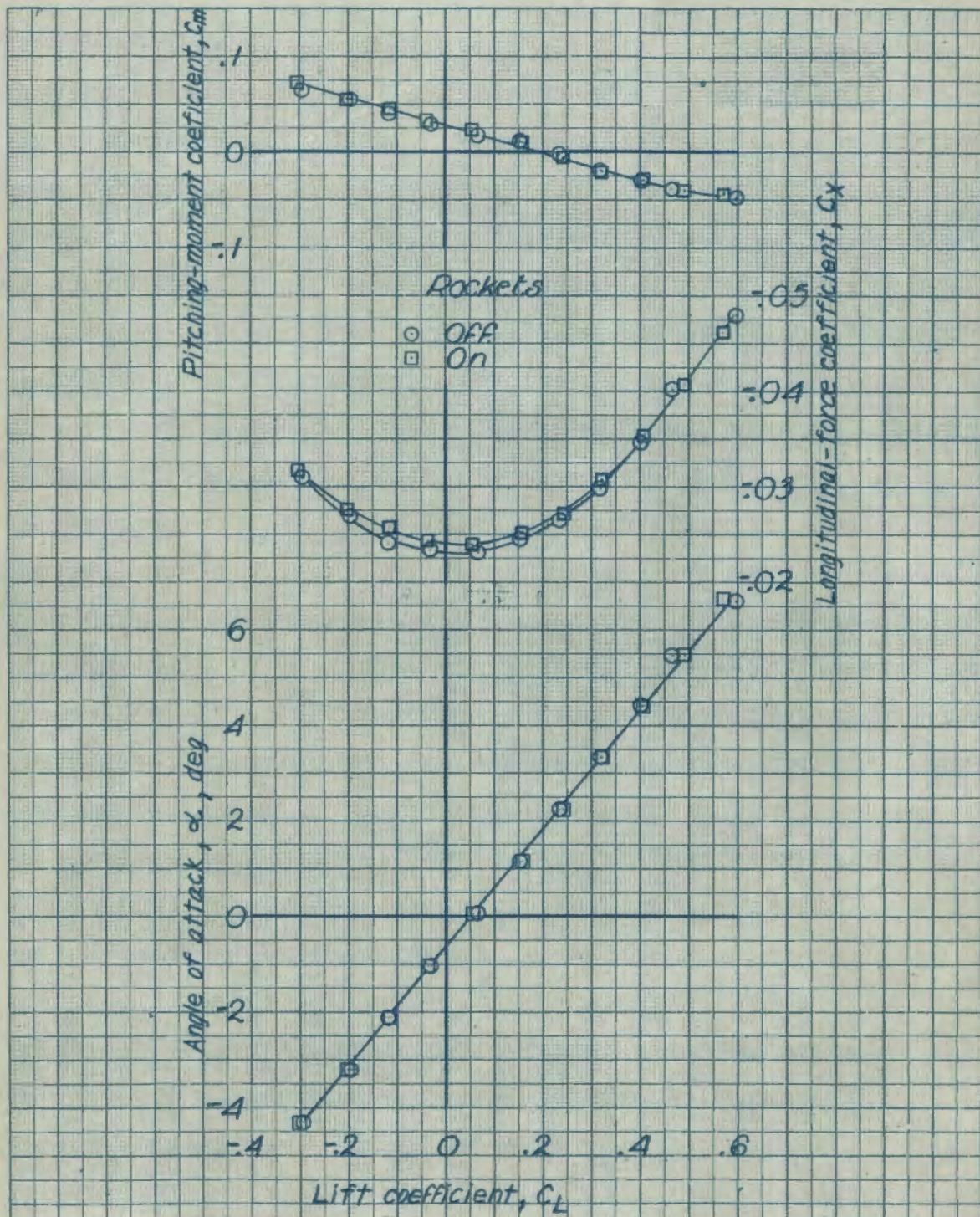


Figure 32.- Effect of rockets on the aerodynamic characteristics in pitch of the 1/5-scale model of the Republic XP-84 airplane with revised horizontal tail. Idling power; cruising configuration;  $\alpha = 0^\circ$ .

NATIONAL ADVISORY  
COMMITTEE FOR AERONAUTICS.

182033

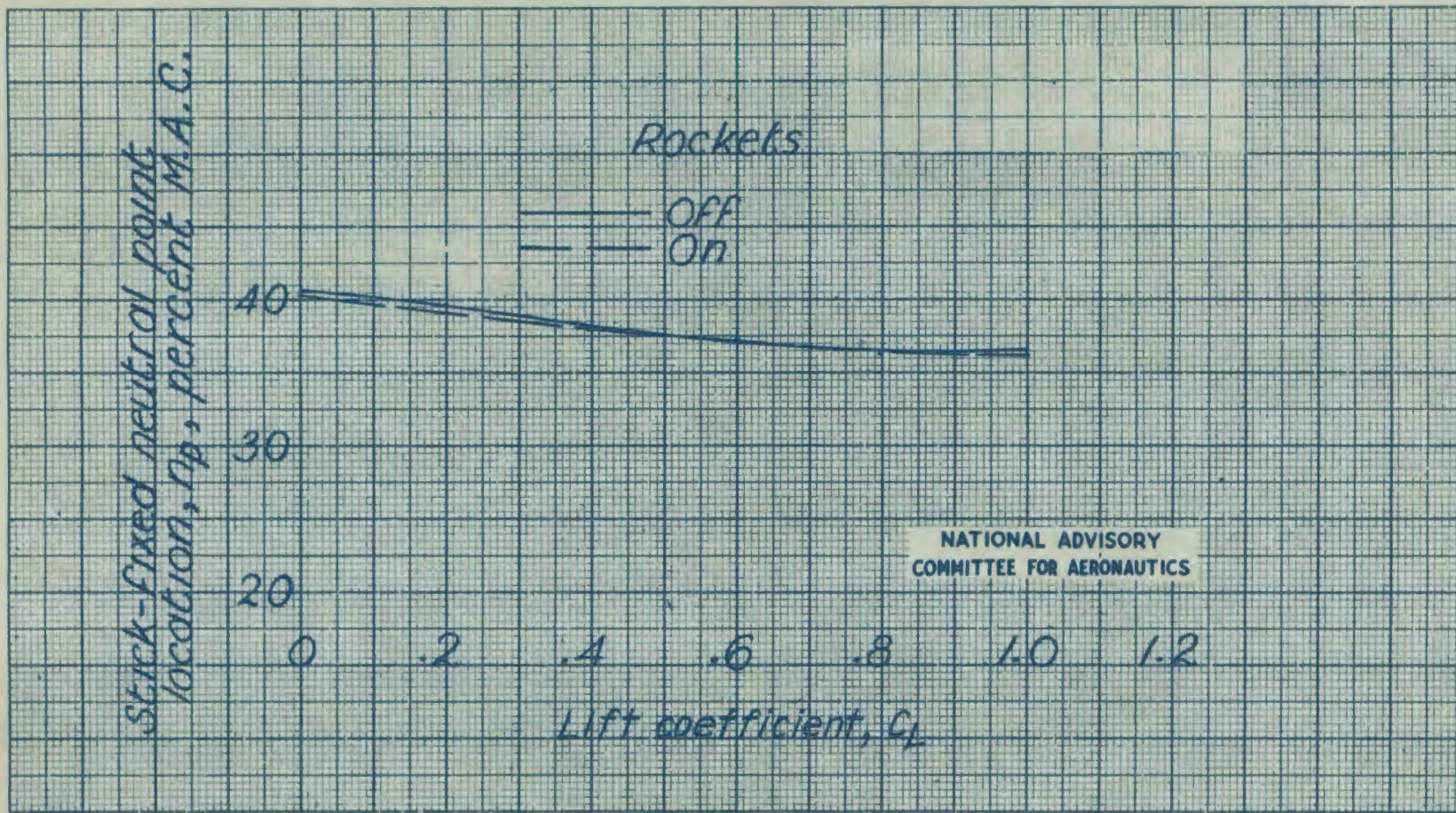
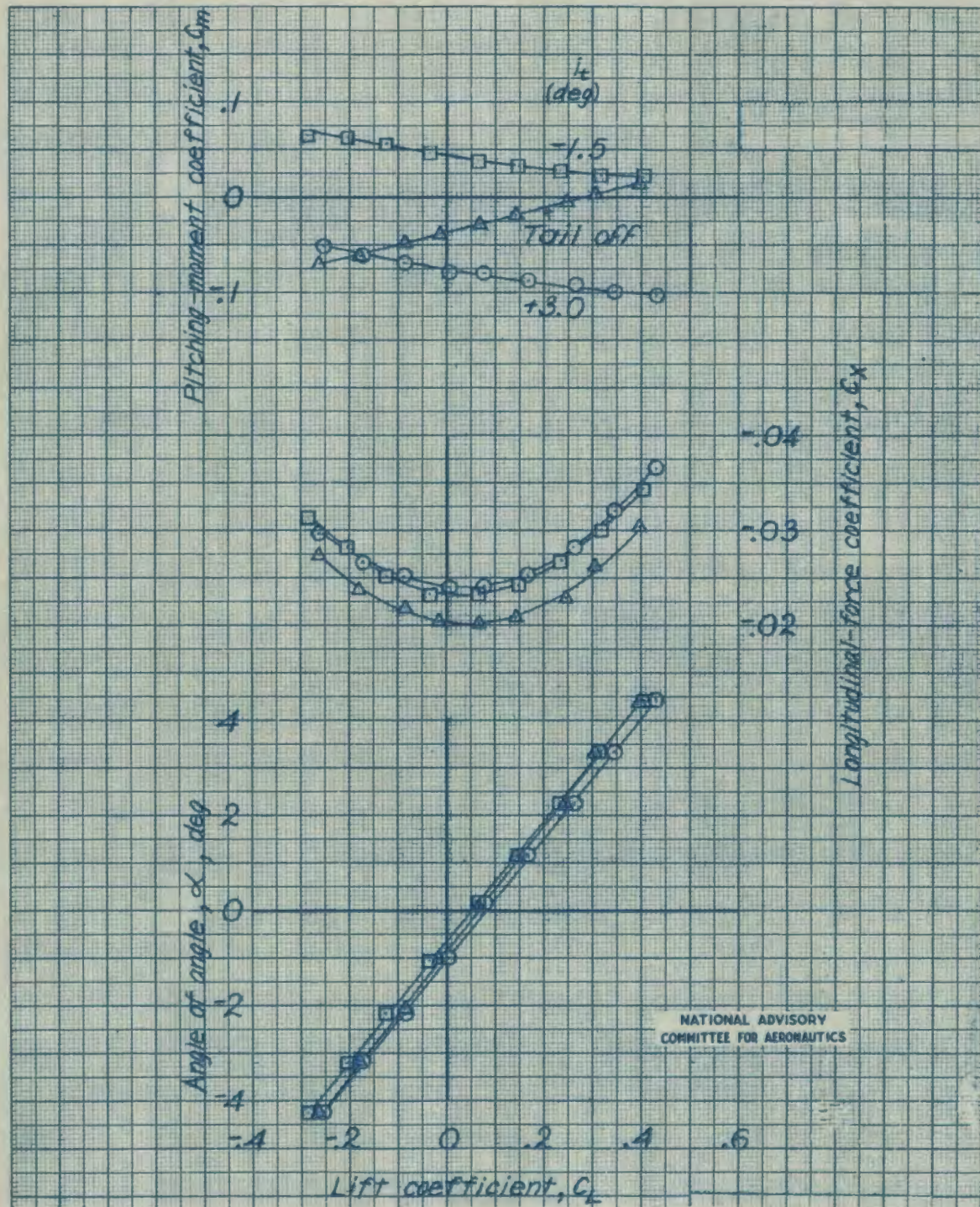


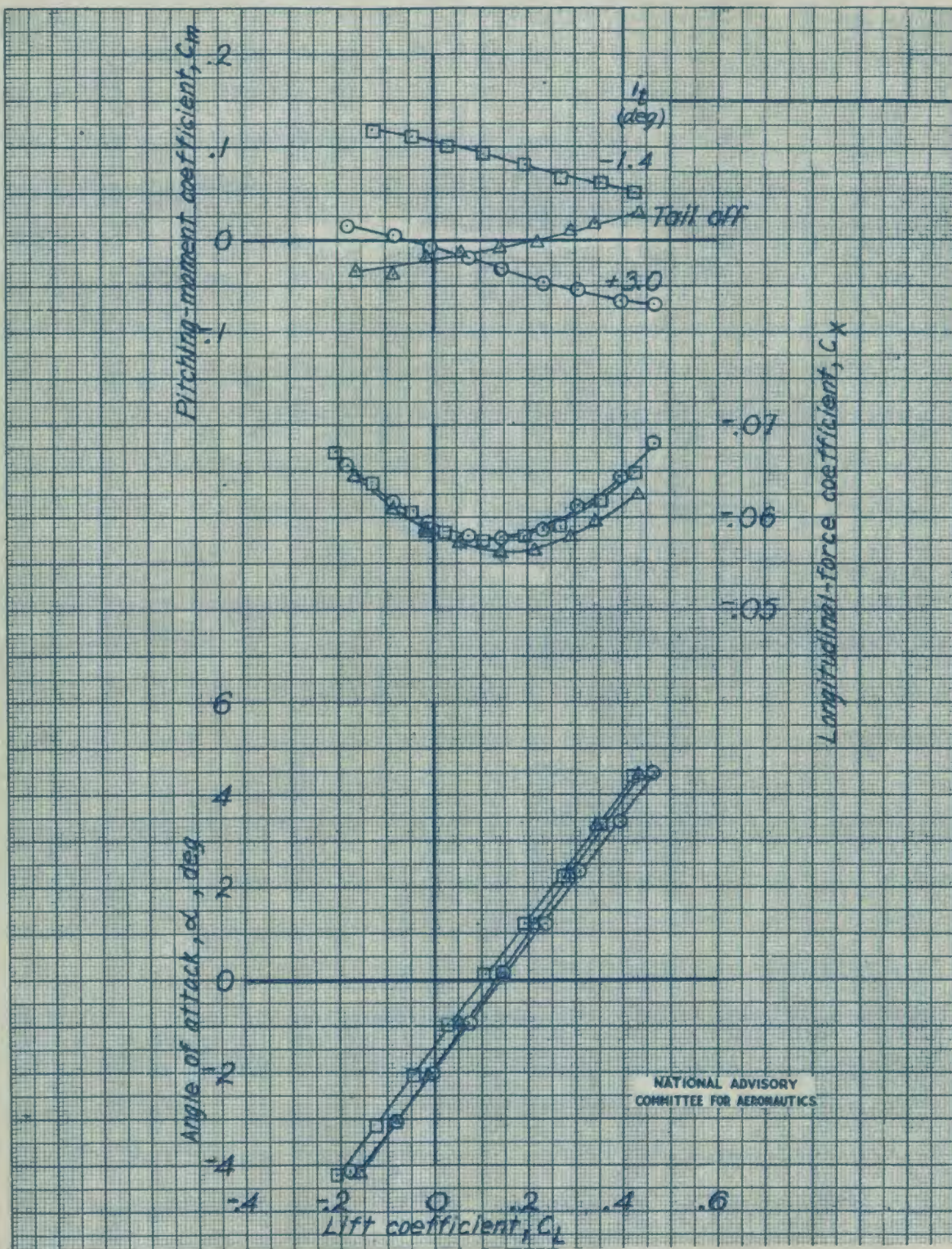
Figure 33.- Effect of rockets on the stick-fixed neutral points of the Republic XP-84 airplane with revised horizontal tail, as determined from tests of the 1/5-scale model. Idling power; cruising configuration.

MR No. L6F25



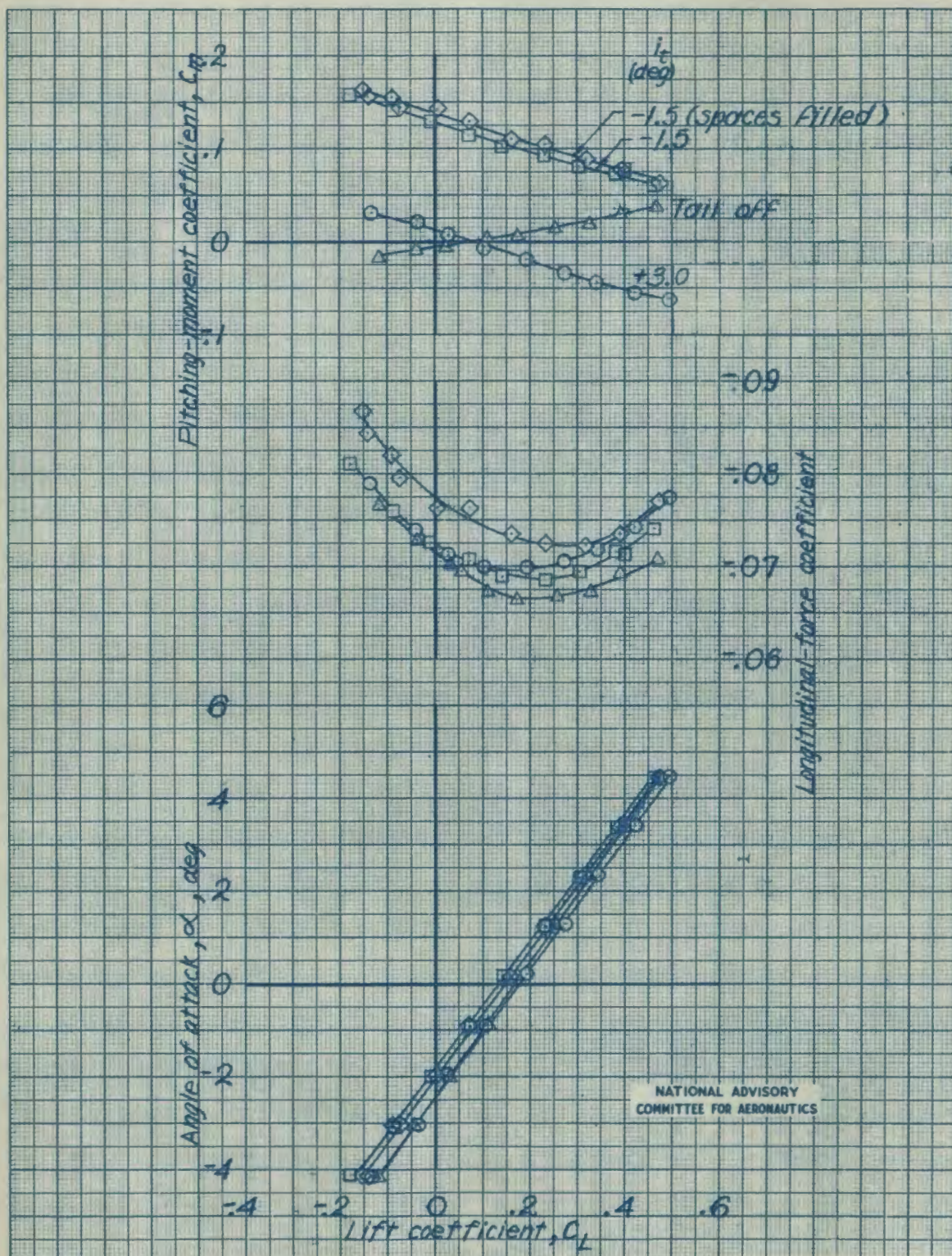
(a) Dive brakes retracted.

Figure 34 - Effect of fuselage dive-brake deflection on the aerodynamic characteristics in pitch of the 1/5-scale model of the Republic XP-84 airplane with original horizontal tail. Idling power, cruising configuration.



182031

MR No. L6F25



(c) Diye brakes deflected 90°

Figure 34.- Concluded.

182036

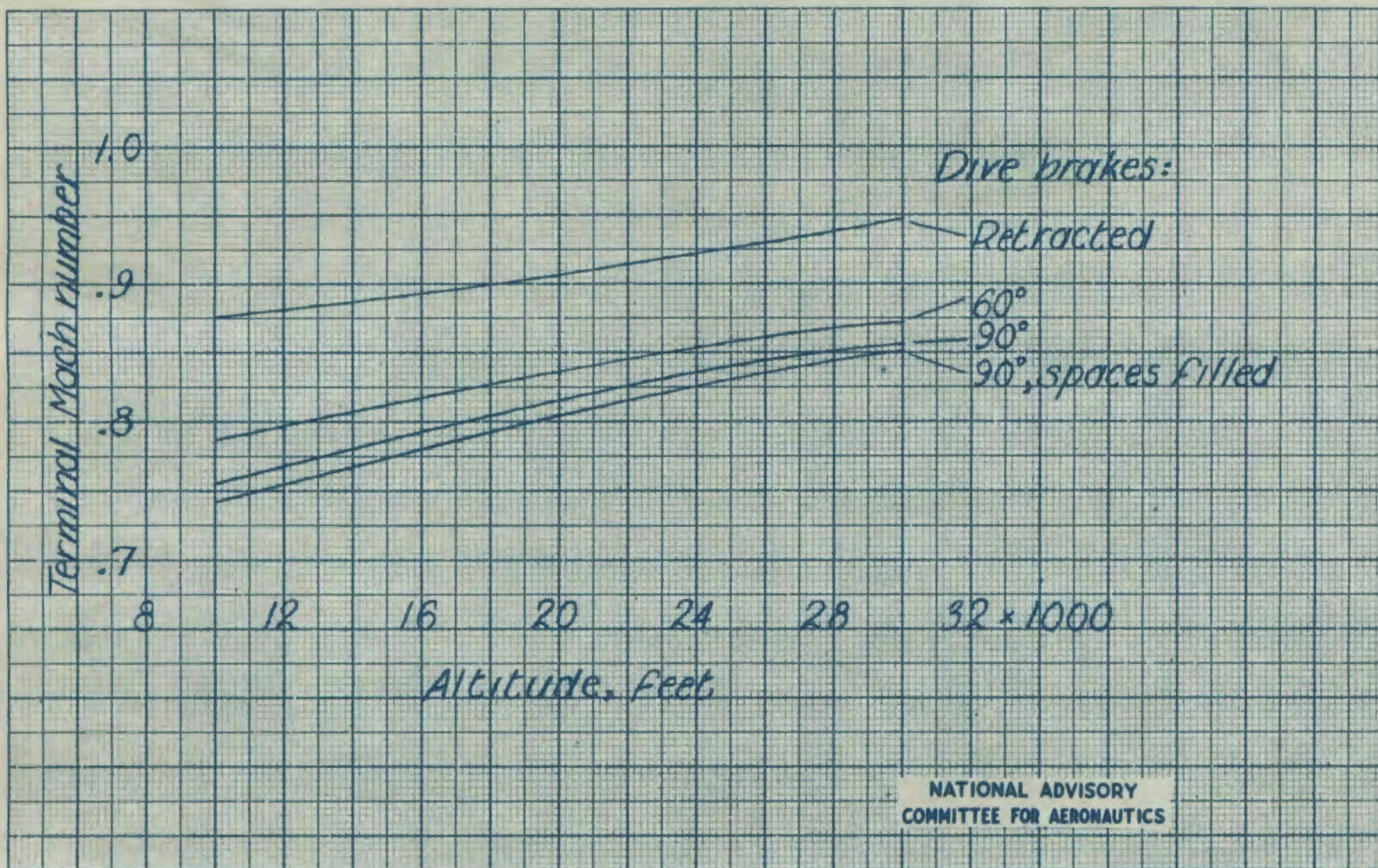
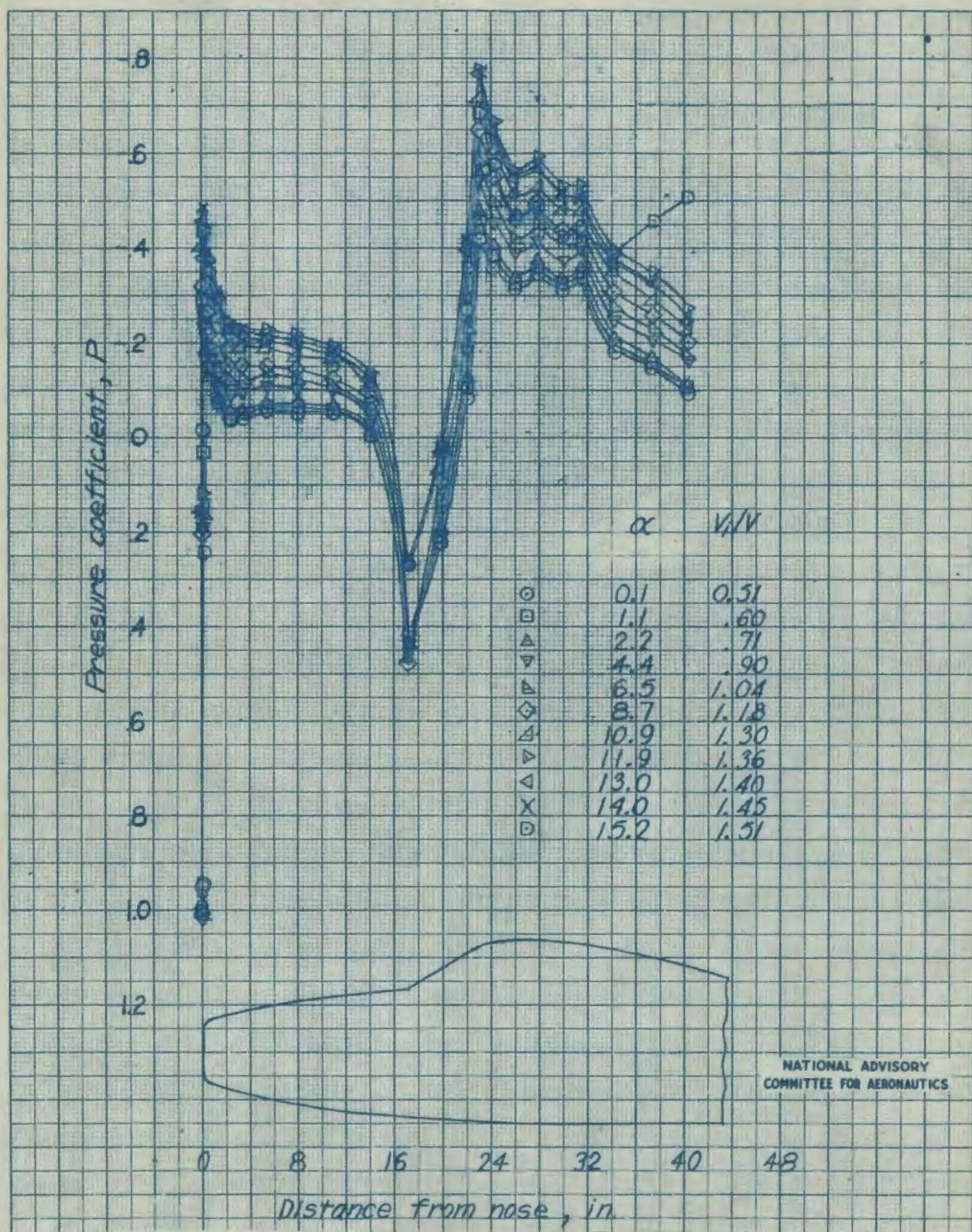


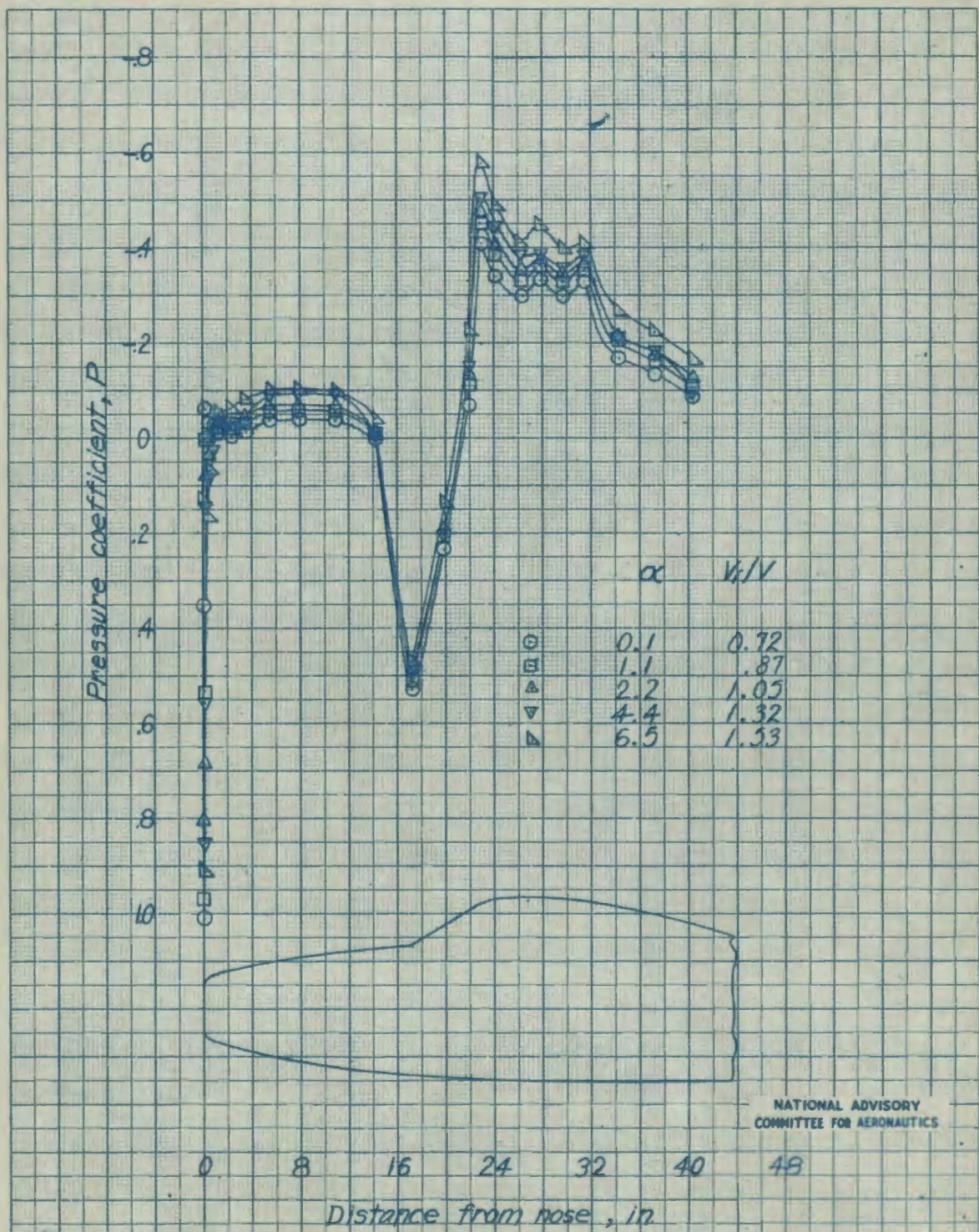
Figure 35 .- Effect of fuselage dive brakes on the estimated terminal Mach numbers of the Republic XP-84 airplane in vertical dives. Estimates based on wing critical Mach number of 0.755. Gross weight = 13,524 lb.

MR No. L6F25



(a) Power condition A [idle power (90 percent rpm) at sea level;  
approximately full power (100 percent rpm) at 30,000 feet]

Figure 36.- Pressure distribution over the top of the fuselage of the  
1/5-scale model of the Republic XP-84 airplane with the original canopy.

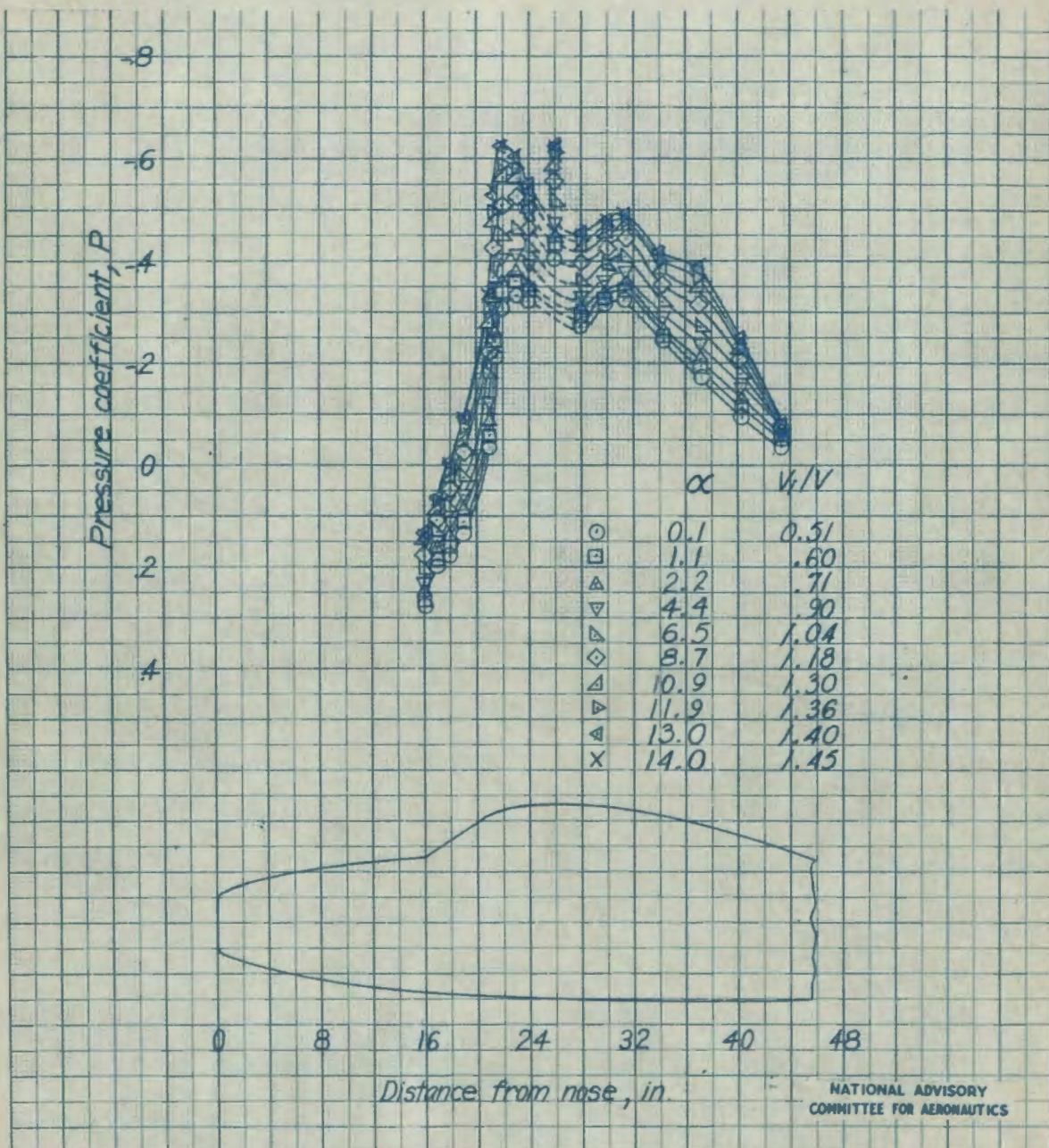


(b) Power condition B [full power (100 percent rpm) at sea level]

Figure 36.- Concluded.

18051

MR No. L6F25

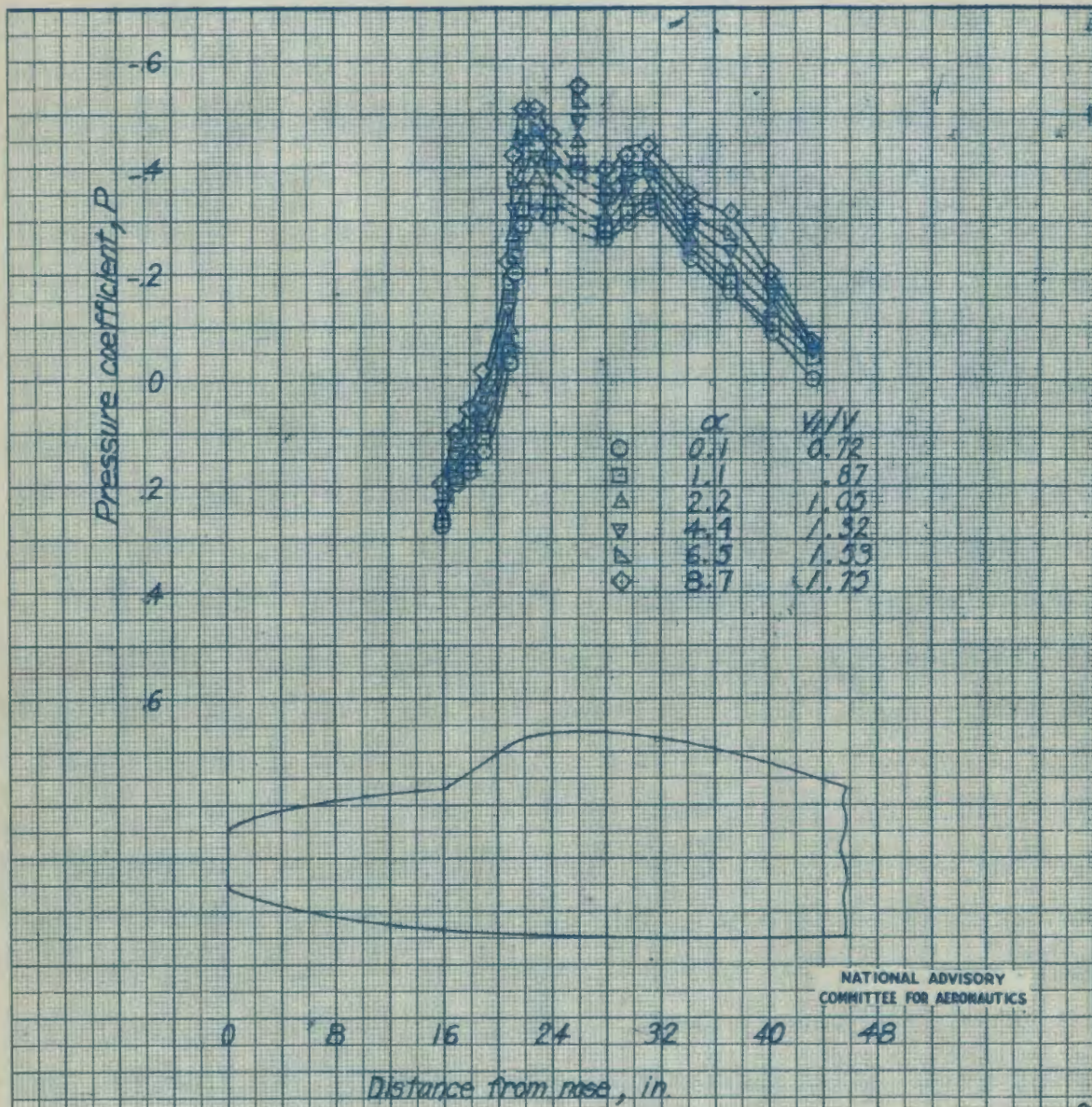


(a) Power condition A [idling power (80 percent rpm) at sea level; approximately full power (100 percent rpm) at 30,000 feet]

Figure 37.- Pressure distribution over the top of the V-front canopy tested on the 1/5-scale model of the Republic AP-84 airplane.

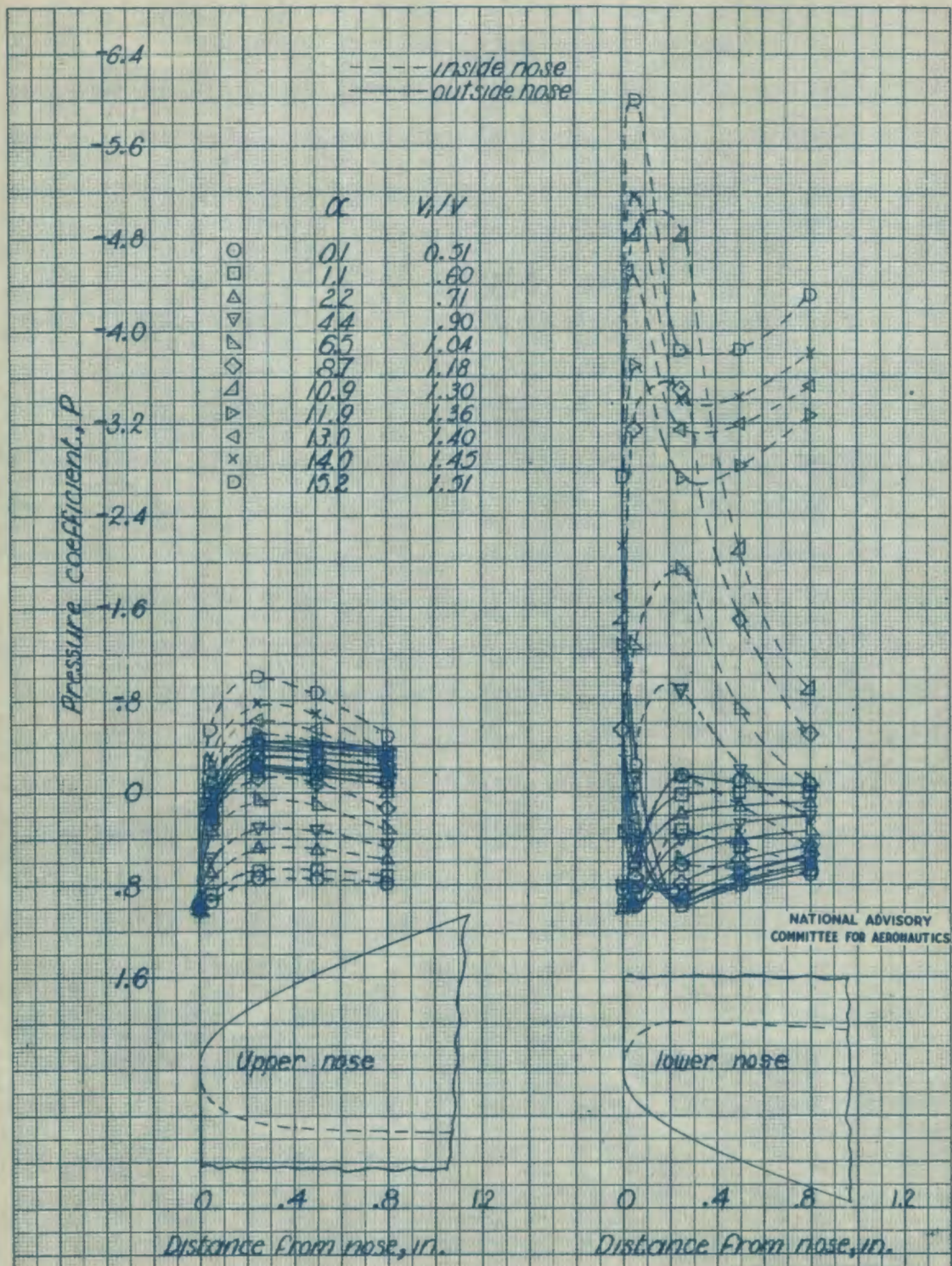
182031

MR No. L6F25



(b) Power condition B [full power (100 percent rpm) at sea level]

Figure 37.- Concluded.

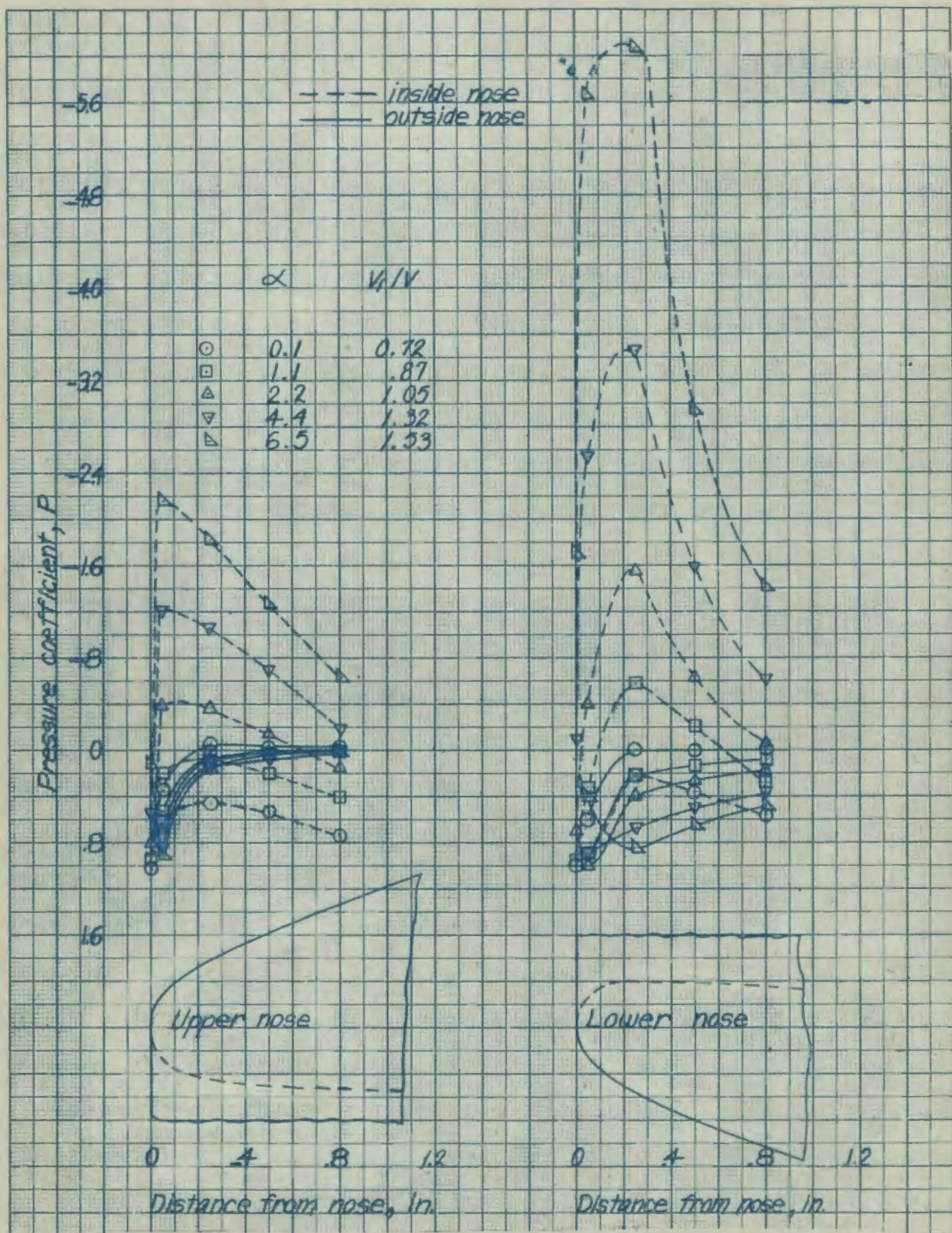


(a) Power condition A [idling power (80 percent rpm) at sea level; approximately full power (100 percent rpm) at 30,000 feet]

Figure 38.- Pressure distribution over the nose of the entrance duct of the 1/5-scale model of the Republic XP-84 airplane.

132038

MR No. L6F25



(b) Power condition B [full power (100 percent rpm) at sea level]

Figure 38.- Concluded.

NATIONAL ADVISORY  
COMMITTEE FOR AERONAUTICS.

182039

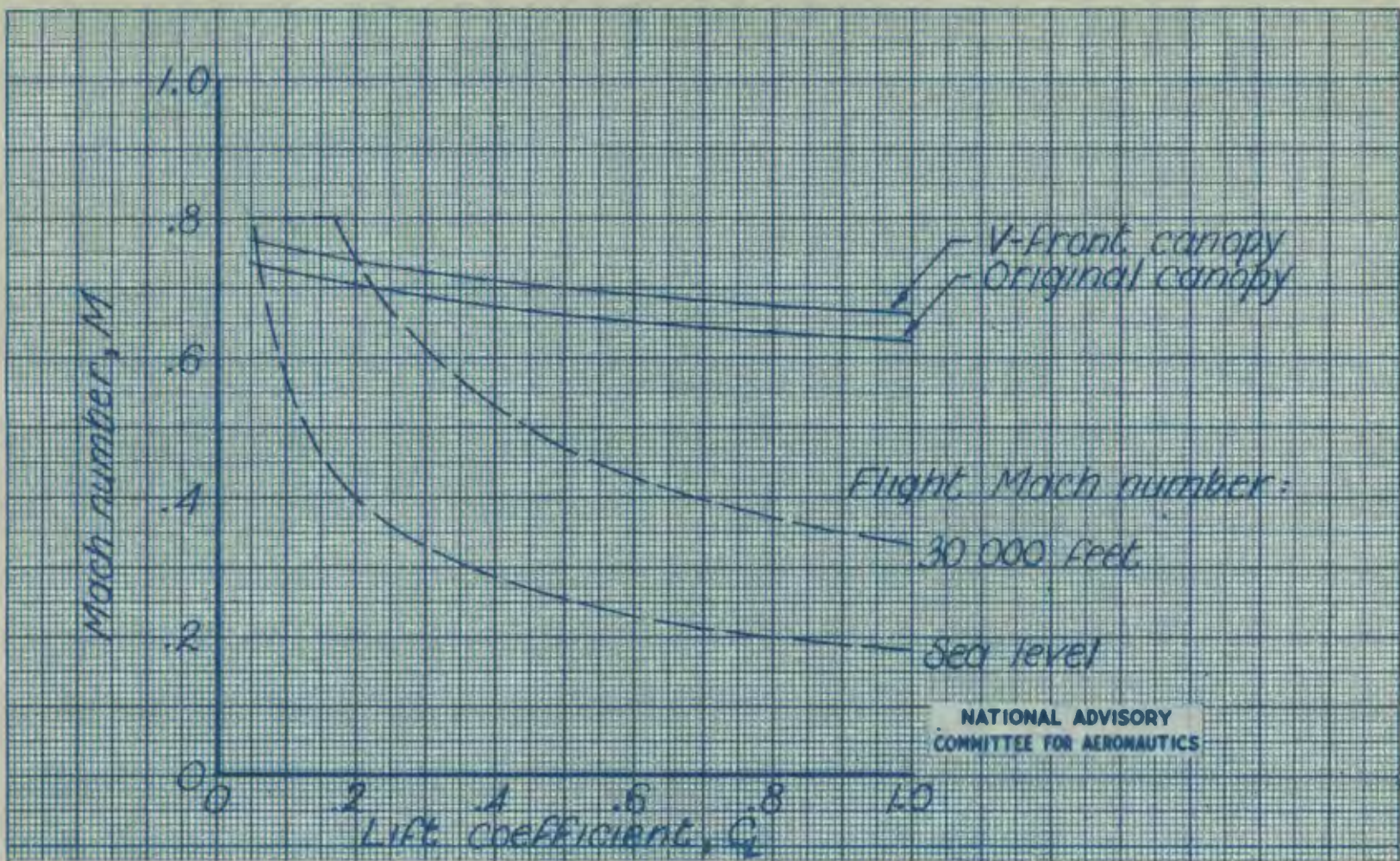


Figure 39.- Critical Mach numbers of two canopies for the Republic XP-84 airplane, as estimated from pressure-distribution tests of the 1/5-scale model. Power conditions A and B.

162040

MR No. L6F25

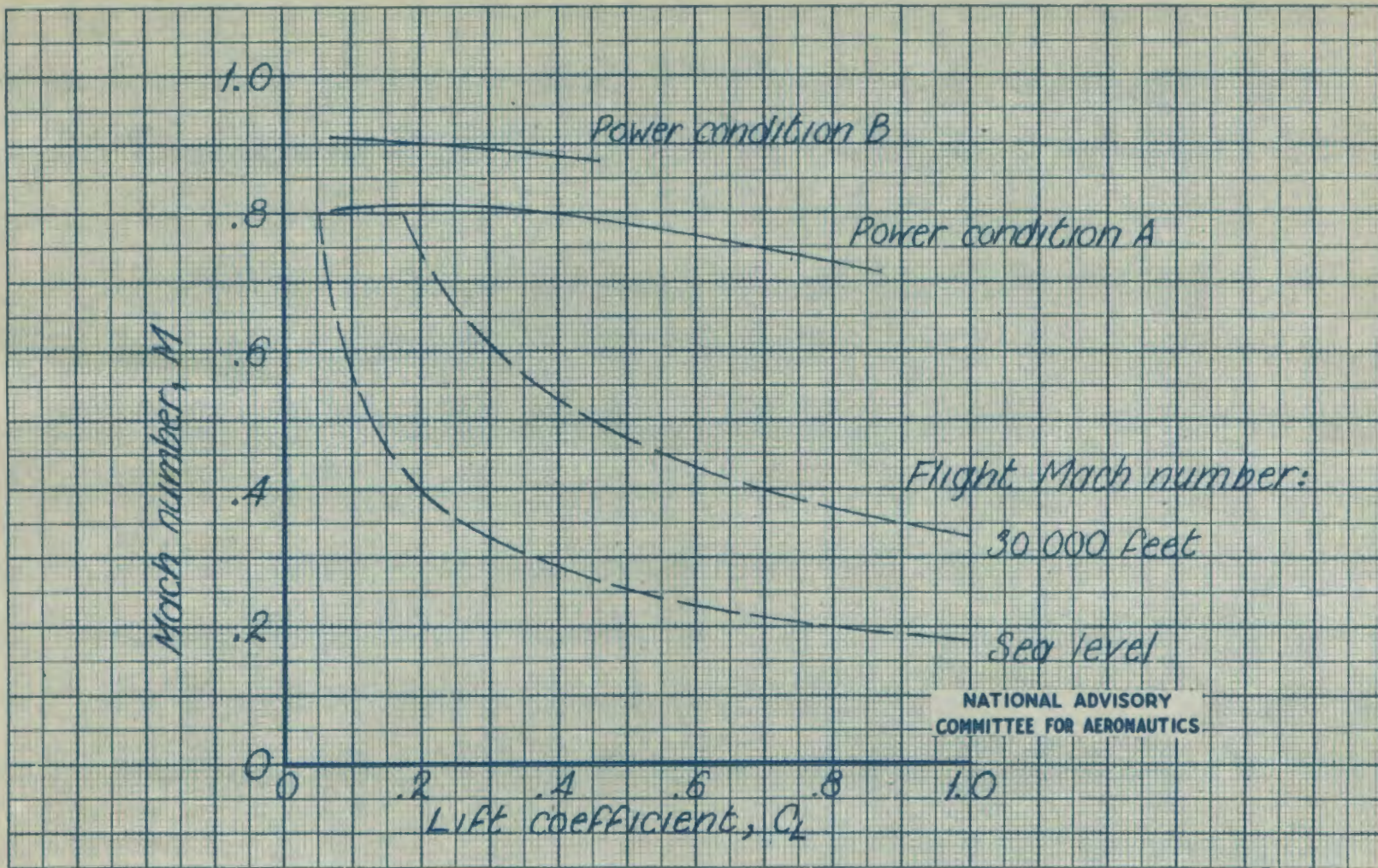


Figure 40.- Critical Mach numbers of the outside of the upper nose of the entrance duct of the Republic XP-84 airplane, as estimated from pressure-distribution tests of the 1/5-scale model.